Fall 12-20-2019

HDAC1 is a Required Cofactor of CBFβ-SMMHC and a Therapeutic Target in Inversion 16 Acute Myeloid Leukemia

Lisa E. Richter
University of Nebraska Medical Center

HDAC1 IS A REQUIRED COFACTOR OF CBFβ-SMMHC AND A THERAPEUTIC TARGET IN INVERSION 16 ACUTE MYELOID LEUKEMIA

By

Lisa E. Richter

A DISSERTATION

Presented to the Faculty of
the University of Nebraska Graduate College
in Partial Fulfillment of the Requirements
for the Degree of Doctor of Philosophy

Biochemistry & Molecular Biology Graduate Program

Under the Supervision of Professor R. Katherine Hyde

University of Nebraska Medical Center
Omaha, Nebraska

December, 2019

Supervisory Committee:
Shantaram Joshi, Ph.D.
Steven Caplan, Ph.D.
David Klinkebiel, Ph.D.

HDAC1 IS A REQUIRED COFACTOR OF CBFβ-SMMHC AND A THERAPEUTIC TARGET IN INVERSION 16 ACUTE MYELOID LEUKEMIA

Lisa E. Richter, Ph.D.

University of Nebraska, 2019

Supervisor: R. Katherine Hyde, Ph.D.

Acute myeloid leukemia (AML) is a neoplastic disease characterized by the uncontrolled proliferation and accumulation of immature myeloid cells. A common mutation in AML is the inversion of chromosome 16 [inv(16)], which generates a fusion between the genes for core binding factor beta (*CBFB)* and smooth muscle myosin heavy chain (*MYH11*), forming the oncogene *CBFB-MYH11*. The expressed protein, CBFβ-SMMHC, forms a heterodimer with the key hematopoietic transcription factor RUNX1. Although CBFβ-SMMHC was previously thought to dominantly repress RUNX1, recent work suggests that CBFβ-SMMHC functions together with RUNX1 to activate transcription of specific target genes.

Targeting the activity of CBFβ-SMMHC is a promising approach for treating inv(16) AML, although currently there are no inhibitors of CBFβ-SMMHC ready for clinical use. An alternative approach is to indirectly target the fusion protein by inhibiting the activity of other proteins which are recruited to CBFβ-SMMHC and are required for its activity. One possible target is the epigenetic regulator histone deacetylase 1 (HDAC1), which was previously shown to colocalize with CBFβ-SMMHC on gene promoters. We hypothesized that HDAC1 was recruited to the CBFβ-SMMHC:RUNX1 complex and inhibitors of HDAC1 could be used to indirectly target its leukemogenic activity.

In this study, we demonstrate that HDAC1 forms a complex with CBFβ-SMMHC, confirmed its colocalization with RUNX1 and CBFβ-SMMHC on the promoters of known fusion protein target genes, and determined that *Hdac1* is required for expression of these genes. These results imply that HDAC1 is an important component of the CBFβ-SMMHC transcriptional complex, and that leukemia cells expressing the fusion protein may be sensitive to treatment with HDAC1 inhibitors. Both *Hdac1* knockdown and treatment with the HDAC1 selective inhibitor entinostat *in vitro* results in a decrease in colony-forming ability and an increase in differentiation in CBFβ-SMMHC$^+$ cells, implying that HDAC1 is required to maintain the differentiation block in the leukemia cells. Using a knock-in mouse model expressing CBFβ-SMMHC, we found that *in vivo* treatment with entinostat decreased leukemic burden and induced differentiation and apoptosis of leukemia cells. Importantly, entinostat treatment specifically targeted the leukemia cells with minimal toxicity to normal cells. We also tested the same treatment strategy on survival of the mice but found that leukemia cells were able to continue to grow after cessation of treatment. Overall, our results demonstrate the strict requirement for HDAC1 in CBFβ-SMMHC$^+$ cells and reveal that it is a promising therapeutic target for treatment of inv(16) AML.

Table of Contents

Abbreviations

°C	degrees Celsius
µg	microgram
µL	microliter
µm	micrometer
µM	micromolar
Å	angstrom
aa	amino acid
ACD	assembly competence domain
ACK	Ammonium-Chloride-Potassium lysing buffer
ALL	acute lymphocytic leukemia
AML	acute myeloid leukemia
ANOVA	analysis of variance
ATP	adenosine triphosphate
BM	bone marrow
bp	base pair
BSA	bovine serum albumin
CBC	complete blood count
CBF	core binding factor

CBFB	core binding factor beta; gene symbol
CBFβ	core binding factor beta; protein symbol
cDNA	complementary DNA
CFA	colony-forming assay
CFU	colony-forming units
cGy	centigray
ChIP	chromatin immunoprecipitation
ChiP-seq	chromatin immunoprecipitation sequencing
CLL	chronic lymphocytic leukemia
CM	CBFB-MYH11 or CBFβ-SMMHC
cm	centimeter
CM^{+}	leukemia cells from knock-in mice with a conditional *Cbfb-MYH11* allele (*Cbfb*$^{+/56M}$) under the control of the *Mx1-Cre Recombinase* (*Mx1-Cre*$^{+}$) transgene
CML	chronic myeloid leukemia
CNS	central nervous system
CR	complete remission
diH_2O	deionized water
DMEM	Dulbecco's Modified Eagle Medium
DMSO	dimethyl sulfoxide

DNA	deoxyribonucleic acid
DTT	dithiothreitol
E	embryonic day
EC_{50}	half-maximal effective concentration
EDTA	ethylenediaminetetraacetic acid
EGS	ethylene glycol bis(succinimidyl succinate)
ENU	N-ethyl-N-nitrosourea
ESC	embryonic stem cell
FACS	flow cytometry and cell sorting
FBS	fetal bovine serum
FC	flow cytometry
FISH	fluorescent *in situ* hybridization
FRET	fluorescence resonance energy transfer
GFP	green fluorescent protein
H&E	hematoxylin and eosin stain
HABD	high-affinity binding domain
HAT	histone acetyltransferase
HBS	HEPES-buffered saline
HDAC	histone deacetylase
HDACi	HDAC inhibitor

HEPES	4-(2-hydroxyethyl)-1-piperazineethanesulfonic acid
His	histidine
HRP	horseradish peroxidase
HSC	hematopoietic stem cell
Inv(16)	inversion 16
IP (injection)	intraperitoneal
IP	immunoprecipitation
IPTG	Isopropyl β-D-1-thiogalactopyranoside
IRES	internal ribosome entry site
KAT	lysine acetyltransferase, another name for HAT
kb	kilobase
kD	kilodalton
KD	knockdown
KDAC	lysine deacetylase, another name for HDAC
kg	kilogram
KI	knock-in
KO	knockout
Leu	leucine
LIC	leukemia-initiating cell
Lin^-	lineage-depleted bone marrow

LSC	leukemia stem cell
M	molar
MDS	myelodysplastic syndrome
mg	milligram
mL	milliliter
mM	millimolar
MPN	myeloproliferative neoplasm
MPP	multipotent progenitor cell
MYH11	smooth muscle myosin heavy chain; gene symbol
NAD	nicotinamide adenine dinucleotide
NAT	N-terminal acetyltransferase
NES	nuclear export signal
ng	nanogram
NLS	nuclear localization signal
OD	optical density
PBS	phosphate-buffered saline
PCR	polymerase chain reaction
PEG	polyethylene glycol
pH	power of hydrogen
PVDF	polyvinylidene difluoride

qRT-PCR	quantitative real-time polymerase chain reaction
RHD	runt homology domain
RNA-seq	RNA sequencing
RNA	ribonucleic acid
rpm	revolutions per minute
RPMI	Roswell Park Memorial Institute media
RUNX1	runt-related transcription factor 1
SCF	stem cell factor
SEM	standard error of the mean
shRNA	short hairpin RNA
SMMHC	smooth muscle myosin heavy chain; protein symbol
TBS-T	tris-buffered saline with tween
TCR	T-cell receptor
TE	tris EDTA buffer
TF	transcription factor
Trp	tryptophan
TSA	trichostatin A
V	volts
VPA	valproic acid
WB	western blot

WT	wild-type
YPD	Yeast Extract–Peptone–Dextrose media
Zn	zinc

List of Figures

List of Tables

Acknowledgements

I would first like to thank my advisor, Dr. Kate Hyde, for giving me the amazing opportunity to join the lab and initiate a brand-new project. Thank you for your patience and hard work molding me into an independent scientist and for always being an incredible role model. Your constant optimism in the wake of a string of failed experiments kept me going on too many occasions to count. None of this would have been possible without your guidance.

Thank you to my coworkers for making our work environment fun and supportive, and for the help you gave me with this project. Yiqian Wang, you have been a daily inspiration to me through your dedication and persistence. I can't wait to see all your hard work pay off in your career. Michelle Becker, thank you for being supportive through the ups and downs of life and graduate school. I am never afraid to just be myself around you whether it's a good day or a bad day, and that is such a great gift. Thank you for letting me be a part of your family and for making me the other Aunt Lisa. Jake Williams, thank you for always being able to lighten the mood and keep things fun.

I am also thankful to the many students who temporarily worked with me in the lab. Ankita Sarawagi, Rachel Coburn, Jay Jiang, Josephine Peitz, Alex Pieper, and Arjun Dhir, you have all helped me to become a better teacher and mentor. Thank you for your various contributions to this project.

A special thank you to my supervisory committee members who have helped guide and shape this project from the beginning. Dr. Shantaram Joshi, Dr. Steve Caplan, and Dr. David Klinkebiel, thank you for your roles in mentoring me and providing constructive feedback on my project.

I would like to thank the UNMC Department of Biochemistry and Molecular Biology for supporting me as a student. Most labs in the department have contributed resources and expertise to this project in some way. A special thank you to the Challagundla lab, the Teoh-Fitzgerald lab, the Oberly-Deegan lab, and the Mott lab for continued use of your equipment.

I really don't think I could have succeeded in graduate school without the help of an amazing support group of fellow students, especially Brandon Griess, Bailee Sliker, Brittany Poelaert, and Megan Zavorka Thomas. Thanks for the vent sessions and many fun times outside of the lab. You were all instrumental in the completion of this project and more importantly in the maintenance of my sanity.

Finally, thank you to my wonderful family: Fran, Nancy, and Andy Richter. Dad, you were the one who encouraged me to go to graduate school and were there to see me off. I wish you were here to see me finish, but you never doubted I would get to this point. Mom, thank you for always being there in good times and bad and loving me unconditionally. There aren't words to thank you for everything you do for me. I don't deserve you, but I am endlessly thankful that I am your daughter. Andy, thanks for your support and being genuinely interested in what I've been working on all these years. My time in Omaha has also resulted in a new family, for whom I am so thankful. Jim and Jodi Booth, thank you for making me part of your family and giving me a home-away-from-home full of puppy snuggles, tasty food, and love. And finally, Nathan Booth, my favorite person and future husband, thank you for your endless love and support during this process. I love you so much and I think our future is going to be pretty great.

Chapter I

Introduction

1. Overview and Rationale

The process of mature blood cell formation, or hematopoiesis, is a complex system that requires the precisely regulated activity of countless transcription factors, epigenetic regulators, and signaling pathways. This process malfunctions in leukemia, resulting in an accumulation of immature blood cells. Mutations in transcription factors involved in the regulation of hematopoiesis are a common cause of leukemia. Such is the case in inversion 16 acute myeloid leukemia [inv(16) AML], which results from the gene for core binding factor beta (*CBFB*) fusing with the gene for smooth muscle myosin heavy chain (*MYH11*) (1).

Inv(16)(p13;q22) is one of the most common recurrent mutations found in AML and accounts for roughly 10% of all AML cases (2–4). Standard treatment for inv(16) AML leads to high levels of remission, classifying inv(16) as a favorable prognosis mutation (2,5–8). However, this treatment is not specific to the leukemia cells, resulting in high toxicity for patients (5,9). Furthermore, 50% of patients will quickly relapse, indicating that treatment is ineffective at complete eradication of the disease (8,10). The five-year survival for inv(16) AML is only 50-60% (2,7,8), demonstrating a pressing need for innovative targeted therapies for inv(16) AML patients.

New treatments which target the activity of the inv(16) fusion protein, CBFβ-SMMHC, have been investigated as targeted therapy for the disease (11–13). These studies have demonstrated the efficacy of this approach, but the compounds used in these studies are not suitable for clinical trials. Another possibility is identifying and targeting other binding partners of the inv(16) fusion protein complex which are required for its leukemogenic activity and targeting these cofactors for therapy.

One possible candidate is histone deacetylase 1 (HDAC1) which was found to colocalize to gene promoters with CBFβ-SMMHC, suggesting that it might be regulating the activity of the fusion protein (14). HDAC1 is also a known binding partner of runt-related transcription factor 1 (RUNX1), the DNA-binding subunit of protein complexes including CBFβ and CBFβ-SMMHC (15–17). Because RUNX1 is a required binding partner of CBFβ-SMMHC in inv(16) AML cells, it is possible that HDAC1 could be binding to the RUNX1: CBFβ-SMMHC complex (18). Additionally, certain HDAC inhibitors have already been FDA approved, allowing for faster translation for clinical use if these drugs are effective for inversion (16) AML treatment. This hypothesis is the basis for the current study, in which we investigated the role of HDAC1, and to a lesser extent HDAC2 and HDAC3, in inv(16) AML.

2. Hematopoiesis

2.A. Overview

Hematopoiesis is a tightly regulated, hierarchical process that results in the generation of all mature blood cells (Figure 1). At the apex of the hierarchy is the long-term hematopoietic stem cell (HSC) that is capable of self-renewing or differentiating. The multipotent progenitor (MPP) population of cells is the last cell type capable of becoming either myeloid or lymphoid. Further differentiation from the MPP results in a cell committed to either the myeloid lineage or the lymphoid lineage. The common myeloid progenitor gives rise to either the megakaryocyte-erythrocyte progenitor or the granulocyte-monocyte progenitor. At the base of this pyramid lies the final mature form of each type of myeloid cell: megakaryocyte, erythrocyte, the granulocytes (basophils, eosinophils, neutrophils), and monocytes. The lymphoid lineage begins with the common lymphocytic progenitor which can then mature into B cells, T cells, or natural killer cells.

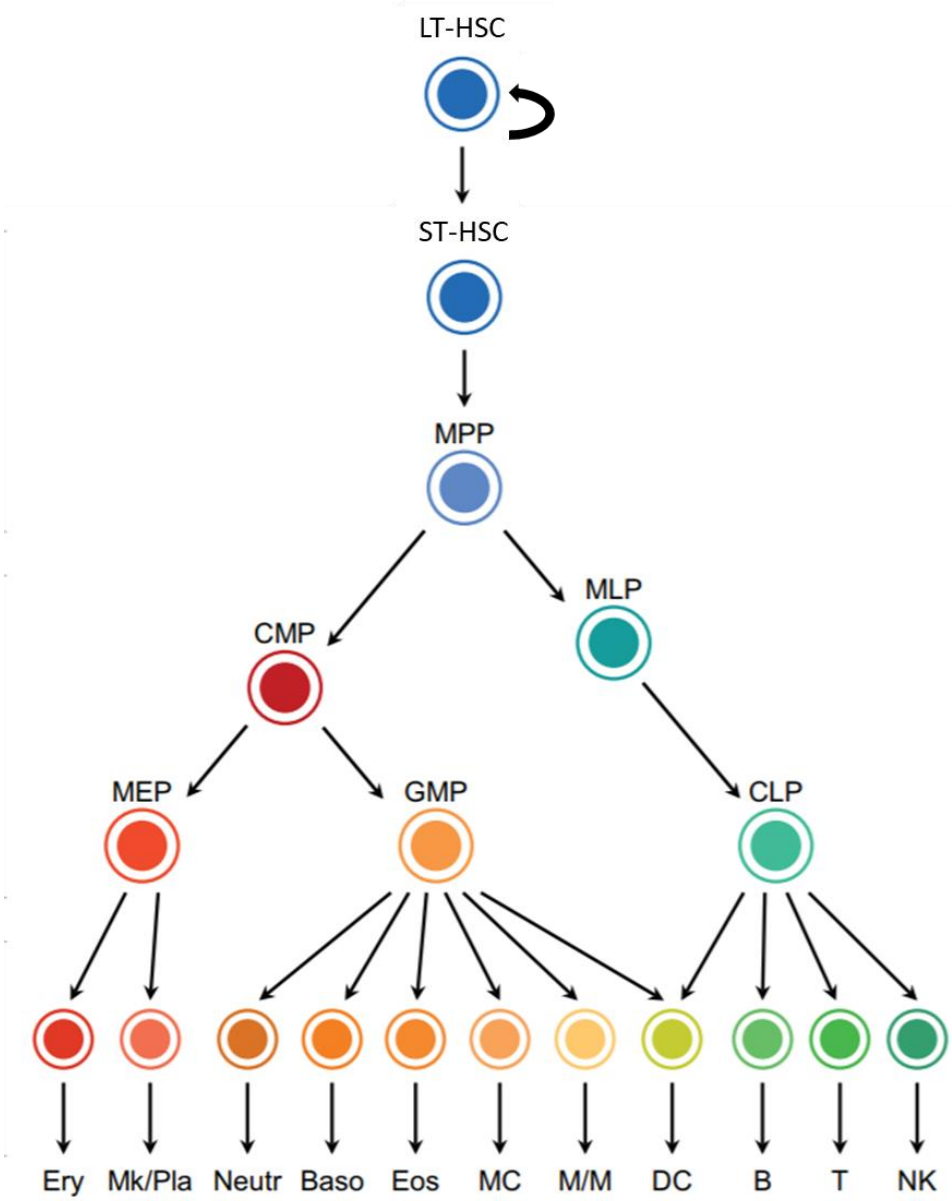

Figure 1. The hierarchical model of hematopoiesis. Human hematopoietic cells arise from self-renewing long-term hematopoietic stem cells (LT-HSC). Abbreviations: Short-term hematopoietic stem cell (ST-HSC), multipotent progenitor (MPP), multilymphoid protenitor (MLP), common lymphoid progenitor (CLP), common myeloid progenitor (CMP), granulocyte-macrophage progenitor (GMP), megakaryocyte-erythrocyte progenitor (MEP), natural killer cell (NK), T cell (T), B cell (B), dendritic cell (DC), monocytes/macrophages (M/M), mast cells (MC), eosinophils (Eos), basophils (Baso), neutrophils (Neutr), megakaryocyte/platelets (Mk/Pla), erythrocytes (Ery). Adapted from Antoniani C, Romano O, Miccio A. Concise Review: Epigenetic Regulation of Hematopoiesis: Biological Insights and Therapeutic Applications. Stem Cells Transl Med. 2017;6(12):2106–14.

2.B. Location of hematopoiesis

The site of hematopoiesis changes according to the stage of development. In humans, hematopoiesis starts in the yolk sac around day 15-17 post-fertilization (19). This initial phase is termed “primitive” hematopoiesis and is mainly for producing red blood cells to facilitate rapid growth (20). The next wave of more adult-like hematopoiesis is termed “definitive” hematopoiesis. In humans it begins by day 60 after fertilization, first taking place in the aorta-gonad mesonephros region where HSCs are first produced, followed by a transition to the fetal liver. During the 11^{th} week of human development, blood cell formation begins in the bone marrow, where it remains for the remainder of life (19,20). In rare circumstances, extramedullary hematopoiesis can occur in the liver or spleen during times of infections or diseased states where the bone marrow niche no longer supports hematopoiesis (21).

2.C. Transcriptional control of hematopoiesis

The temporal specific expression of transcription factors (TFs) is key to the hierarchical differentiation scheme. Active transcription factors control cell surface receptor expression, cytokine excretion for paracrine or autocrine signaling, cell-type specific proteins, and hematopoietic stem cell self-renewal and commitment to differentiation. Thus the expression of transcription factors has to be tightly regulated, often by many transcription factors regulating the expression of a single other transcription factor (22). Regulation of the activity of transcription factors is also critical and is often influenced by the presence of other transcription factors at the same promoter. Because of the critical role of transcription factors in hematopoiesis, it is not surprising that mutation of key transcription factors is a common initiating mutation in leukemia.

2.D. Core binding factor

One of the most important hematopoietic transcription factor complexes, and among the most mutated transcription factor families in leukemia, is core binding factor (CBF) (23–25). CBF is composed of two subunits, which during hematopoiesis consist of the alpha subunit RUNX1 and beta subunit CBFβ. Both subunits are critical for hematopoiesis, as knockout of either gene in mice results in embryonic lethality (26–28), but each subunit has distinct roles as well. RUNX1 directly interacts with DNA (29), while CBFβ stabilizes the interaction and prevents RUNX1 degradation (Figure 2) (16,30,31). Both RUNX1 and CBFβ have critical roles in the molecular pathology of inv(16) AML, and therefore will be examined in greater detail in the following sections.

2.D.i. Core binding factor beta (CBFβ)

2.D.i.a. Heterodimerization

Human core binding factor beta (*CBFB*) is located on chromosome 16 (16q22.1), and is made up of six exons (32). The expression of *CBFB* results in a protein of roughly 22 kilodaltons, CBFβ, and is ubiquitously expressed in human and mouse tissues (33). CBFβ, formerly referred to as polyomavirus enhancer-binding protein 2 beta (PEBPB2), is one subunit of core binding factor (CBF), heterodimerizing with the alpha subunit which can be either RUNX1, 2, or 3 (Figure 2) (34).

Mutational studies have demonstrated that the heterodimerization region of CBFβ is located on the N-terminal 135 amino acids (35). Expression of only the first 135 amino acids maintains a similar structure to full-length CBFβ and can also bind to the RUNX:DNA complex with similar affinity as full-length CBFβ. The residues on CBFβ which are involved with RUNX binding are spread out throughout this region, with RUNX

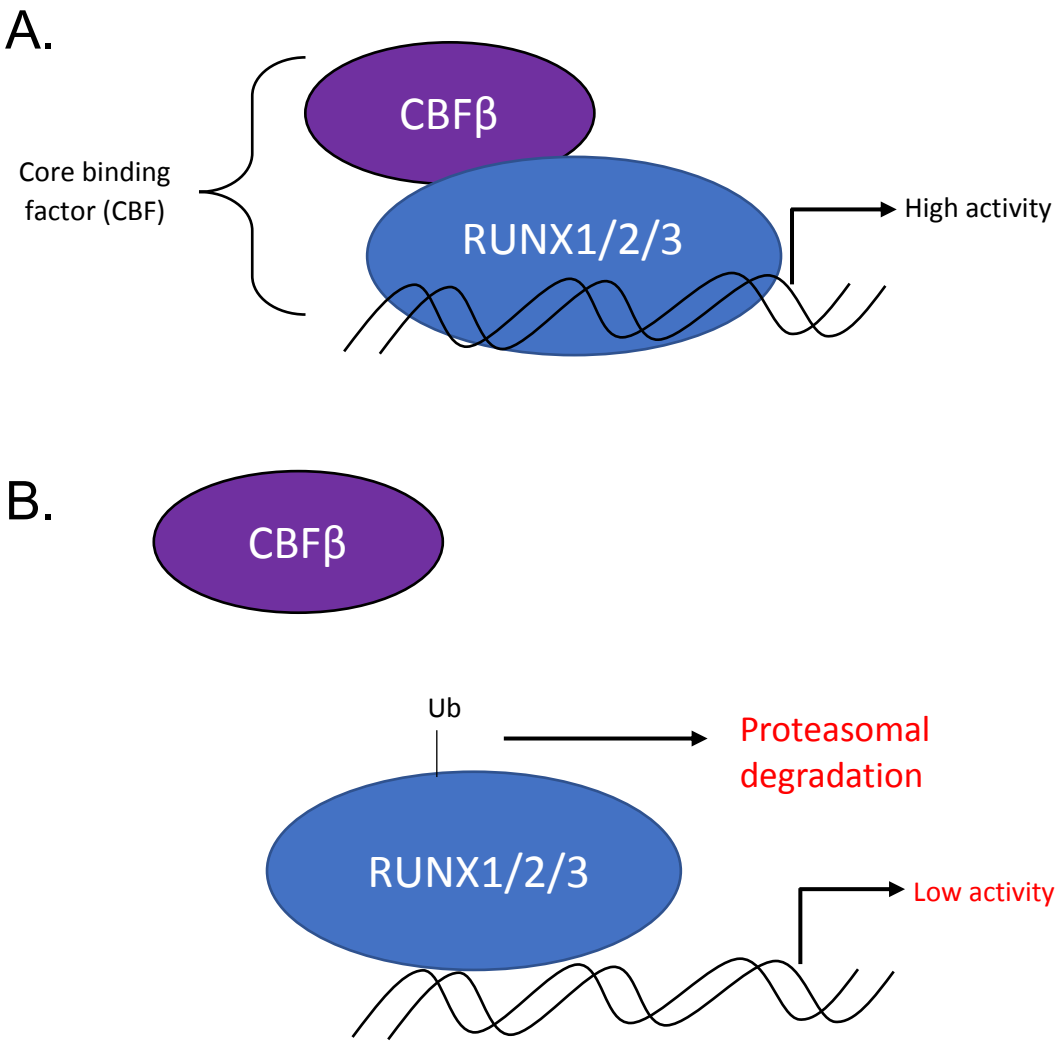

Figure 2. Core binding factor. Core binding factor (CBF) is a transcription factor composed of two subunits, CBFβ and either RUNX1, RUNX2, or RUNX3. When CBFβ is bound to RUNX, the interaction between RUNX1 and DNA is stabilized and proteasomal degradation of RUNX1 is inhibited (**A**). Without CBFβ, RUNX1 can still bind to DNA but its transactivation ability is much lower and it is ubiquitinated and degraded much faster (**B**).

relying upon many different contact points within the higher structure of the CBFβ protein (36,37).

2.D.i.b. Role in normal hematopoiesis

Structural analysis revealed that CBFβ binding to RUNX1:DNA results in a conformational shift in the RUNX protein leading to additional hydrogen bonding with DNA (38). CBFβ itself does not directly bind to DNA, but it decreases the rate at which RUNX dissociates from DNA, therefore stabilizing the interaction (16,30). While RUNX is capable of binding to DNA as a monomer, its affinity for DNA is 5- to 10-fold greater when CBFβ is part of the complex (16,30). CBFβ, in turn, relies on RUNX1 for proper subcellular localization. CBFβ is localized to both the cytoplasm and nucleus but does not contain a nuclear localization signal (NLS), and enters the nucleus only through interaction with RUNX, which does have a NLS (39,40).

Beyond allosteric regulation of RUNX, a second important role for CBFβ is to increase the half-life of the RUNX protein. CBFβ decreases the rate at which RUNX is degraded by the ubiquitin-proteasome pathway. RUNX1/2/3 protein levels are stabilized by the addition of exogenous CBFβ, and heterodimerization is required for this activity by blocking ubiquitination on the runt domain of RUNX (31).

Knockout mouse models have demonstrated the importance of CBFβ *in vivo*. *Cbfb*$^{-/-}$ mice die between embryonic days 11.5 and 13.5 (E11.5 to E13.5) due to hemorrhage in the central nervous system (26,41). While primitive hematopoiesis remained intact in *Cbfb*$^{-/-}$ mice, they completely lacked definitive hematopoiesis as evidenced by lack of hematopoietic cells in the fetal liver by E12.5 (26). *Cbfb*$^{-/-}$ mice had low RUNX1 expression due to the elimination of CBFβ's key function as an inhibitor of

RUNX proteosome-mediated degradation (31). Altogether, these studies provide strong evidence that CBFβ is essential for RUNX activity.

2.D.ii. Runt-related transcription factor 1 (RUNX1)

The alpha subunit of core binding factor is one of three runt-related transcription factor (RUNX) proteins: RUNX1, RUNX2, or RUNX3 (formerly AML1/CBFα2, AML3/ CBFα1, or AML2/ CBFα3, respectively) (34). Each of the alpha subunits binds to CBFβ to regulate gene expression in various tissues. RUNX genes arose early in evolution and maintained extensive homology in vertebrates (42), especially within the runt-homology domain (RHD) which is responsible for binding to DNA and CBFβ (29). While RUNX2 is important in bone tissue and RUNX3 in the central nervous system, RUNX1 is the primary regulator of hematopoiesis (43,44). The *RUNX1* gene was originally identified because of its involvement in the frequent leukemia-associated translocation *RUNX1-RUNX1T1* (45). Because of its importance in regulating hematopoiesis, *RUNX1* is the most frequently mutated gene in human leukemia (23,24).

2.D.ii.a. Role in normal hematopoiesis

RUNX1 is a direct regulator of gene transcription and controls hematopoiesis along with many other transcription factors. It is expressed in almost all hematopoietic stem and progenitor cells, as well as cells of the myeloid lineage and B- and T-cells (46,47). RUNX1 directly binds to the DNA consensus sequence 5’-PuACCPuCA-3’ through the runt-homology domain (29,48). RUNX1 regulates genes involved in a wide range of cellular activities including hematopoietic differentiation, cytokine production, and cell cycle. There are many bona fide RUNX1 target genes including IL-3, GM-CSF, and T-cell Receptor (TCR) components in T-cells, and CSF1R (M-CSFR), MPO, p14, and p21 in myeloid cells (49).

Studies in knockout mice have identified the requirement for RUNX1 during development. RUNX1-nullizygous mice die *in utero* due to a failure to progress from primitive to definitive hematopoiesis (27,28). In contrast, depletion of *Runx1* in adult mice does not cause a complete loss of hematopoiesis. Instead, an inducible *Runx1* deletion results in an immediate increase in HSCs and myeloid progenitors but impaired development of lymphocytes and megakaryocytes (50–52). With time, *Runx1* deletion results in splenomegaly due to an expansion of the myeloid compartment, a decrease in thymus size concurrent with an increase in immature $CD4^{-}CD8^{-}$ thymocytes, cytopenia in the peripheral blood, and an increase in immature cells in the bone marrow indicative of a myelodysplastic syndrome (52–54).

2.D.ii.b. Post-translational modifications

The activity of RUNX1 is further controlled by post-translational modifications, including phosphorylation and acetylation. RUNX1 has numerous serine, threonine, and tyrosine phosphorylation sites (55–57). Phosphorylation of RUNX1 at serine/threonine promotes its transactivation ability by releasing RUNX1 from association with the corepressor Sin3A (58) and histone deacetylase (HDAC) 1 and 3 (15). In myeloid lineage cells, tyrosine phosphorylation results in a similar increase in transactivation ability by increasing DNA binding and decreasing contacts with HDACs (59).

RUNX1 activity is also critically regulated through acetylation. The histone acetyltransferases (HATs) p300 and MOZ are capable of interacting with and acetylating RUNX1 and stimulating its transcriptional activity *in vitro* (60,61). The acetylation sites of RUNX1 were mapped to the region N-terminal to the Runt domain at lysines 24 and 43 of the RUNX1b variant (62). Mutation of these residues indicated that acetylation at these sites is important for p300-mediated transcriptional activation of RUNX1. Furthermore, in *in vitro* experiments, acetylation enhanced DNA binding, but did not alter

CBFβ binding ability of RUNX1 (62). RUNX1 acetylation is also important for regulating its activity in the context of the leukemia fusion protein RUNX1-RUNX1T1. Lysines 24 and 43 were confirmed as the RUNX1 acetylation sites on RUNX1-RUNX1T1 as well, and p300 controls the acetylation of these sites (58). Acetylation at these sites is essential for RUNX1-RUNX1T1-induced leukemogenesis in mice, particularly at lysine 43 (58).

While these studies have made it clear that acetylation of RUNX1 is critical for its activity, no studies have examined the regulators of RUNX1 deacetylation. Additionally, there are no investigations into the role of RUNX1 acetylation in the context of CBFβ-SMMHC and inv(16) AML, which is likely to be important based on the requirement for RUNX1 activity in this disease. We will explore these topics further in the discussion chapter, as one possible future direction for our study.

2.D.ii.c. RUNX1 in leukemia-associated fusion proteins

RUNX1 is itself part of several leukemia-associated fusion proteins such as RUNX1-RUNX1T1 and RUNX1-EVI1 in AML, and TEL-RUNX1 in acute lymphoblastic leukemia (ALL). These fusion proteins share some common features such as the recruitment of other transcription factors and epigenetic regulators to regulate chromatin dynamics and gene expression (63).

The translocation resulting in the fusion gene *RUNX1-RUNX1T1* (*AML1-ETO, AML1-MTG8*), t(8;21)(q22;q22), is present in 12-15% of AML cases and is the most commonly observed recurring chromosomal abnormality in AML (64,65). The t(8;21)(q22;q22) translocation retains the N-terminal 177 amino acids of RUNX1, including the runt-homology domain, fused to the majority of the RUNX1T1 protein (66). RUNX1T1, formerly called ETO (eight twenty-one, MTG8) is an evolutionarily conserved,

nuclear-localized protein that does not bind DNA itself but is part of transcription factor complexes due to its ability to recruit coactivators and corepressors (67). RUNX1-RUNX1T1 disrupts the normal gene regulation of RUNX1 by recruitment of HATs, HDACs, and other epigenetic regulators to regulatory regions of RUNX1 target genes. While most RUNX1-RUNX1T1 activity is centered around the repression of genes involved in cell growth or differentiation, the fusion is also involved in gene activation (68). Thus, RUNX1-RUNX1T1 has many similar features to CBFβ-SMMHC, the fusion protein in inv(16) AML discussed in subsequent sections. This could indicate some common features of leukemia-associated fusion proteins that could be exploited to generate more targeted therapies for these particular subtypes of AML.

3. Leukemia

The first description of a patient suffering from leukemia was published in 1811, noting the milky appearance of the serum and the treatment of the patient with blood-letting (69). Leukemia, literally meaning “white blood”, has since been identified as a heterogeneous cancer of the blood cells. Leukemia is not the only cancer of blood cells, however. Myeloma and lymphoma are the two other major types of blood cancer, arising from a more mature blood cell type compared to the HSC or progenitor cell type which is the cell of origin for leukemia. Other hematological disorders including myelodysplastic syndrome (MDS) or myeloproliferative neoplasms (MPN) are generally less aggressive but may transform to leukemia with additional mutations. Usually leukemia that develops is “primary” or “*de novo*”, meaning that it developed independently of other known conditions. However, in 10-20% of leukemia cases, it is “therapy-related” or “secondary”, and was caused by the treatment of a previous disease (70).

Leukemia is a clonal disorder, meaning that the highly proliferative leukemia blast cells can be traced back to founder cells, called leukemia stem cells (LSCs) or

leukemia-initiating cells (LICs) (71). Before a cell can cause leukemia, it must acquire multiple types of mutations: at least one mutation which blocks differentiation and at least one mutation which allows for uninhibited proliferation (72). A cell can acquire one of these mutations long before the other, remaining in a pre-leukemia-initiating state for years or decades (73). Once a patient has cancer, selective pressure leads to the outgrowth of a major clone over the course of the evolution of the disease (74,75). These leukemic cells are arrested at an immature stage and cannot perform the functions of normal blood cells. As the leukemic cells continue to multiply, they eventually crowd out the bone marrow and prevent the production of healthy, mature blood cells. Patients commonly die due to infection or bleeding, due to their lack of functioning immune cells and platelets (76).

Leukemia is divided into four major subtypes based on the maturation status and growth rate of the cells (chronic, acute) and the lineage of the transformed cell type (myeloid, lymphoid): acute lymphoblastic leukemia, acute myeloid leukemia, chronic myeloid leukemia (CML), and chronic lymphoblastic leukemia (CLL) (Figure 3A). While each type of leukemia can occur at any age, some are more commonly found in a specific population. For instance, the average age of diagnosis is 15 years for ALL and 68 years for AML (77).

3.A. Causes of leukemia

While pinpointing the exact cause of a patient's leukemia is often impossible, there are many genetic and environmental factors that can predispose one to its development. Lifestyle factors such as smoking or obesity and environmental factors such as ionizing radiation, benzene, and pesticide exposure correlate with leukemia development (78,79). Therapy-related leukemia is usually the result of exposure to radiation, alkylating agents or topoisomerase II inhibitors that were used to manage a

Figure 3. Subdivisions of leukemia and AML. (A) New cases of leukemia in the United States in 2016. Percentages of new cases of leukemia classified according to subtype. Abbreviations: Acute lymphoblastic leukemia (ALL), chronic lymphoblastic leukemia (CLL), acute myeloid leukemia (AML), chronic myeloid leukemia (CML). Data was retrieved from the National Cancer Institute Surveillance, Epidemiology, and End Results (SEER) program available online at seer.cancer.gov. **(B)** AML can be divided into subtypes based on cytogenetic abnormalities. Recurrent chromosomal abnormalities account for approximately half of *de novo* AML cases. Inv(16) and t(16;16) account for about 8-10% of total cases of AML. Adapted from Kayser S, Döhner K, Krauter J, Köhne C-H, Horst HA, Held G, et al. The impact of therapy-related acute myeloid leukemia (AML) on outcome in 2853 adult patients with newly diagnosed AML. Blood. 2011 Feb 17;117(7):2137–45.

A.

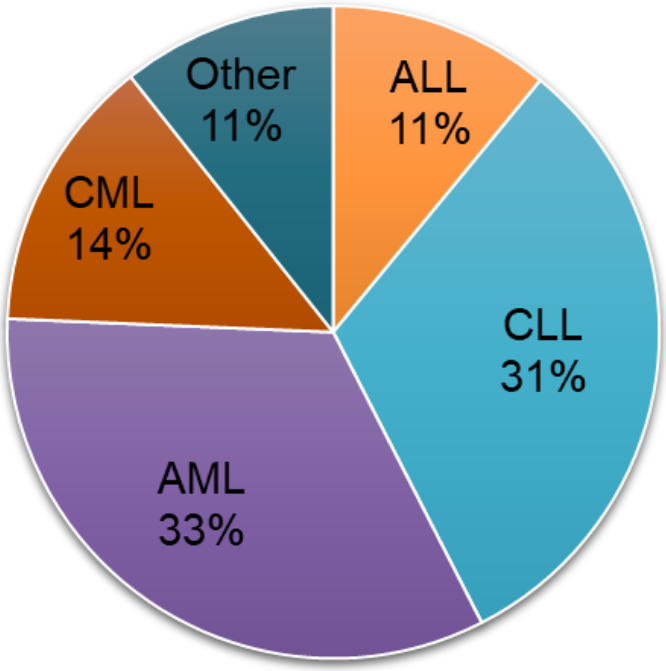
Other
11%
ALL
11%
CML
14%
CLL
31%
AML
33%

B.

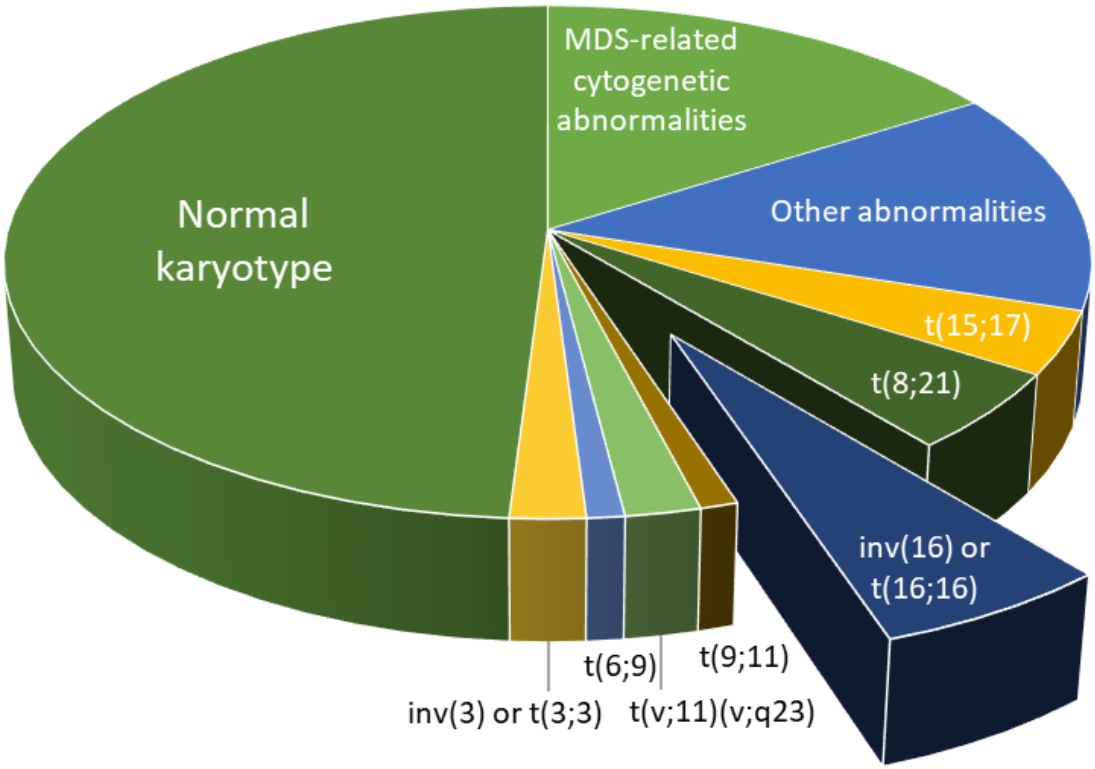
MDS-related
cytogenetic
abnormalities
Other abnormalities
Normal
karyotype
t(15;17)
t(8;21)
inv(16) or
t(16;16)
t(6;9)
t(9;11)
inv(3) or t(3;3)
t(v;11)(v;q23)

prior condition (80,81). Pre-existing hematopoietic disorders that disrupt proper blood formation such as certain types of anemia or myeloproliferative neoplasms can progress to leukemia. Like most cancers, age is a risk factor for developing leukemia, due to the acquisition of somatic mutations over a lifetime. There is no way to prevent leukemia but avoiding the lifestyle and environmental risk factors may decrease its likelihood of development.

3.B. Diagnosis

In the United States, leukemia is one of the top ten most common types of newly diagnosed cancer. Across all cancer types in adults, leukemias account for 3% of all new cancer cases in females and 4% in males (82). It accounts for a much larger percentage of childhood cancer, making up 29% of new diagnoses (82). In 2018, 60,300 new cases of leukemia were diagnosed in the United States. CLL and AML are the most common forms of leukemia, each accounting for about one-third of new leukemia cases (Figure 3A) (83). Patients usually present with symptoms of recurrent infection, abnormal bruising or bleeding, or more general fatigue, fever, or weight loss (84,85). Complete blood counts (CBC) and analysis of cellular morphology is used to confirm the presence of leukemia. Further cytogenetic analysis and genomic sequencing is used to characterize the specific type of leukemia present and other potentially targetable cooperating mutations (84,86). Previously, the presence of at least 20% leukemic cells, or blasts, was required for an official diagnosis. However the presence of specific leukemia-associated mutations can result in a diagnosis with a lower blast count (87).

3.C. Survival statistics

Deaths from leukemia account for 4% of all cancer related deaths in adults in the United States, with 24,370 reported deaths from leukemia in 2018 (82). There are major

disparities among the survival rates between the subtypes of leukemia and between ages at diagnosis. The chronic leukemias have the highest five-year survival rates, with CML at 68.0% and CLL at 86.2%. The acute leukemias are more deadly, with a five-year survival of 71.0% for ALL, and remarkably lower rate of survival for AML at 27.4% alive at five years after diagnosis (82). Children under 15 years old diagnosed with ALL or AML experience much higher five-year survival, at 91.8% and 66.4%, respectively (82). Explanations for this age-related survival outcome include the ability of children to undergo and recover from harsher treatment regimens as well as an increase in high-risk mutations in older patients (88,89). Overall, outcomes for leukemia patients have drastically improved since the 1970's, attributable in part to refinements in dosing schedules, advances in diagnostics and targeted treatments (77,88). However, outcomes specifically for patients over 60 years of age have not seen large improvements over the same period of time due in part to their inability to tolerate high dose chemotherapy regimens (88).

3.D. Treatment

Treatments for leukemia vary based on subtype, mutations present, age, and comorbidities present at diagnosis. As screening for common recurrent mutations becomes easier, it allows for more targeted therapy for each individual case. For chronic leukemias, intensive therapies are less common. CLL patients are often monitored without treatment upon diagnosis, while tyrosine kinase inhibitors are employed in the case of Philadelphia chromosome-positive CML (87). Acute leukemias can progress rapidly and therefore usually require immediate intensive treatment. Intensive chemotherapy is utilized, sometimes accompanied by allogenic transplantation (84). Many subtypes benefit from the addition of a hypomethylating agent to the chemotherapy regimen or as a replacement of chemotherapy altogether in patients

unable to undergo intensive chemotherapy (90,91). Other epigenetic therapies, kinase inhibitors, T cell therapies, or monoclonal antibodies are being investigated as potential treatments in clinical trials (70,87). There is clearly a need for acute leukemia treatments that can compliment or replace chemotherapy in patients who cannot handle the toxicity of conventional treatment, and this will be a main focus of our study.

While initial treatment is often successful, it is common for leukemia patients to experience relapse. In AML, although 40-65% of patients achieve remission, 85% of patients will relapse within 3 years (70). Often upon recurrence of disease the patient is resistant to the initial treatment. This is likely due to LSCs escaping the initial therapy and acquiring new mutations due to selective pressure during treatment (92). Treatment for relapse, such as allogenic stem cell transplant, remains largely ineffective with a three-year survival of under 20% after transplant in acute leukemia patients (93). Thus, reducing the occurrence of relapse is a major obstacle facing scientists and clinicians in further improving the overall survival of leukemia patients. Because of the role of LSCs in relapse, our study includes *in vitro* and *in vivo* investigations into the activity of LSCs after drug treatment in an effort to address whether we can inhibit the occurrence of relapse.

4. Inversion 16 AML and the *CBFB-MYH11* fusion

4.A. Mutational landscape of AML

AML is a heterogeneous disease, broadly categorized as cytogenetically normal or abnormal. Approximately 40-50% of patients have cytogenetically normal AML (Figure 3B) (94). This is a diverse group of patients that have recurring molecular mutations in *FLT3*, *NPM1*, *IDH1/IDH2*, and many other genes. The remainder of patients fall into the cytogenetically abnormal category, where nonrandom and recurrent chromosomal

abnormalities are important indicators of risk and outcome. Over 300 different chromosomal translocations or inversions have been identified in AML patients (95). The most prevalent are mutations in core binding factor genes. Over one dozen AML gene rearrangements involve *RUNX1* or *CBFB*, including t(8;21)(q22;q22) and inv(16)(p13;q22) which encode the fusion genes *RUNX1-RUNX1T1* and *CBFB-MYH11*, respectively. *RUNX1-RUNX1T1* is the most common mutation in adult AML, present in about 12% of cases (66). Second most common is *CBFB-MYH11,* which is present in about 8-10% of total AML cases (Figure 3B) (2–4). *CBFB-MYH11* is the mutation found in patients with inversion 16 [inv(16)] AML.

4.B. *CBFB-MYH11* gene fusion

Inv(16)(p13;q22) is the result of DNA breaks occurring within the introns of the genes *CBFB* (16q22) and *MYH11* (16p13) and a subsequent pericentric inversion. The chromosome is reattached in-frame which results in the fusion gene *CBFB-MYH11* (1) (Figure 4). The reciprocal fusion gene product of *MYH11-CBFB* is not detected in cells (96).

4.B.i. Translocation of chromosome 16

Inversion 16 is not the only mutation to cause the fusion of *CBFB* to *MYH11*. A related translocation, t(16;16)(p13;q22), results from breaks in both chromosomes occurring at the same sites as in inv(16) AML (97). This translocation results in an identical *CBFB-MYH11* fusion gene and indistinguishable clinical characteristics (96,98,99). Consequently, the t(16;16) patients are usually combined with inv(16) AML patients for research and clinical purposes. The t(16;16) mutation is much rarer than inv(16) and is estimated to make up less than 10% of core binding factor AMLs and less than 1% of total AML patients (99,100).

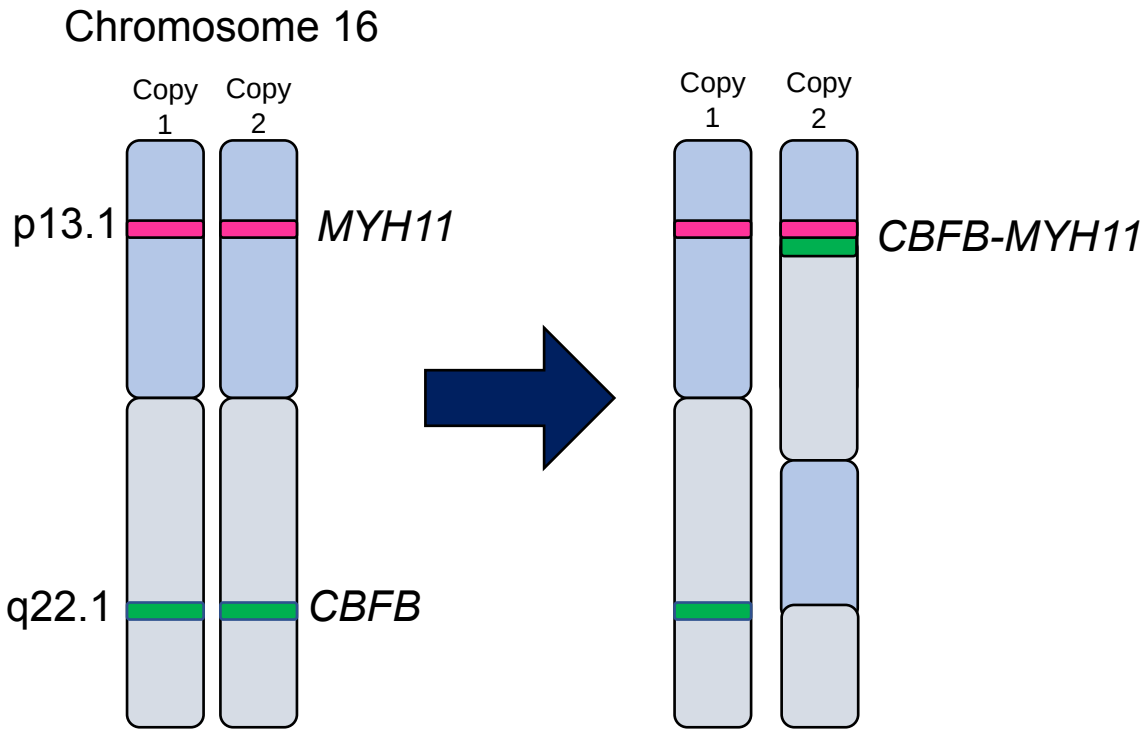

Figure 4. Inversion of chromosome 16 leads to the *CBFB-MYH11* gene fusion. In inv(16) AML patients, one copy of chromosome 16 is mutated after double stranded breaks occur between the *MYH11* and *CBFB* genes. The chromosome is inverted and rejoined which results in the fusion of *CBFB* to *MYH11.* The other copy retains the normal *CBFB* allele.

4.B.ii. Variants of *CBFB-MYH11*

Several different variants of *CBFB-MYH11* have been described in patients. To date, 11 different *CBFB-MYH11* transcripts have been detected, named A-K (95,96,101). Type A is by far the most common, present in 80-85% of patients (95,96,102,103). Type A contains the first 495 nucleotides of *CBFB* which account for the first five exons, fused to *MYH11* nucleotides 1,921-3,259 for a combined total length of 611 amino acids. The other variants have different starting or ending nucleotides in the *MYH11* region, contain less nucleotides of *CBFB*, or a combination. Type D and type E are the second most common, each accounting for about 5% of cases, while the remainder of *CBFB-MYH11* variants are extremely rare (102). Non-type A mutations are more common in therapy-related inv(16) AML (9). Little is known about the clinical relevance of different *CBFB-MYH11* variants, although one report has demonstrated unique gene expression profiles and secondary mutations associated with non-type A variants (102), suggesting that there might be differences in the disease characteristics of different variants. The experiments discussed in this dissertation have all been conducted using the type A variant of *CBFB-MYH11*.

4.B.iii. Breakpoints

Because *CBFB-MYH11* is a common recurring mutation in AML, there has been interest in determining what features of the genome result in the common breakpoints around these genes. Type A *CBFB-MYH11* rearrangements result from breakpoints in a 15 kb intron located between exons 5 and 6 of *CBFB* which contains many repetitive elements. Additionally, breakpoints in *MYH11* are located in intron 30, a 370 bp intron with no repetitive elements but which did have a V(D)J recombinase signal sequence (104). Because the spatial proximity of genes in the nucleus has been important in other

cases of chromosomal translocations, the proximity of *CBFB* to *MYH11* in hematopoietic stem cells was investigated. Interestingly, the genes were located closer together in hematopoietic stem cells compared to mesenchymal stem cells, peripheral blood lymphocytes, or fibroblasts. Additionally, *CBFB* was located closer to *MYH11* than a control gene that was located closer in terms of number of base pairs of separation (105). Although there is no single definitive answer for why *CBFB* and *MYH11* so often break and reattach together, these studies provide possible explanations for its frequency.

4.C. CBFβ-SMMHC functional domains

The protein product of the fusion gene *CBFB-MYH11* is CBFβ-SMMHC. Several functional domains exist within CBFβ-SMMHC and are critical for the activity of the fusion protein. The CBFβ portion of the fusion retains its binding domain for RUNX1, its normal heterodimeric transcription factor partner (17). The SMMHC portion contains a coiled-coil multimerization domain, a second RUNX1 binding site, and a repression domain (Figure 5,6) (106–109).

4.C.i. High-affinity binding domain

The SMMHC portion of CBFβ-SMMHC contains one functional region that is located proximal to CBFβ, the high-affinity binding domain (HABD), comprising amino acids 179-221. The HABD region binds to RUNX1, which along with the CBFβ site gives the fusion protein two sites for RUNX1 binding and the ability to outcompete wild-type CBFβ for RUNX1 binding (Figure 6) (106).

However, one rare fusion variant found in patients omits this region of CBFβ-SMMHC (110), indicating that it is not a required region for leukemogenesis. Indeed,

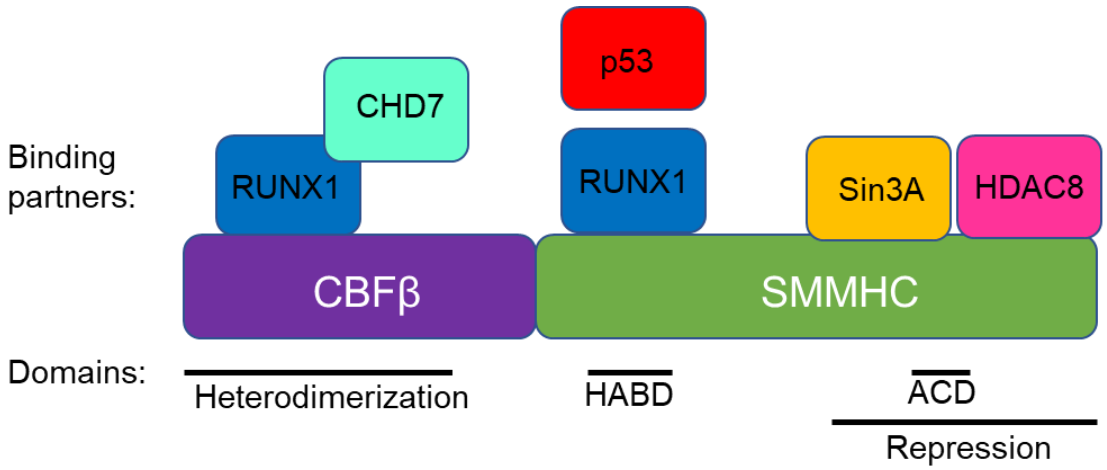

Figure 5. Domains of CBFβ-SMMHC and approximate locations of binding partner interactions. Model of the CBFβ-SMMHC protein domains and the approximate locations of binding for protein-protein interactions. CHD7 requires RUNX1 for interaction with CBFβ-SMMHC. p53 binds in the HABD region but it is not known if it binds through RUNX1. HDAC8 binds to the C-terminal 95 amino acids. Sin3A binds in the repression domain and is not required for HDAC8 binding. Abbreviations: high-affinity binding domain (HABD), assembly competence domain (ACD).

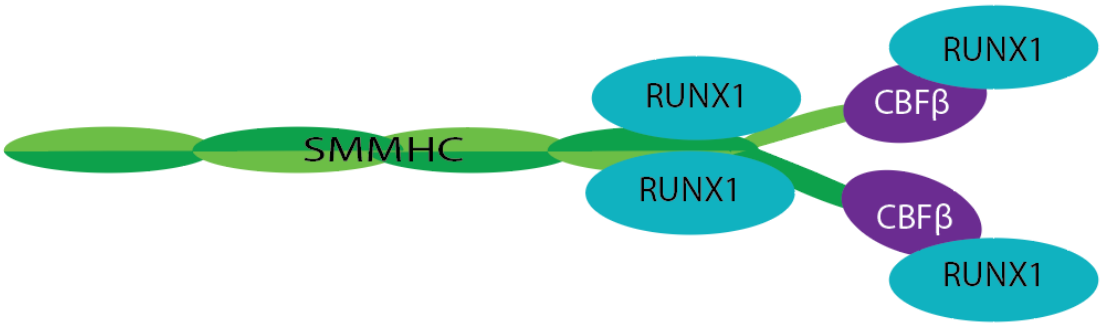

Figure 6. Model of CBFβ-SMMHC:RUNX1 protein complex. RUNX1 binds to two sites of CBFβ-SMMHC, one in the CBFβ region and one in the HABD of the SMMHC tail. The multimerization domain in SMMHC facilitates dimerization, resulting in a protein complex resembling the one modeled above.

eliminating the high-affinity binding domain in mice actually resulted in accelerated leukemogenesis even though it partially rescued RUNX1 and CBFβ activity (111).

4.C.ii. Multimerization or assembly competence domain

The assembly competence domain (ACD), or multimerization domain, is a short region in the C-terminus of CBFβ-SMMHC that is required for self-dimerization (108). Dimerization is important for CBFβ-SMMHC localization to the nucleus and for its leukemogenic activity (108). Expression of CBFβ-SMMHC in normal human or mouse myeloid progenitors causes a decrease in proliferation, a defect which is rescued when the ACD is removed (112). In addition, mice transplanted with CBFβ-SMMHC$^+$ leukemia with ACD deletion do not develop leukemia within the same time frame as mice with full-length CBFβ-SMMHC$^+$ leukemia due to an inability of ACD mutant mice to arrest myeloid development (113). Mice which were designed with specific point mutations to disrupt the multimerization domain without deleting any other regions do not develop leukemia even when treated with a mutagen, further emphasizing the importance of this domain in leukemia development (114).

4.C.iii. Repression domain

The repression domain is a large region of the C-terminus of CBFβ-SMMHC spanning amino acids 449-611, roughly one-third of the total SMMHC portion (115). This region includes the ACD, but is considered a distinct region because of the binding of multiple corepressors within this region. The repression domain was first identified through *in vitro* promoter assays in which CBFβ-SMMHC repressed transcription of RUNX1 target genes. However, a deletion of 95 amino acids from the end of CBFβ-SMMHC resulted in a rescue of the repression, and so it was concluded that this region was part of a repression domain (107). A knock-in mouse model with this deletion

(*Cbfb*$^{+/MYH11\Delta C95}$) rescued the defects in primitive and definitive hematopoiesis seen in *Cbfb*$^{+/MYH11}$ mice and prevented the onset of leukemia, demonstrating its requirement for the activity of CBFβ-SMMHC in inv(16) AML (116) .

The repression domain is also required for interaction with Sin3A and HDAC8, proteins involved in the recruitment of repressor complexes or gene repression, respectively (12,115). This implies that other proteins can be recruited to CBFβ-SMMHC to mediate its activity, and that they are potential drug targets.

4.D. CBFβ-SMMHC:RUNX1 activity

Based on *in vitro* work, it was proposed that CBFβ-SMMHC dominantly suppresses the function of the RUNX1:CBFβ dimer. CBFβ-SMMHC stabilizes RUNX1 to a greater extent and has a higher affinity for RUNX1 than does CBFβ (31,117), providing a mechanism for the dominant suppression activity. Overexpression of CBFβ-SMMHC resulted in sequestration of RUNX1 to the cytoplasm of cells, where CBFβ-SMMHC was associated with actin filaments, supporting a dominant negative model of activity (39). In support of this, mice homozygous for a null allele of either *Cbfb* (*Cbfb*$^{-/-}$) or *Runx1* (*Runx1*$^{-/-}$) exhibit embryonic lethality, a block in definitive hematopoiesis, and central nervous system hemorrhaging that is indistinguishable from that in mice heterozygous for a knock-in *Cbfb-MYH11* allele (*Cbfb*$^{+/MYH11}$)) (28,41,118).

However, immunohistochemistry in inv(16) patient samples demonstrates that at endogenous levels, CBFβ-SMMHC is localized to the nucleus and not sequestered in the cytoplasm (119). Furthermore, if a dominant repressor model fully described the fusion protein's activity, one would predict that loss of *RUNX1* would be equivalent to expression of the fusion protein. However, knock-in mice expressing *Cbfb-MYH11* from the endogenous *Cbfb* locus (*Cbfb*$^{+/MYH11}$) have defects in primitive hematopoiesis, a

phenotype that is not observed in *Cbfb*$^{-/-}$ or *Runx1*$^{-/-}$ embryos (120). In addition, the *Cbfb*$^{+/MYH11}$ animals have a more severe block in hematopoietic differentiation and show deregulated expression of a unique set of genes as compared *Runx1*$^{-/-}$ or *Cbfb*$^{-/-}$ mice (120). Microarray data showed *Cbfb*$^{+/MYH11}$ embryos have 658 genes differentially expressed compared to wild-type littermates, while *Cbfb*$^{-/-}$ embryos had only 174 changed genes (120). Finally, humans with homozygous deletion of RUNX1 have a more immature AML subtype with poor prognosis (121), a different clinical presentation than inv(16) patients. This data suggests that CBFβ-SMMHC has unique activities in addition to suppression of core binding factor's normal activity.

A more complete model for CBFβ-SMMHC activity may include activity as a transactivator. Chromatin immunoprecipitation studies demonstrated that CBFβ-SMMHC colocalizes with Histone H3 acetylation and RNA Polymerase II, markers of actively transcribed genes (14). In addition, chromatin immunoprecipitation (ChIP) and RNA-seq in a CBFβ-SMMHC inducible-expression cell line revealed that of genes two-fold or more altered by CBFβ-SMMHC expression, two-thirds were upregulated (14). The majority of genes were also upregulated in *Cbfb*$^{+/MYH11}$ embryos compared to *Cbfb*$^{+/+}$ (120). Together these studies provide convincing evidence that a model describing CBFβ-SMMHC activity must include CBFβ and RUNX1 repression-independent activities.

Nevertheless, RUNX1 is required for inv(16) leukemia. Mice expressing *Cbfb-MYH11*, but with significantly reduced RUNX1 activity, have impaired *Cbfb-MYH11*-induced changes in gene expression and myeloid differentiation (18). In addition, RUNX1 knockdown in CBFβ-SMMHC^{+} mouse leukemia (122) or ME-1 cells, an inv(16) patient-derived cell line, (123) resulted in an increase in apoptosis. An inhibitor of RUNX1, Ro5-3335, decreases viability of ME-1 cells in a dose-dependent fashion, reduces viability and colony-forming ability of lineage-depleted (Lin^{-}) CBFβ-SMMHC^{+}

mouse leukemia cells *in vitro*, and decreases leukemic burden and extends survival in CBFβ-SMMHC^{+} leukemic mice treated with the drug *in vivo* (11). Additionally, RUNX1-inactivtaing mutations are never found in patients with inv(16) AML (124,125), further supporting the requirement for RUNX1 in inv(16) AML pathogenesis.

4.E. Binding partners of CBFβ-SMMHC

The fusion protein CBFβ-SMMHC does not operate in isolation but exerts its leukemogenic function through collaboration with other proteins. RUNX1 is a major player as discussed in the preceding sections, but other proteins are recruiting and are being recruited by CBFβ-SMMHC. Mass spectrometry and ChiP-Seq analysis revealed a host of general transcription factors and hematopoietic transcription factors are either binding to CBFβ-SMMHC or are in close proximity to CBFβ-SMMHC on gene promoters (14). Future research is required to determine the significance of these factors in the pathogenesis of inv(16) AML. Some of the proteins recruited to the CBFβ-SMMHC: RUNX1 complex are epigenetic regulators, which are directly regulating the fusion protein's activity and represent potential therapeutic targets, such as Sin3A, HDAC8, and CHD7 which are further discussed below (Figure 5).

4.E.i. Sin3A

Sin3A is found as part of large corepressor complexes, one of which is the Sin3/HDAC complex, a homologue of yeast Rpd3S complex (126). Sin3A does not contain any DNA-binding or enzymatic activity itself, but it can bind to many proteins at once, recruiting HDACs to transcription factors (127). Sin3A was identified as a binding partner of CBFβ-SMMHC that does not require RUNX1 to mediate the interaction (107,115). It binds through the corepressor domain of CBFβ-SMMHC, implying that

Sin3A or proteins it recruits to CBFβ-SMMHC could be critical for its transcriptional repression activities (115).

4.E.ii. HDAC8

Histone deacetylase 8 (HDAC8) is a member of the Class I histone deacetylase family in addition to HDAC1, HDAC2, and HDAC3. HDAC8 binds to CBFβ-SMMHC in the repression domain but does not bind through Sin3A, consistent with HDAC8 not being recruited into corepressor complexes (115). CBFβ-SMMHC also binds to p53 and brings HDAC8 and p53 together, where HDAC8 promotes the transformation of CBFβ-SMMHC^{+} leukemia stem cells by deacetylating p53 (12). Specific inhibition of HDAC8 prevents p53 deacetylation resulting in its activation. Inhibitor treatment prevents leukemia initiation in CBFβ-SMMHC^{+} cells and causes apoptosis in transformed leukemia cells (12).

4.E.iii. CHD7

Chromodomain Helicase DNA Binding Protein 7 (CHD7) is an ATP-dependent chromatin remodeler. CHD7 interacts with the RUNX1:CBFβ-SMMHC complex through RUNX1. Genetic depletion of CHD7 in conditional CBFβ-SMMHC-expressing mice (*Chd7*$^{f/f}$*, Mx1-Cre, Cbfb*$^{+/56M}$) results in a delay in leukemia development by slowing the expansion of leukemia progenitor populations compared to CBFβ-SMMHC-expressing mice with CHD7 (128). CHD7 also interacts with the RUNX1:CBFβ complex (128), so it is not a specific target to inhibit CBFβ-SMMHC activity. However, it demonstrates that RUNX1 interacting partners may also have important activities in inv(16) AML. Overall, it is evident that one of the functions of CBFβ-SMMHC is in acting as a protein complex scaffold and that this activity is part of the molecular pathology of inv(16) AML.

4.F. Secondary mutations in Inv(16) AML

A common feature of leukemia is the requirement for a minimum of one mutation that blocks differentiation and one mutation that induces uncontrolled proliferation, called the two-hit hypothesis of leukemia development (129). Accordingly, the expression of the *CBFB-MYH11* fusion gene and CBFβ-SMMHC fusion protein is not sufficient for leukemia (130). Cells which harbor *CBFB-MYH11* without additional cooperating mutations are in a pre-leukemic state (131). However, when cooperating mutations are acquired which induce uncontrolled proliferation, the cells can progress to frank leukemia. Inv(16) cells often harbor coexisting chromosome mutations and always harbor at least one mutation in a gene which causes unchecked proliferation (132).

4.F.i. Secondary mutations in genes

In inv(16) AML patients, 80-90% have identifiable secondary mutations in genes and many of these genes are involved in known proliferation or survival pathways (133,134). An analysis of 176 inv(16) AML patients quantified the mutation status of known co-occuring mutations. They determined the most common gene mutations were in *NRAS* (45%), *KIT* (37%), *FLT3* (17%), and *KRAS* (13%) (133), and other studies corroborated these findings (134,135). Overall, 53% of patients had mutations in *RAS* genes, with some patients harboring both *NRAS* and *KRAS* mutations. The landscape of secondary gene mutations was not different between *de novo* and therapy-related inv(16) AML patients (133). The prognostic relevance of each mutation is not yet clear, and study designs have led to contradictory results in many cases. However, *FLT3* and *KIT* mutations may have an adverse effect on patient outcomes overall (133,135,136).

While the presence of cooperating mutations in patients implies that they are necessary for leukemia development, studies in mice prove that they are required.

CBFB-MYH11 itself is not sufficient for frank leukemia development in mice. *Cbfb*$^{+/MYH11}$ mice do not develop leukemia within one year, but injection with the mutagen N-ethyl-N-nitrosourea (ENU) (130) or disruption of genes through retroviral insertional mutagenesis (137) induces leukemia within months after injection. Leukemia in mice can also be accelerated by specifically introducing a secondary gene mutation in a gene regulating survival and/or proliferation pathways, such as *KIT* (138) or *Nras* (139). Importantly, these mouse models allow the study of clinically relevant inv(16) cooperating mutations and should help to uncover unique molecular pathways and therapeutic targets for specific mutations.

4.F.ii. Co-occurring chromosomal aberrations

Co-occurrence of additional chromosomal aberrations occurs in 35-40% of inv(16) AML cases (133). The most common mutations are trisomy 22, trisomy 8, 7q deletion, and trisomy 21 (133,134,140). In therapy-related inv(16) AML patients, the prevalent mutations and their frequency are similar to *de novo* patients (141). The presence of additional chromosomal abnormalities in general have positive prognostic implications (7,142), although the sample sizes in these studies are small. Overall, the additional mutations found in inv(16) AML patients reveal that there is vast heterogeneity even within this particular AML subtype. The collection of mutations within a single patient may be tremendously important in determining response to treatment, but the lack of research into the molecular pathways that are involved is a major gap in the field which needs to be addressed.

4.G. Clinical features of Inv(16) AML

Almost all inv(16) AML patients are associated with a distinct clinical subtype of AML, formerly French-American-British subtype M4Eo, characterized by large numbers

of dysplastic eosinophils in the bone marrow (9). Inv(16) AML can present in patients of any age, but is more common in adults with a median age of 40-50 years (2,6,9). A definitive diagnosis of inv(16) AML can be accomplished using cytogenetic analysis with fluorescent *in situ* hybridization (FISH) or with quantitative real-time polymerase chain reaction (qRT-PCR) which is more sensitive and can determine the precise variant of *CBFB-MYH11* that is present (143).

The current standard treatment for inv(16) AML was developed in the 1960's and has changed very little in ensuing decades (143,144). It is composed of high dose cytarabine combined with an anthracycline (doxorubicin, daunorubicin, idarubicin). Usually this takes place in a "7+3" dosing schedule, with cytarabine given for 7 days and the anthracycline given in combination for the first 3 days. This induction therapy regimen results in 90% complete remission (CR) rate (5,6). Induction therapy is ideally followed by consolidation therapy with high-dose cytarabine for 3-4 cycles, although the toxicity may not be tolerated in older patients (5,9). Due to the high success rate using high-dose cytarabine in achieving CR, hematopoietic stem cell transplant is not usually considered in first complete remission, and in fact has no significant benefit at first remission (145). However, it can be useful for relapsed or high risk patients (143).

AML subtypes are broadly classified as favorable, intermediate, or unfavorable based on their cytogenetic risk category. Due to the low survival rates found in AML as a whole, the inv(16) subtype is classified as a favorable prognosis mutation with a 50-60% 5-year overall survival rate (2,7,8). However, the relapse-free survival is estimated to be less than 50% (8,10). Relapse in inv(16) AML patients after first complete remission occurs within an average of 10 months (146). Overall survival three years after relapse is about 60% (146). Because inv(16) AML patients have distinct clinical features compared

to other subtypes of AML, it is important to understand the activity of the underlying CBFβ-SMMHC mutation in order to improve survival.

5. Histone acetyltransferases and histone deacetylases

The mutations which cause leukemia affect secondary pathways, such as epigenetic control. Commonly, epigenetic regulation is hijacked to allow for the gene expression changes which result in the leukemic phenotype. Many types of leukemia alter chromatin dynamics by recruiting epigenetic factors and this feature can be targeted therapeutically to disrupt the block in differentiation (147,148). In inv(16) AML, the misregulation of acetyltransferases and deacetylases is of particular interest and may represent a mechanism that can be targeted therapeutically.

5.A. Acetylation

Acetylation is a protein modification in which an acetyl moiety is transferred from acetyl-CoA onto an amino acid residue of a protein. There are two types of protein acetylation: N-terminal acetylation (N^{α}-acetylation) and acetylation of the ε-amino group of a lysine residue. N-terminal acetylation is less understood, but surprisingly common, occurring in 80-85% of eukaryotic proteins (149–151). Here, the addition of an acetyl group to the first amino acid of a protein is catalyzed by an N-terminal acetyltransferase (NAT) and is an irreversible modification. The functional importance of this modification is only beginning to emerge, but is suggested to effect the protein half-life, mediate protein interactions, and determine subcellular localization (150). Acetylation of the ε-amino group of a lysine residue is a reversible post-translational modification which is an evolutionarily conserved process (151). In this case, the enzyme responsible for transferring the acetyl group onto a protein is a histone acetyltransferase while a histone deacetylase catalyzes the removal of the acetyl group (Figure 7). HATs and HDACs are

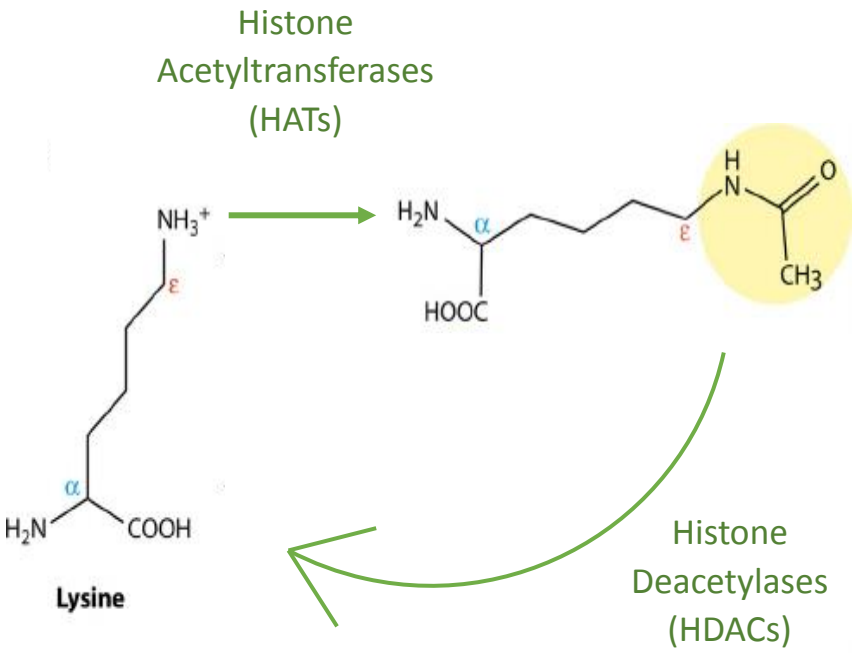

Figure 7. Protein acetylation and deacetylation. A lysine side chain is acetylated by the enzymatic activity of histone acetyltransferases and deacetylated by histone deacetylases. Adapted from: Hentchel KL, Escalante-Semerena JC. Acylation of Biomolecules in Prokaryotes: a Widespread Strategy for the Control of Biological Function and Metabolic Stress. Microbiol Mol Biol Rev. 2015;79(3):321–46.

regulators of the highly dynamic process of acetylation and deacetylation both on histones and on non-histone proteins.

In the 1960's, histones were the first protein to be identified as acetylated, resulting in the name histone acetyltransferase/deacetylase (152). The acetylation of lysine residues on the N-terminal histone tails leads to an open chromatin structure that is accessible to transcriptional machinery and cofactors, while deacetylation of histone tails leads to a transcriptionally repressed state (Figure 8) (153,154). This is due to the positive charge of lysine which is masked by the addition of an acetyl group (155,156). The acetyl group may also serve to recruit proteins which contain bromodomains, which can regulate gene expression by "reading" the acetyl group and assembling transcription-regulating protein complexes (157). Additionally, transient acetylation of histones after they are synthesized is crucial for their localization and deposition onto chromatin (151).

While this modification of histones has widespread implications for gene expression regulation, it is clear that the acetylation status of other proteins is also essential in many cellular processes and a true picture of the "acetylome" of a cell is now emerging. The first non-histone protein to be identified as acetylated was the tumor suppressor and cell cycle regulator p53, followed by members of the basal transcriptional machinery (158,159). In rodents, over 15,000 acetylation modifications on 4,500 proteins were identified (160). Because of the numerous proteins regulated by HATs and HDACs, some scientists refer to these proteins as lysine acetyltransferases (KATs) or lysine deacetylases (KDACs), although the traditional nomenclature is more widely used (161).

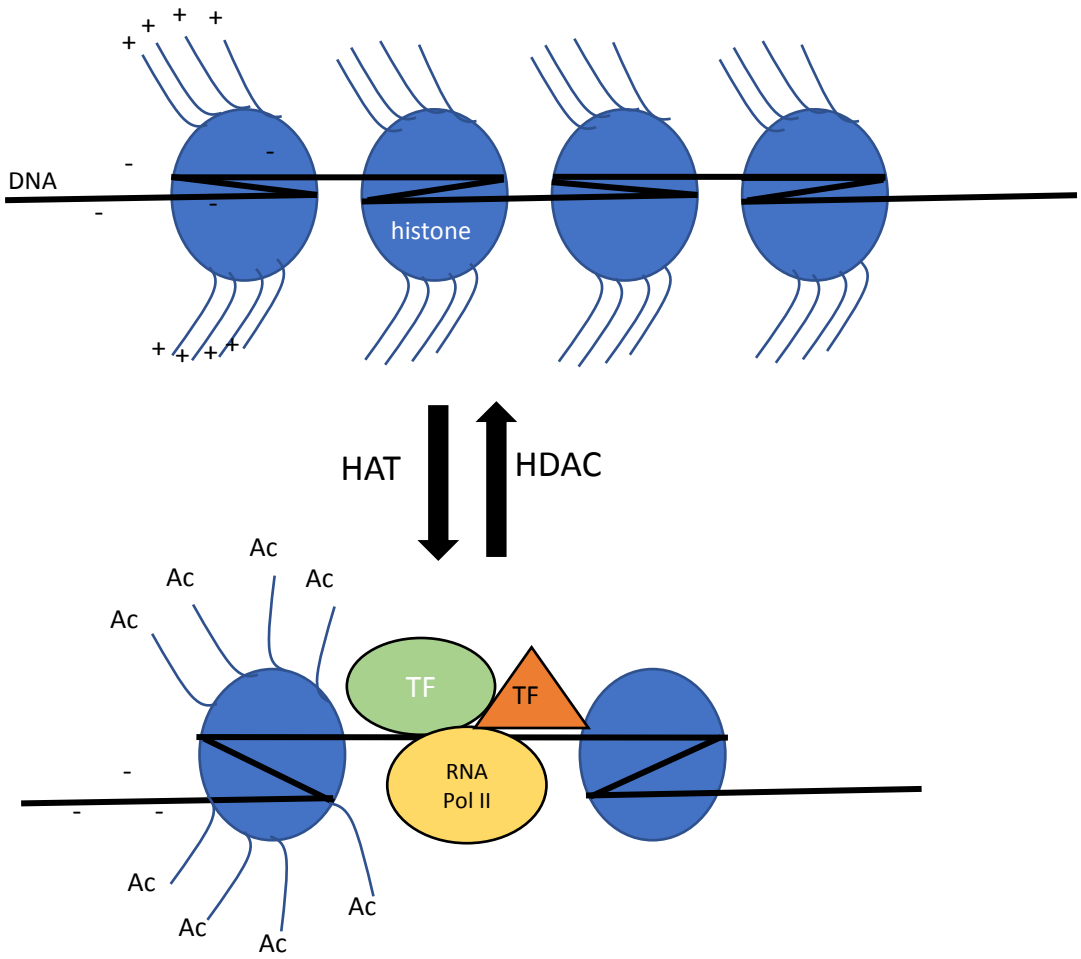

Figure 8. Canonical view of histone acetylation and deacetylation. Acetylation by histone acetyltransferases (HATs) results in more open chromatin structure allowing for transcription factor (TF) and RNA Polymerase II (RNA Pol II) binding to activate gene expression. Histone deacetylation by histone deacetylases (HDACs) results in more closed chromatin structure due to attraction in charges between positive lysine residues and negative DNA.

5.B. Non-canonical activities of HATs and HDACs

HAT and HDAC activities must remain in strict equilibrium. Any deviation from a normal balance of acetylation and deacetylation due to genetic or environmental factors can contribute to disease development. Rather than operating independently of each other to facilitate gene transcription or repression, studies have suggested that there is an interplay between HATs and HDACs that helps maintain that balance. Observations that histone acetylation and deacetylation can have a half-life as short as 7 minutes in certain regions of actively transcribed chromatin established the likelihood of the colocalization of HATs and HDACs (162). Co-immunoprecipitation and FRET analysis indicated that class I HDACs physically interact with HATs in the nucleus of HeLa cells and that HATs are recruited to HDAC complexes (163). ChIP-Seq analysis of the genome-wide binding patterns of HATs and HDACs surprisingly revealed that both are present at the sites of most active genes but few repressed genes, and HDACs are present at the promoter regions to remove the acetyl groups placed by HATs at active genes (164). These observations suggest that the role of HDACs as transcriptional repressors is only a partial view of their activity, and HDACs can also be required for gene activation.

In addition to the hypothesis that turnover of acetylation and deaceylation of histones is required for gene activation and elongation, several other mechanisms have been proposed to explain the possible role for HDACs in gene activation. A certain combination of acetylation and deacetylation at specific lysines on histones may be required to recruit different transcription factors. Analysis of global acetylation patterns in yeast using DNA microarrays show that histone H3K9/18/27 hyperacetylation and hypoacetylation at H4K16 and H2BK11/16 is correlated with transcriptional activity (165). It is possible that HDACs are responsible for eliminating steric hindrance caused by

acetylated residues to allow for DNA binding by transcription factors (166). HDACs can also influence gene expression through the deacetylation of transcription factors and other gene regulatory factors (149). While it is likely that HDACs influence the recruitment of the basal transcriptional machinery to many genes through deacetylation of specific proteins, the mechanism has not yet been elucidated. HDACs also act downstream of signaling pathways to regulate gene expression, and studies using HDACi have demonstrated that they are required for the proper activation of those responsive genes (166). From these observations, it is clear that HDACs have activities beyond the deacetylation of core histone proteins and are actually required for both activation and repression of transcription.

5.C. Histone acetyltransferases (HATs)

Histone acetyltransferases are responsible for catalyzing the removal of the acetyl group from acetyl-CoA and attachment onto select lysine residues of proteins. When a HAT adds this modification to lysines on N-terminal histone tails, the classical result is the activation of gene expression. There are 22 human proteins that possess HAT activity, and these HATs are grouped into three major families: GNAT, MYST, and p300/CBP (151). HATs generally function as part of multiprotein complexes, the components of which help dictate the activity, localization, and substrate specificity of the HAT (167). The balance of acetylation is maintained in cells through the activity of the enzyme that oppose the activity of HATs, histone deacetylases.

5.D. Histone deacetylases (HDACs)

Histone deacetylases catalyze the removal of the acetyl moiety from the ε-amino group of a lysine residue on a protein, unmasking the positive charge of the lysine residue. When HDACs deacetylate the N-terminus of histone proteins it results in a

tighter connection between histones and DNA, leading to the classical definition of HDACs as transcriptional repressors. There are 18 individual HDACs in humans, which are further classified into four families based on their homology to yeast counterparts: class I, class II, class III and class IV (149,151). Class III, otherwise known as the sirtuins, are comprised of seven different human enzymes (SIRT1-7) which are NAD^+-dependent for their enzymatic activity (151). Class I, II, and IV are comprised of eleven enzymes (HDAC1-11) which are zinc-dependent (Figure 9).

5.D.i. Class I HDACs

Class I HDACs (HDAC1, HDAC2, HDAC3, HDAC8) are ubiquitously expressed in tissues and mostly localized to the nucleus. Class I HDACs have one deacetylase domain with high homology within the group to the yeast deacetylase Rpd3 (168). Each member will be discussed in greater detail below.

5.D.i.a. HDAC1

Histone deacetylase 1 (HDAC1) was first identified in 1996 and originally named “HD1” (169). Its mRNA expression is ubiquitous in all tissues (170,171). While the mRNA expression of HDAC1 does not change during progression through the cell cycle, protein expression is linked to the cell cycle, with low expression in G_0 and an increase in G_1/S (170). HDAC1 in mouse and humans is 482 amino acids in length (169,170) with several important domains (outlined in Figure 10) (172–174). HDAC1 has deacetylase activity against all core histones when purified or when immunoprecipitated to retain its native complex (174). However, recombinant isolated protein has much lower deacetylase activity than endogenous complexes implying a requirement for cofactors for its full activity (175).

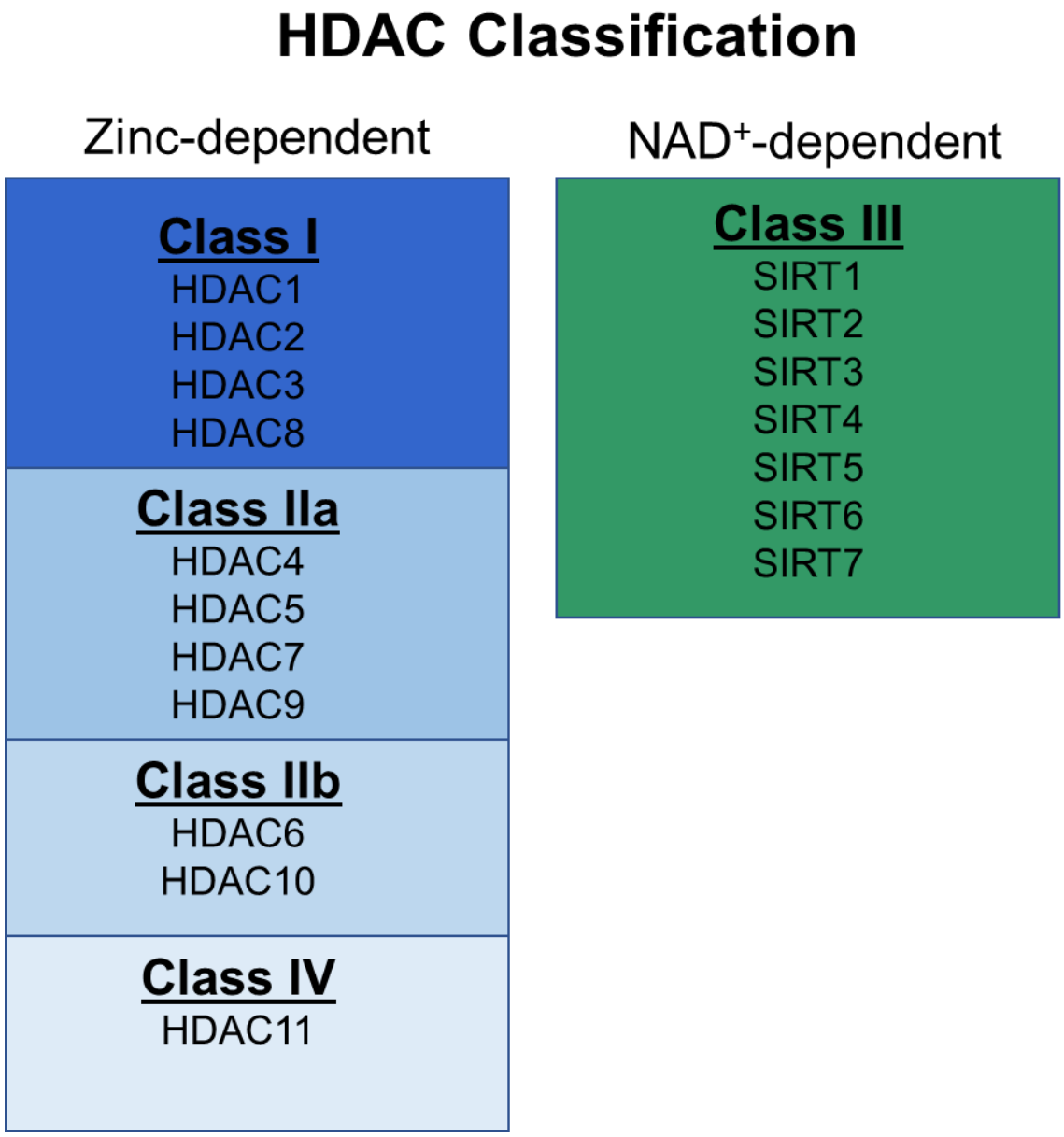

Figure 9. Histone deacetylase (HDAC) classification. HDACs are broadly classified as zinc or NAD^+ dependent and are further sub-divided based on homology to yeast counterparts.

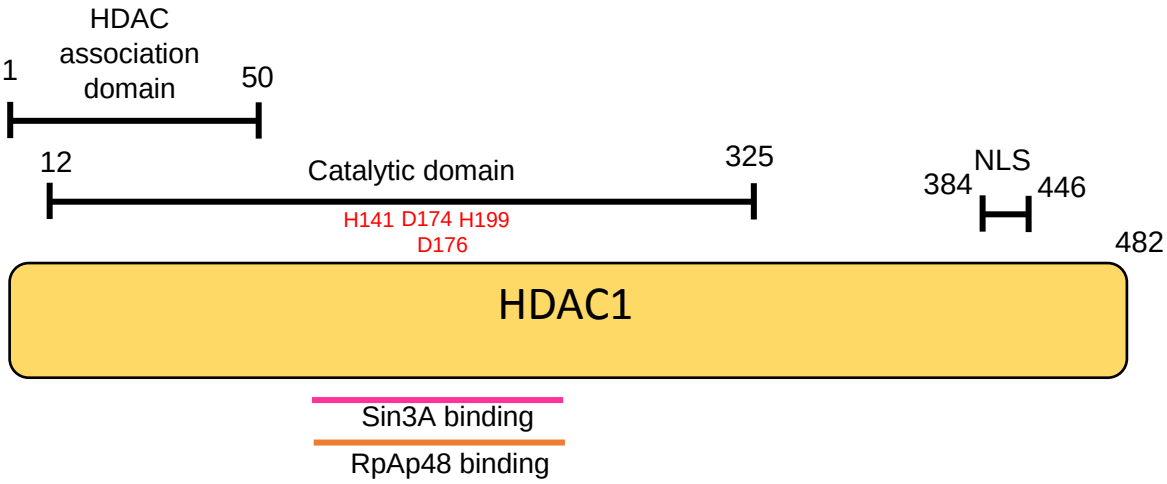

Figure 10. Histone deacetylase 1 (HDAC1) domains. HDAC association domain mediates homodimerization and heterodimerization (Taplick 2001). The catalytic domain encompasses the majority of the protein (Brunmeir 2009). Amino acids highlighted in red are critical residues of the HDAC1 active site that abolish enzymatic activity when mutated and that also maintain association with Sin3A and RpAp48 (Hassig 1998). NLS = nuclear localization signal. Numbers represent amino acids numbering.

Of note, HDAC1 does not contain a DNA-binding domain and relies on recruitment to DNA by other transcription factors. It can be recruited by DNA-binding factors such as E2F, YY1, p53 or Sp1/2 (173). It can also be recruited by the DNA-binding protein RUNX1 in hematopoietic cells, which colocalizes with HDAC1 on gene promoters implying that it may be capable of recruiting HDAC1 to DNA (14). HDAC1 can also be recruited to DNA as a member of a large corepressor complex. Sin3A, NuRD, and CoREST are well characterized HDAC1 containing complexes involved in gene regulation; however many additional HDAC1-containing complexes have been discovered. Sin3A binds to CBFβ-SMMHC and RUNX1 (115,176) and so may be predicted to assemble HDAC1 into a complex with these proteins as well.

While mice heterozygous for HDAC1 have a normal phenotype, homozygous knockout of HDAC1 in mice leads to early embryonic lethality at E10.5, indicating that other deacetylases cannot fully compensate for its loss, at least during early development (177). HDAC1 knockout in embryonic stem cells (ESCs) in one study resulted in a decrease in cell proliferation and increased levels of p21 and p27 (177), although these changes were not observed in a second study (178). HDAC1 knockout in ESCs also revealed that HDAC1 is required for both gene repression and gene activation. While a fairly small subset of genes was changed upon HDAC1 deletion (7%), two-thirds of genes were upregulated and one-third was downregulated (179). This implies that HDAC1 can have a multifaceted role in gene transcription that extends beyond acting as a corepressor.

In hematopoietic cells, HDAC1 has a unique expression pattern that reflects its activity. mRNA and protein expression is low in HSCs, increases in more differentiated progenitors, and remains increased in cells of the erythrocyte/megakaryocyte or lymphoid lineage while expression drastically decreases during differentiation into the

myeloid lineage (180). HDAC1 knockdown directs cells toward myeloid differentiation while HDAC1 overexpression results in a block in myeloid differentiation (180). In mice, *Hdac1*/*Hdac2* double knockout results in anemia and thrombocytopenia due to loss of the erthyrocyte/megakaryocyte lineage (181,182). Monoallelic expression of *Hdac1*, but not *Hdac2*, rescues the defect, implying that HDAC1 is more important for differentiation of this lineage and that HDAC2 cannot fully compensate for HDAC1 at specific stages of hematopoiesis (181). In contrast, only double knockout of *Hdac1* and *Hdac2* resulted in a defect in HSC homeostasis in mice with conditional tissue specific deletion, indicating redundancy in early hematopoietic cells (181). These results imply that HDAC1 plays a direct role in mediating cell fate decisions during hematopoiesis.

5.D.i.b. HDAC2

Histone deacetylase 2 (HDAC2) has many of the same features as HDAC1, due to extensive homology with HDAC1 (82% identical in human), likely from a gene duplication event in a common ancestor of vertebrates (173). However unlike HDAC1, HDAC2 is dispensable during embryonic development and knockout of HDAC2 results in viable, although slightly smaller mice (183). HDAC2 is also ubiquitously expressed, although it is expressed more highly in the brain than HDAC1/3 and may have a unique function in the CNS (171).

5.D.i.c. HDAC3

Histone deacetylase 3 (HDAC3) is also ubiquitously expressed (171), although its subcellular localization differs from HDAC1/2 in that it can be found in both the nucleus and the cytoplasm due to the presence of both an NLS and an nuclear export signal (NES) (184). While HDAC3 shares the characteristic of requiring cofactor binding for enzymatic activity, its complexes are distinct from those of HDAC1/2 (174,185).

HDAC3 is part of the NCoR and SMRT corepressor complexes which are involved in priming chromatin for transcription and maintaining heterochromatin through deacetylation of core histones (184,186). Global deletion of HDAC3 in mice results in embryonic lethality by E9.5, suggesting its requirement in development (187).

5.D.i.d. HDAC8

While ubiquitously expressed, protein levels of HDAC8 are generally much lower than other class I HDACs in most tissues (188). Unlike other class I HDACs, the activity of HDAC8 does not depend on the presence of additional cofactors. Histones may or may not be a target of HDAC8 deacetylase activity; experiments *in vitro* demonstrate they are a substrate of HDAC8 but it has not been able to be replicated *in vivo* (189,190). Therefore, non-histone proteins may be the more relevant targets of HDAC8, such as p53 and ERRα, which are deacetylated by HDAC8 (190). Global deletion of HDAC8 results in perinatal lethality due to skull malformation, indicating its requirement in early development and a possible unique role in bone formation (191).

5.D.ii. Class I HDACs in leukemia

Deregulated histone deacetylation by HDACs, especially HDAC1, has been implicated as a factor leading to leukemogenesis. HDAC1 has been shown to interact with several other leukemia fusion oncoproteins, including RUNX1-RUNX1T1 (192–194). HDAC1 is expressed in primary AML patient leukemic blasts and at significantly higher levels than in non-leukemic controls (180,195,196). Accordingly, lower HDAC1 expression levels correlated with longer survival in leukemia patients (196). Knockdown of HDAC1 in cell lines derived from AML patients inhibited cell proliferation and induced cell cycle arrest, showing the potential benefit of HDAC1 inhibition in AML treatment

(196). In addition, several HDAC inhibitors are used clinically or are in clinical trials for other hematological malignancies (197,198).

The results from several studies indicate that HDAC1 may function in CBFβ-SMMHC-induced leukemia. First, RUNX1 is known to interact directly with HDAC1 (115,199). Additionally, ChIP-Seq experiments on CBFβ-SMMHC-expressing ME-1 cells found the colocalization of RUNX1, CBFβ-SMMHC, and HDAC1, indicating a possibility that HDAC1 could be in a complex with RUNX1:CBFβ-SMMHC (14). Sin3A, known to recruit HDAC1 to protein complexes, binds to the SMMHC region of CBFβ-SMMHC (107,115). Therefore, HDAC1 has the potential to be recruited to the RUNX1:CBFβ-SMMHC complex through several possible mechanisms.

6. HDAC inhibitors (HDACi)

6.A. Overview of HDACi

HDAC inhibitors have been explored for the treatment of a wide range of conditions from cancer to cardiovascular disease, psychiatric disorders, and neurodegeneration. While there are currently only four FDA approved HDACi for treatment of two types of hematological malignancies (Vorinostat, Romidepsin, and Belinostat for T-cell lymphoma, Panobinostat for multiple myeloma), there are over 10 compounds in ongoing phase II or phase III clinical trials for treatment of various types of cancer (200,201).

HDACi are found extensively in nature as natural defenses against bacteria, fungi, parasites, and higher organisms. For example, trichostatin A is an anti-fungal HDACi secreted by some species of bacteria (202). HDACi are even produced by plants that humans eat regularly, such as sulforaphane found in broccoli (203). It has been suggested that the evolutionary origin for the secretion of HDACi by prokaryotes may be

due to capitalizing on differences in prokaryotic vs. eukaryotic chromatin packaging (201). However, this also suggests that eukaryotes would have evolved mechanisms to resist the transcriptional changes induced by HDACi present in the environment. One group has recently suggested that this eukaryotic resistance mechanism to HDACi could explain why clinical trials using HDACi in cancer therapy have been largely unsuccessful (201,204).

HDAC inhibitors are classified according to their chemical structure, and include four major classes: hydroxamates (e.g. vorinostat, TSA), cyclic peptides (e.g. romidepsin), benzamides (e.g. entinostat), and aliphatic acids (e.g. valproic acid, sodium butyrate) (205,206). HDAC inhibitors tend to exhibit structural similarity to the lysine substrates, containing a metal chelating region, a linker region of similar size to the lysine side chain, and a cap region that interacts with the moieties at the surface of the zinc binding pocket (207). Therefore, HDAC inhibitors which target Class I, II, and IV have a similar mechanism of action. They block HDAC activity by chelating the zinc ion in the HDAC catalytic site which is required for HDAC activity (206). Thus, the class III HDAC sirtuins are not affected by the same inhibitors due to NAD^+ rather than Zn^+ in their active sites.

6.B. Specificity of HDAC inhibitors

6.B.i. HDAC isoform selectivity

There is considerable interest in developing isoform specific HDAC inhibitors to offset toxicities associated with pan-inhibition. However, the high level of homology in the structures of the different HDAC proteins have prevented their development. Nevertheless, inhibitors have been developed with high selectivity towards a particular HDAC isoform over the others, such as the HDAC3 inhibitor RGFP966 (208) or the

HDAC8 inhibitor PCI-34051 (208–210). The challenge of creating isoform specific inhibitors stems from highly conserved residues lining the 11 Å channel that contains the zinc ion in the active site of HDACs (211). It is possible that resolving the crystal structures of each individual isoform will reveal differences in the active sites of each isoform that can be exploited for isoform selective inhibitors. However, there are already established differences in the moieties surrounding the entrance to the binding pocket such that steric hindrance can be exploited to create class-selective inhibitors (207,211). It is possible that differences in this region could be exploited to create isoform selective inhibitors.

Another factor mediating HDAC inhibitor specificity is the multi-protein complexes that recruit HDACs and are required for maximal HDAC activity. Since multiple complexes can recruit a single HDAC isoform, the binding partners that are present at a given time can dictate the efficacy of the inhibitor. One groundbreaking study found that a panel of HDAC inhibitors which were thought to be selective for certain HDAC isoforms based on activity assays conducted using purified enzymes are only selective for these isoforms when they are in some complexes but not others (212). The necessity of taking into account the components of an HDAC complex when trying to design inhibitors also leads to the possibility of designing inhibitors to specific complexes rather than the HDAC isoforms themselves (213).

6.B.ii. Specificity for leukemia cells vs. normal cells

The use of HDACi have been beneficial in treating many types of cancer due to their ability to cause cell differentiation, arrest cell cycle, or cause apoptosis of malignant cells while exhibiting low toxicity toward normal cells (198). For the treatment of AML, HDACi have shown promise when used in combination with chemotherapeutic agents both in the laboratory (214–217), and in early stage clinical trials (218–220).

While HDACi are active against both normal and malignant cells, they consistently exert greater toxicity towards malignant cells. Many mechanisms have been proposed to explain this phenomenon, which is likely to be cell-type and/or mutation-type specific. Leukemia-associated fusion proteins are uniquely sensitive to HDACi treatment and several mechanisms underly this observation. First, both leukemia-associated fusion proteins and HDACi treatment have been shown to increase levels of DNA damage in cells, and the combination of fusion protein expression plus HDACi treatment uniquely sensitizes the leukemia cells to apoptosis (221). Second, many leukemia-associated fusion proteins bind HDACs and require their activity. Therefore, these cells are uniquely sensitive to treatment with HDACi compared to their normal counterparts.

6.C. Entinostat

Entinostat (MS-27-275, MS-275, SNDX-275) was found to be a potent histone deacetylase inhibitor through a screen of synthetic benzamide derivatives in an effort to find compounds that would have an increased half-life in the blood and greater *in vivo* activity than previously identified HDACi such as sodium butyrate or trichostatin A (Figure 11) (222). Entinostat is not a pan-HDACi, but rather is selective to HDAC1 compared to HDAC2 or HDAC3, and has no activity against HDAC8 or other classes of HDACs (223–225). The interest in using entinostat for treating disease gained traction due to its favorable toxicity profile in patients and relatively long half-life of 33-150 hours (226). It is a well-tolerated drug whose common side effects including fatigue, nausea, and anemia, are easily manageable (226,227).

Entinostat has been tested as a drug candidate in many cancers, both for solid tumors and hematological malignancies. It has demonstrated preclinical antitumor activity in models of lung, prostate, breast, pancreas, and renal cell carcinoma (226).

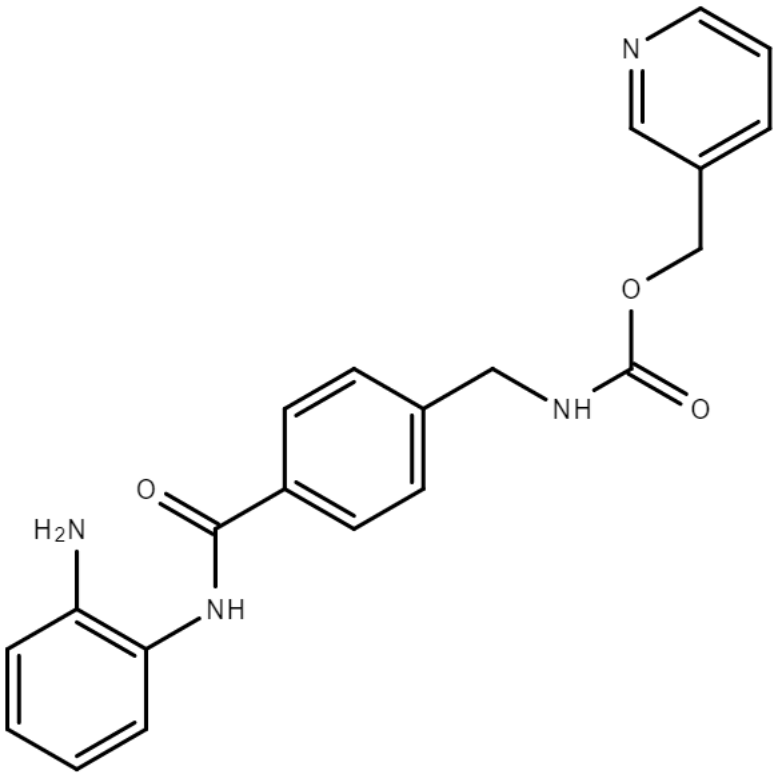

Figure 11. Chemical structure of entinostat.

Recently, a phase II clinical trial demonstrated the efficacy of entinostat treatment in patients with hormone receptor-positive advanced breast cancer, leading to FDA designation of entinostat as a Breakthrough Therapy for this disease (228).

Entinostat treatment has shown promise in *in vitro* and *in vivo* models of leukemia. A study on human leukemia cell lines treated with entinostat demonstrated that at lower concentrations (1 μM) the cells underwent cell cycle arrest and differentiation while at higher concentrations (5 μM) cells incurred mitochondrial damage resulting in apoptosis (229). Treatment of cytogenetically normal AML cells *ex vivo* resulted in a decrease in cell viability and colony-forming ability, and *in vivo* treatment extended the average survival of mice (230). Additionally, entinostat treatment was found to reverse silencing of genes which resulted in apoptosis of leukemia cells (231,232).

To date, clinical trials incorporating entinostat into leukemia treatment have not been successful. A Phase I trial demonstrated increased acetylation of histones in bone marrow mononuclear cells with entinostat treatment in patients with advanced AML, but did not observe a clinical response (233). A phase II trial conducted on MDS and AML patients tested azacytidine, which prevents DNA methylation, with or without entinostat and found that entinostat did not increase the efficacy of azacytidine alone (234). Interestingly hypomethylation and hyperacetylation status were not predictive of response (233,234). It is possible that several factors influenced the failure of these studies, such as the advanced stage of leukemia of the cohort tested or the many different cytogenetic subtypes pooled together for analysis. Not differentiating between leukemic subtypes for analysis could mask positive outcomes occurring in less common subtypes. In addition, the dosing schedule may have been flawed in this particular study. Because azacytidine acts on proliferating cells by incorporation into DNA and HDACi

block proliferation, the simultaneously administration of these drugs may have resulted in antagonism. Therefore, use of entinostat in AML should not be discounted until the limitations in these initial trials are addressed. Research into the molecular pathology of leukemia subtypes will direct better clinical trials in the future.

7. Hypothesis

Current treatments for inv(16) AML are highly toxic and nonspecific. Because inhibitors for CBFβ-SMMHC are not currently available for use in the clinic, we propose that one way to specifically target the activity of CBFβ-SMMHC is by identifying druggable cofactors which bind to the fusion protein and are required for its leukemogenic function.

HDAC1 can bind to RUNX1, colocalizes with CBFβ-SMMHC and RUNX1 at promoters in leukemia cells, and is often recruited into complexes by Sin3A, a known binding partner of CBFβ-SMMHC (14,115). HDAC1 inhibitors are FDA approved and could be quickly translated into clinical use for inv(16) leukemia (200,201). Therefore, HDAC1 is an attractive candidate for targeting the CBFβ-SMMHC complex if it is recruited to the complex and required for inv(16) leukemia. I hypothesize that HDAC1 is a required cofactor for CBFβ-SMMHC in inv(16) AML and that the leukemogenic activity of the fusion protein can be inhibited by the HDAC inhibitor entinostat.

Chapter II

Methods

1. Mouse models

Cbfb$^{+/56M}$*, Mx1-Cre*$^{+}$ or *Cbfb*$^{+/56M}$*, Mx1-Cre*$^{+}$, *Gt(ROSA)26Sor*$^{tm4(ACTB-tdTomato,-EGFP/Luo}$*/J)* (*Rosa26*$^{tdT/GFP}$) (Jackson Laboratory, Bar Harbor, ME) mice were genotyped and treated to develop leukemia, as previously described (18,235–237). Leukemia cells from primary mice were expanded by transplantation into congenic C57Bl6/129S6 F1 mice (Taconic, Hudson, NY) as previously described (120).

For *in vivo* studies, 1x10^{5} – 1x10^{6} cells from *Cbfb*$^{+/56M}$*, Mx1-Cre*$^{+}$*, Rosa26*$^{tdT/GFP}$ mice were transplanted into sub-lethally irradiated (600 cGy) congenic mice. When green fluorescent protein (GFP) in peripheral blood averaged 10-20%, mice were treated by IP injection or oral gavage with 10 mg/kg/day entinostat (Cayman Chemical, Ann Arbor, MI) prepared in PBS with 2.5% DMSO,1% Tween-80 and 5.1% PEG-400, or vehicle alone for seven days. Tissues were collected for analysis the day after the last treatment. Peripheral blood was collected in 2 mL ACK buffer, centrifuged at 4°C at 1800 rpm for 5 minutes, and incubated a second time in ACK buffer for 5 minutes on ice followed by washing in FACS buffer (5% FBS in PBS) and staining for flow cytometry. Bone marrow was collected and lineage negative (Lin^{-}) cells were selected using the EasySep Mouse Hematopoietic Progenitor Cell Isolation Kit (Stemcell Technologies) according to the manufacturer's recommendations and stained for flow cytometry analysis. For histological analysis, tissues were fixed in 4% paraformaldehyde for 48 hours, embedded in paraffin, sectioned, and stained with hematoxylin and eosin. Slides were examined using a Leica DM4000 B LED microscope at 20X magnification.

In vivo knockdown of *Hdac1* was accomplished by generating a leukemia sample obtained from a *Cbfb*$^{+/56M}$*, Mx1-Cre*$^{+}$ leukemic mouse (hereafter *CM*$^{+}$ cells) with the stable integration of an Isopropyl β-D-1-thiogalactopyranoside (IPTG)-inducible shRNA targeting *Hdac1* and GFP expressed from an internal ribosome entry site (IRES). To

accomplish this, *CM*$^{+}$ cells were transduced using the lentiviral method described below. Following transduction, GFP^{+} cells were sorted and transplanted into sub-lethally irradiated C57Bl6/129S6 F1 mice. The development of GFP^{+} leukemia was monitored using flow cytometry. When the mice were moribund from leukemia, the spleen cells were cryopreserved. Prior to *in vivo* studies, the cells were thawed, sorted for GFP expression, and injected into sub-lethally irradiated C57Bl6/129S6 F1 mice. When the mice had 10-20% GFP^{+} cells in the peripheral blood, they were treated with or without 10 mM IPTG in the water bag for seven days with water bags changed on day 4. For gene expression analysis, leukemic cells from the spleen were sorted for GFP expression. All procedures were performed in accordance with guidelines and protocols approved by the Institutional Animal Care and Use Committee (IACUC) of the University of Nebraska Medical Center.

2. Cell culture

Cbfb$^{+/56M}$*, Mx1-Cre*$^{+}$ cells were cultured in RPMI-1640 (ATCC, Manassas, Virginia) supplemented with 20% ESC qualified fetal bovine serum (Thermo Fisher Scientific, Waltham, MA) 1% penicillin/streptomycin, 1% L-glutamine, 10 ng/mL IL-3, 10 ng/mL IL-6, 20 ng/mL SCF (Peprotech, Rocky Hill, NJ) and cryopreserved in RPMI-1640 supplemented with 50% FBS and 10% DMSO. COS-7 cells (ATCC) and HEK293T cells (ATCC) were maintained in DMEM supplemented with 10% fetal bovine serum, 1% penicillin/streptomycin, and 1% L-glutamine. ME-1 cells (kindly provided by P. Liu, NHGRI/NIH) were maintained in RPMI-1640 supplemented with 20% fetal bovine serum, 2.5% of a 10% (w/v) glucose solution, 1% penicillin/streptomycin, 1% L-glutamine, 1% sodium pyruvate, and 2.5% 1M HEPES. Kasumi-1 cells (ATCC) and 32D cl3 INV/CB6 cells (238) were maintained according to ATCC recommended protocols. 32D cl3

INV/CB6 cells were maintained under selection at 1.2 mg/mL G418. All cells were incubated at 37°C, 5% CO_2.

3. Assays

3.A. COS-7 transfection

The day before transfection, low-passage COS-7 cells were plated at 400,000 cells per well in a 6-well plate with 2 mL media and incubated overnight. The following day, the media was removed and 2 mL fresh media was added to each well. Transfection mixtures were prepared as follows: 500 µL Optimem (Gibco), 1 µg total plasmid DNA, 8 µL Lipofectamine LTX (Thermo Fisher). If needed, pBluescript empty plasmid was used to bring the total plasmid DNA to 1 µg for each reaction. Each reaction was briefly vortexed, centrifuged, and incubated at room temperature for 30 minutes. Each reaction was added dropwise to one well and put back in the incubator for 5 hours. Next, the media was removed and 2 mL new media was added. Cells were placed back in the incubator and harvested approximately 48 hours later.

3.B. Immunoprecipitation

Nuclear lysates were prepared from cells for IP as follows:10mM HEPES pH 7.5, 1.5mM $MgCl_2$,10mM KCl, 0.5mM DTT, and protease inhibitors (Sigma, St. Louis, MO) were added to the cell pellet, resuspended gently, and incubated on ice for 15 minutes. Cells were centrifuged for 30 seconds at 12,000 rpm and supernatant removed (or saved for cytosolic fraction). Next, the previous buffer with the addition of 0.05% NP-40 was added to the cell pellet, vortexed, and centrifuged again. The supernatant was discarded. The pellet was resuspended in 20mM HEPES pH 7.5, 25% glycerol, 0.42M NaCl, 0.2mM EDTA, 0.5mM DTT, and protease inhibitors. The samples were alternately incubated on ice for 5 minutes and vortexed a total of five times, then centrifuged for 15

minutes at 13,000 rpm. The nuclear extract was removed for IP. 1 µg (transfected cells) or 2 µg (*CM*$^{+}$, ME-1 cells) of the pulldown antibody was added to each sample and incubated with the lysates overnight with rotation at 4°C. The following day, lysates were incubated for 40 minutes with protein A Dynabeads (Thermo Fisher Scientific) at room temperature, and washed five times with 150mM NaCl, 20mM HEPES pH 7.5, 0.2% NP-40, 0.1% Tween and protease inhibitors. Beads were resuspended in 2x Laemmli buffer and boiled at 95°C for 5 minutes.

3.C. Western Blot

Western blotting was performed on 4-12% Bis-Tris gels (Invitrogen) at 200V according to manufacturer's recommendation. Proteins were transferred onto a PVDF membrane (Invitrogen) at 30V according to manufacturer's recommendations. The membrane was blocked in blocking buffer (5% dry milk in TBS-T) for approximately 1 hour. After 5 minute wash in TBS-T, the membrane was incubated overnight with the indicated antibodies in 5% BSA in TBS-T. The following day, the membrane was washed 5x for 5 minutes in TBS-T. The membrane was incubated in HRP-conjugated secondary antibody for 1 hour in blocking buffer. After 5x washes for 5 minutes in TBS-T, the membrane was incubated with Supersignal Pico/Femto chemiluminescent substrate (Thermo Scientific) for 2 minutes in the dark and subsequently exposed to film and developed. A list of antibodies used can be found in Table 1.

3.D. Chromatin Immunoprecipitation

Chromatin Immunoprecipitation (ChIP) was performed using MagnaChip A Chromatin Immunoprecipitation Kit (EMD Millipore, Billerica, MA) with some modifications. $10x10^{6}$ cells were crosslinked with 1.5 mM final concentration of ethylene glycolbis (succinimidylsuccinate) (EGS) for 30 minutes followed by 10 minutes

Table 1. List of antibodies, manufacturer, and catalog number used for western blot (WB), immunoprecipitation (IP), chromatin immunoprecipitation (ChIP) and flow cytometry analysis (FC).

Antibody	**Manufacturer**	**Catalog Number**	**Use**
SMMHC (MYH11) (discontinued)	Novus Biologicals	21370002	IP, WB, ChIP
SMMHC (MYH11)	Origene	TA323339	ChIP
HDAC1	Abcam	ab7028	WB, ChIP
HDAC1	Sigma	SAB1400121	WB
HDAC2	Cell Signaling	5113S	WB
HDAC3	Abcam	ab7030	WB, IP, ChIP
GAPDH	Ambion	AM4300	WB
FLAG	Sigma	F1804	IP
CBFβ	Aviva Systems Biology	P100598_p050	WB, IP
RUNX1	Active Motif	39000	IP, WB, ChIP
RUNX1	Invitrogen	MA5-15814	WB
Acetyl-lysine	Novus	NB100-74339	WB
Normal rabbit IgG	Millipore	12-370	IP, ChIP
Mac-1 (CD11b) BV421	BD Biosciences	562605	FC
Gr-1 (Ly-6G/C) BV510	BD Biosciences	563040	FC
Annexin V APC	BD Biosciences	550475	FC
Kit (CD117) APC-eFlour780	Invitrogen	47-1171-82	FC
Anti-mouse secondary	Vector Laboratories	PI-2000	WB
Anti-rabbit secondary	Vector Laboratories	PI-1000	WB

crosslinking with 1% final concentration paraformaldehyde. Chromatin was sheared using a Bioruptor Plus (Diagenode, Denville, NJ) for 30 total cycles of 30 seconds on/30 seconds off. 5 µg of antibody was used in each pulldown with lysate from approximately $2x10^6$ cells and incubated overnight with 20 µL protein A magnetic beads. The following day, beads were washed as indicated in kit instructions. Reverse crosslinking was achieved with a 5 hour incubation at 62°C with frequent gentle mixing. ChIP was followed by qRT-PCR with *CDKN1A*, *MPO*, *CSF1R*, and *CEBPD* ChIP primers described previously (239). Antibodies used for ChIP can be found in Table 1 and primer sequences can be found in Table 2.

3.E. Virus Production

To produce the virus used for shRNA-mediated knockdowns, 2 $x10^6$ low-passage HEK293 cells were plated two days before transfection in 10 cm plates with 10 mL DMEM. On the day of transfection, 6 µg JPC9, 10 µg JPC10A, 5 µg JPC11 third generation lentiviral plasmids (240) plus 24.6 µg Mission 3xLacO-IPTG plasmid engineered to contain GFP for selection and either HDAC1 shRNA or control with no known target (NT shRNA) were combined in a microcentrifuge tube. HDAC1 and control shRNA were a gift from Saverio Minucci, University of Milan (241). Sterile buffered water was added to bring the volume up to 500 µL. 50 µL of 2.5 M $CaCl_2$ was added, followed by 500 µL 2x HBS (pH 7.05) and air was forced into the tube by vigorously pipetting up and down at the liquid surface for five seconds. The tubes were incubated for 25 minutes at room temperature, followed by dropwise addition onto the 10 cm plates of HEK293 cells. The cells were placed back in the incubator for 8 hours. The media was removed, the cells were carefully washed with 5 mL PBS, and 7 mL DMEM was added to each plate. 48 hours later, the media was collected, filtered through a 0.45 µm syringe filter,

Table 2. List of forward (Fw) and reverse (Rv) primers used for quantitative real-time PCR (qRT-PCR) for chromatin immunoprecipitation (ChIP).

Primer	Primer sequence
Cdkn1a Fw	gcggctgtttttcttggtag
Cdkn1a Rv	agacgaggaaagcagttcca
Mpo Fw	ttgctccttagccaagatgg
Mpo Rv	agagaaggacccagagctga
Csf1r Fw	agaagaaggcaagggaatga
Csf1r Rv	gcatagtccgtttgctgtga
Cebpd Fw	ccaagaagaaatgccagagc
Cebpd Rv	cgaaccctctccagctacac
Gene desert Fw	caatgcatgggtccagattt
Gene desert Rv	attggcacggaagtagtgct

and concentrated using PEG-it (System Biosciences) according to manufacturer's recommendations or used directly to transduce leukemia cells.

3.F. Viral transduction for shRNA-mediated knockdown

For transduction, 1 x 10^6 *CM*$^+$ cells/mL were added to the viral supernatant collected as outlined above, with the addition of 10 ng/mL IL-3, 10 ng/mL IL-6, 20 ng/mL SCF, 57 μM beta-mercaptoethanol and 8 μg/mL polybrene. Cells were spinfected at 2,000 rpm for 90 minutes, followed by a 6 hour incubation and a second spinfection. 24 hours after the start of transduction, Isopropyl β-D-1-thiogalactopyranoside (IPTG) was added to a final concentration of 1 mM in each well. 48 hours after the start of transduction, cells were sorted for GFP expression on a BD FacsAria (BD Biosciences, Franklin Lakes, NJ).

3.G. Quantitative real-time PCR

RNA was extracted from cells using TRIzol Reagent (Thermo Fisher Scientific) according to manufacturer's instructions. First strand cDNA synthesis was accomplished using EcoDry Premix (Clontech, Mountain View, CA) according to manufacturer's instructions. Quantitative real-time PCR (qRT-PCR) was performed on an ABI-PRISM 7000 (Applied Biosystems, Foster City, CA) using SybrGreen 2x Mastermix (Thermo Fisher Scientific) according to manufacturer's instructions. Primers sequences for *Cdkn1a*, *Mpo*, *Csf1r*, and *Cebpd* and *Actb* were described previously (239). qRT-PCR primer sequences are listed in Table 3.

Table 3. List of forward (Fw) and reverse (Rv) primers used for quantitative real-time PCR (qRT-PCR) for mRNA gene expression.

Primer	Primer sequence
CBFB-MYH11 Fw	gagaaggacacgcgaatttgaagatag
CBFB-MYH11 Rv	tctcctcattctgctcgtcc
Actb Fw	ccctaaggccaaccgtgaa
Actb Rv	cagcctggatggctacgtaca
Csf1r Fw	gcgatgtgtgagcaatggcagt
Csf1r Rv	agaccgttttgcgtaagacctg
Cdkn1a Fw	cggtggaactttgacttcgt
Cdkn1a Rv	aaatctgtcaggctggtctgc
Mpo Fw	tttgacagcctgcacgatga
Mpo Rv	gtcccctgccagaaaacaag
Gapdh Fw	accacagtccatgccatcac
Gapdh Rv	tccaccaccctgttgctgta
Cebpe Fw	gctacaatcccctgcagtacc
Cebpe Rv	tgccttcttgcccttgtg
Csf3r Fw	ctgatcttcttgctactcccca
Csf3r Rv	ggtgtagttcaagtgaggcag
Ly6g Fw	ttgtattggggtcccacctg
Ly6g Rv	ccagagcaacgcaaaatcca
Itgam Fw	ccatgaccttccaagagaatgc
*Itgam*_Rv	accggcttgtgctgtagtc
Cebpa Fw	aaagccaagaagtcggtggac
Cebpa Rv	ctttatctcggctcttgcgc
Cbfb Fw	gcaagaagacagcaagaccc
Cbfb Rv	gaaaccaactgcagtccctc
Hdac1 Fw	tgaagcctcaccgaatccg
Hdac1 Rv	gggcgaatagaacgcagga

3.H. Flow cytometry

Cells were stained with the indicated fluorophore-conjugated antibody or dye according to manufacturer's recommendations. Antibodies used in flow cytometry experiments can be found in Table 1. Flow cytometry analysis or sorting was performed on a BD LSRII or FACSAria (BD Biosciences), respectively. Data was analyzed in FlowJo v.10.0.8 (FlowJo, LLC, Ashland, OR).

3.I. Cytospin

Cells were prepared at a concentration of 1 x 10^5 cells/100 µL in 0.5% BSA in PBS. Cells were centrifuged in a Shandon Cytospin 3 (Thermo Fisher) for 5 min. at 2,000 rpm (fast acceleration setting) onto positively charged slides. Slides were dried overnight, and then stained with Wright-Giemsa (Protocol Hema 3 kit, Thermo Fisher), and examined using an Olympus BX51 microscope at 100x magnification.

3.J. Colony-forming assay

Colony-forming assays (CFA) were performed using MethoCult™ GF M3534 and SmartDish meniscus-free plates (Stemcell Technologies, Vancouver, Canada). Cells were plated in triplicate in MethoCult mixed with a final concentration of 1 µM entinostat (Cayman Chemical) vorinostat (Active Motif, Carlsbad, CA), RGFP966 (Selleck Chemicals, Houston, TX) or Ro5-3335 (EMD Millipore) or equivalent DMSO control. Cells were incubated at 37°C, 5% CO_2, for 14 days and colonies were counted or stained as indicated.

3.K. Viability assay

Cells were treated with increasing doses of Entinostat or RGFP966 and viability was assessed using PrestoBlue Cell Viability Reagent (Thermo Fisher Scientific)

according to the manufacturer's instructions after 72 hours in culture. Fluorescence was detected on a Tecan Infinite M200 (Tecan, Mannedorf, Switzerland). EC_{50} was calculated using GraphPad Prism 7 (GraphPad Software, La Jolla, CA).

3.L. Site-directed mutagenesis

pMIG-CBFB-MYH11$_{\Delta 179\text{-}221,}$ (provided by P. Liu, NHGRI/NIH) (111), was mutated to CBFB-MYH11$_{N63K,\ N104K,\ \Delta 179\text{-}221}$ using the QuikChangeII Site Directed Mutagenesis Kit (Agilent Technologies, Santa Clara, CA) according to the manufacturer's recommendations. Mutation of pCMV-RUNX1c to RUNX1c$_{K51,70R/Q/A}$ was performed in two rounds of mutagenesis using the double primer method found on www.openwetware.org/Richard_Lab:Site_Directed_Mutagenesis with modifications. PCR was performed by combining 10 µL CloneAmp HiFi PCR Premix (Takara), 1-2 µL 2 µM forward/reverse primers (IDT), and 50 – 500 ng template plasmid with a total volume of 20 µL per reaction. PCR cycling was as follows: 98°C for 30 seconds, 25-30 cycles of 98°C 10 seconds, 60°C 30 seconds, 72°C for 30 sec/kb of plasmid length, 72°C for 5 minutes. 1 µL DpnI restriction enzyme plus CutSmart buffer (NEB) was added directly to each reaction, incubated 2 hours at 37°C, followed by separation on a 1% agarose gel. PCR product was purified using the ZymoClean Gel Purification kit (Zymo Research), and immediately transformed into competent cells. Mutations were confirmed by sequencing. Primers used in RUNX1 mutagenesis were designed using Agilent Primer Design Tool and can be found in Table 4.

The PCR splicing method was used to generate the CBFB-MYH11$_{\Delta 222\text{-}448}$ deletion mutant. The protocol was adapted from http://www.methods.info/Methods/Mutagenesis/PCR_splicing.html. Briefly, 500 ng of CBFB-MYH11 plasmid was combined with 0.2 mM Primers 1 and 2, or Primers 3 and 4 in a separate reaction, with 2.5 µL 10x PCR buffer minus Mg, 0.75 µL 50 mM MgCl2, 0.5

Table 4. List of primers used for site-directed mutagenesis.

Template plasmid	Final Plasmid	Forward Primer	Reverse Primer
CBFB-MYH11$_{\Delta 179\text{-}221}$	CBFB-MYH11$_{N63K,\ \Delta 179\text{-}221}$	aaaactggagagacagcttggttcctgtggccac	gtggccacaggaaccaagctgtctctccagtttt
CBFB-MYH11$_{N63K,\ \Delta 179\text{-}221}$	CBFB-MYH11$_{N63K,\ N104K,\ \Delta 179\text{-}221}$	agataacacagactccttcagaatcatgggagcc	ggctcccatgattctgaagggagtctgtgttatct
RUNX1	RUNX1$_{K24R}$	gctgagcccaggccggatgagcgaggcg	cgcctcgctcatccggcctgggctcagc
RUNX1$_{K24R}$	RUNX1$_{K24R,\ K43R}$	gccctggccggccggctgaggagcgg	ccgctcctcagccggccggccagggc
RUNX1	RUNX1$_{K24Q}$	gctgagcccaggccagatgagcgaggc	gcctcgctcatctggcctgggctcagc
RUNX1$_{K24Q}$	RUNX1$_{K24Q,\ K43Q}$	ccctggccggccagctgaggagc	gctcctcagctggccggccaggg
RUNX1	RUNX1$_{K24A}$	gctgagcccaggcgcgatgagcgaggcg	cgcctcgctcatcgcgcctgggctcagc
RUNX1$_{K24A}$	RUNX1$_{K24A,\ K43A}$	gccctggccggcgcgctgaggagcgg	ccgctcctcagcgcgccggccagggc

µL 10mM dNTP mix, 0.1 µL Platinum Taq (Invitrogen), and water up to 25 µL total volume. PCR cycling conditions were as follows: 94 °C 2 minutes; 35 cycles of 94°C 30 sec, 56°C 30 sec, 72°C 2 min.; 72°C 10 min. After PCR, products were run on a 1% agarose gel, extracted, and diluted 1:10 for second PCR. For second round of PCR, Primers 1 and 4 were combined with 1 µL of the 1:10 diluted first round PCR product plus the other ingredients as stated above. After second round of PCR, PCR product was purified on 1% agarose gel, extracted, digested and cloned back in to the original vector. Sequences for Primers 1-4 can be found in Table 5.

3.M. Yeast two-hybrid assay

The yeast two-hybrid assay was performed as previously described (242). The *Saccharomyces cerevisiae* strain AH109 (kind gift from Steve Caplan, UNMC) was maintained on yeast extract peptone dextrose agar plates. Before transformation, yeast was grown overnight at 30°C with shaking at 250 rpm in liquid YPD medium. The next day, yeast was resuspended in competent solution (TE buffer, 1M lithium acetate, 0.1% salmon sperm DNA). For each reaction, 100 µL of yeast in solution was combined with 1 µg DNA for each plasmid. 600 µL of PEG solution (50% PEG 3350, TE buffer, 1M lithium acetate) was added to each reaction, vortexed, and incubated for 30 minutes at 30°C. 70 µL DMSO was added to each tube followed by heat shock at 42°C for 15-30 minutes. Tubes were centrifuged and pellets resuspended in 20 µL diH_2O. Reactions were plated on minus two (-leucine, -tryptophan) plates and incubated for 2 days at 30°C. Colonies were selected for each reaction and vortexed in 600 µL diH_2O. OD 600 nm was tested and corrected until reading at OD 600 nm was 0.05. 5 µL of each reaction was spotted onto both minus two plates and minus three plates (-leucine, -tryptophan, -histidine) and incubated for 2 days at 30°C.

Table 5. List of primers used for CBFB-MYH11$_{\Delta 222\text{-}448}$ deletion mutagenesis.

	Primer sequence
Primer 1	gctcggatcactagtaacggc
Primer 2	ggacttgaacttggaggcttggagatccct
Primer 3	agggatctccaagcctccaagttcaagtcc
Primer 4	ctctagatgcatgctcgagcg

The cloning for the yeast two-hybrid assay was performed as follows. The plasmids pGBKT7 and pGADT7 AD (kind gift of Steve Caplan, UNMC) were engineered to express fusions of HDAC1 to GAL4 DNA binding domain and CBFB or CBFB-MYH11 to GAL4 activation domain. Specifically, pGBKT7-HDAC1 was created by digesting pcDNA3.1-HDAC1 with EcoRI. Simultaneously, pGBKT7 was digested with EcoRI, followed by Antarctic phosphatase (New England Biosciences) treatment for 30 minutes. Both digested plasmids were run on a 1% agarose gel, then the HDAC1 and pGBKT7 bands were excised and extracted. HDAC1 was ligated into pGBKT7 using Quick Ligase (New England Biosciences), transformed into competent Stellar cells (Clontech), and spread on kanamycin-agaraose plates for selection. DNA sequencing verified the resulting plasmid was correct. The pGADT7-CBFB plasmid was created by digesting both pGEM-CBFB and pGADT7 with EcoRI and XhoI, followed by ligation, plating on carbenicillin-agaraose for selection and verification as outlined above. The pGADT7-CBFB–MYH11 plasmid was created by digesting pGEM-CBFB-MYH11 with EcoRI and NotI, blunt-end ligating into the EcoRV site of pBluescript and then digesting pBluescript-CBFB-MYH11 and pGADT7 with ClaI and BamHI, followed by the ligation and verification steps outlined above.

3.N. Cell cycle analysis

Cells were washed twice in FACS buffer, resuspended in 1 mL 70% ethanol, and incubated on ice for 30 minutes. Cells were centrifuged 5 minutes, 1800 rpm, 4C, washed with 1 mL PBS, and centrifuged again. The pellet was resuspended gently in 500 µL Telford Reagent (For 250 mL: 8.405 mg EDTA, 6.7 mg RNAse A, 12.5 mg Propoidum Iodide, 250 µL Triton X-100, bring up to volume with PBS). Cells were incubated on ice, protected from light, for a minimum of 30 minutes before analysis. No additional wash steps are performed before analysis. Cells were analyzed on a BD

FACSCalibur or BD LSRII flow cytometer and data was analyzed using ModFit LT software (Verity Software House, Topsham, ME).

3.O. Luciferase promoter assay

HEK293 cells were plated for reverse transfection no more than an hour before use. 50,000 HEK293 cells were plated in triplicate in each well of a 96-well plate in 100 µL DMEM. Simultaneously, 1.5 million HEK293 were plated in 1 well of six-well plate for testing transfection efficiency with western blot. To make mastermix for transfection of 3 wells of 96-well plate plus 1 well of 6-well plate: Combine 600 ng pM-CSFR plasmid, 120 ng pRL-TK plasmid, and 1,440 ng total for all other plasmids used in reaction (uniform amount of each plasmid plus empty vector if needed). Add 6 µL Lipofectamine LTX reagent to each tube and bring up to a total volume of 480 µL with Optimem media. Vortex and spin down briefly. Tubes were incubated at room temperature for 30 minutes. 20 µL of the mastermix was added to each well of 96-well plate and 400 µL to 1 well of a 6-well plate, dropwise. 48 hours later, cells were lysed and analyzed for luciferase activity following the protocol from the Dual Luciferase Assay Kit (Promega) or harvested for western blot analysis. Luminescence was detected one well at a time on a Tecan Infinite M200 plate reader in a white 96-well plate, using a 10 second integration time.

4. Statistics

Data was analyzed using either the Student's t-test or ANOVA with Tukey post-hoc test, as appropriate and indicated in the figure legends. Significance for Kaplan-Meier survival curves was calculated using the Log-Rank test. All statistical tests were performed in GraphPad Prism 7. All error bars are plotted as standard error of the mean (SEM). Data was considered statistically significant at a p-value ≤ 0.05. Significance is plotted as follows: * = p≤0.05, ** = p≤0.01, *** = p≤0.001, n.s. = not significant.

Chapter III

Results

Data included in this chapter was previously published in *Molecular Cancer Research.* 2019;17(6):1241-1252.

1. Background

Acute myeloid leukemia (AML) with inv(16)(p13.1q22) or the related translocation t(16;16)(p13.1;q22) represents 8-10% of all AML cases and usually shows monocytic/ granulocytic differentiation and abnormal eosinophils (4,96,243,244). The chromosomal breakpoints for inv(16) occur within the genes *CBFB* and *MYH11*, which encode core binding factor beta (CBFβ) and smooth muscle myosin heavy chain (SMMHC), respectively (1,96). The inverted chromosome results in an in-frame fusion between *CBFB* and the C-terminal coiled-coil region of *MYH11* to generate the oncogene *CBFB-MYH11*. Expression of this oncogene, which produces the protein CBFβ-SMMHC, is the initiating event in inv(16) AML, but additional cooperating mutations are required for transformation to a frank leukemia (130,245).

Core binding factor (CBF) is a heterodimeric transcription factor consisting of one CBFα subunit, which binds DNA, in a complex with CBFβ, which stabilizes the CBFα/DNA interaction. CBFα can be any of the three members of the Runt-related transcription factor family, which includes RUNX1 (AML1, CBFα2), RUNX2 and RUNX3. While the roles of RUNX2 and RUNX3 in blood cells are currently poorly understood, RUNX1 is a well-established, critical regulator of hematopoiesis (25,246–248). CBFβ-SMMHC retains the RUNX binding site in CBFβ and gains a second high-affinity binding domain within the SMMHC region (106,249).

Initial models of CBFβ-SMMHC activity proposed that the fusion protein acts by dominantly repressing normal RUNX1 activity. If this model fully described the fusion protein's activity, one would predict that loss of *RUNX1* would be equivalent to expression of the fusion protein. However, knock-in mice expressing *Cbfb-MYH11* from the endogenous *Cbfb* locus (*Cbfb*$^{+/MYH11}$) have a more severe block in hematopoietic differentiation and show deregulated expression of a unique set of genes as compared

to mice homozygous for a null allele of *Runx1* (*Runx1*$^{-/-}$) (120). These findings imply that CBFβ-SMMHC activity is not solely based on RUNX1 repression and raises the possibility that RUNX1 may be dispensable for the fusion protein's effect. To test this possibility, we generated mice expressing *Cbfb-MYH11*, but with significantly reduced RUNX1 activity (18). We found that loss of RUNX1 activity impaired *Cbfb-MYH11* induced changes in gene expression and myeloid differentiation. Collectively these findings support a new model of CBFβ-SMMHC activity in which the fusion protein doesn't repress RUNX1, but alters its activity, resulting in the changes in gene expression that lead to leukemogenesis. In support of this model, chromatin immunoprecipitation experiments show that RUNX1 and CBFβ-SMMHC colocalize in the inv(16) AML cell line, ME-1. Interestingly, the epigenetic modifier HDAC1 was also found to colocalize with RUNX1 and CBFβ-SMMHC, raising the possibility that HDAC1 may contribute to the fusion protein's transcriptional activity (14).

HDAC1 is a known binding partner of RUNX1 and a member of the class I HDAC family, which also includes HDAC2, HDAC3, and HDAC8. These family members are classified together based on their homology to yeast RPD3, with HDAC1 and 2 being the most similar, and HDAC8 the most divergent (169,250). Class I HDACs' canonical roles are as epigenetic modifiers associated with transcriptional repression. By removing acetyl groups from lysine residues in histone tails, HDACs create a closed chromatin structure which is inaccessible to the transcriptional machinery (251,252). More recently, Class I HDACs have been shown to have additional roles including participation in transcriptional activation and deacetylation of non-histone proteins (164,253).

Based on these findings, we hypothesize that HDAC1 is part of the RUNX1:CBFβ-SMMHC complex and contributes to the gene expression changes associated with inv(16) AML. In this report, we show that HDAC1 binds to CBFβ-SMMHC and contributes to gene expression changes, maintenance of the differentiation

block, and colony growth. In addition, we show that pharmacological inhibition of HDAC1 impairs the growth of CBFβ-SMMHC-expressing leukemia cells *in vitro* and *in vivo*, implying that HDAC1 inhibitors may be effective for the treatment of inv(16) AML.

2. HDAC1 is a member of the CBFβ-SMMHC:RUNX1 complex

Because HDAC1 colocalizes with RUNX1 and CBFβ-SMMHC on gene promoters (14), it is possible that HDAC1 is part of the RUNX1:CBFβ-SMMHC complex. Before testing this, we confirmed that HDAC1 is expressed in leukemia cells from knock-in mice with a conditional *Cbfb-MYH11* allele (*Cbfb*$^{+/56M}$) under the control of the *Mx1-Cre Recombinase* (*Mx1-Cre*$^{+}$) transgene, (hereafter *CM*$^{+}$ cells) and in the human inv(16) AML cell line, ME-1 (18,120,235,254). We detected increased levels of HDAC1 in three different *CM*$^{+}$ mouse samples as compared to bone marrow from wild-type mice. HDAC1 was also readily detectable in ME-1 cells (Figure 12A). As HDAC1 and HDAC2 are known to have overlapping functions in normal hematopoiesis, we also analyzed the expression of HDAC2 in *CM*$^{+}$ and ME-1 cells (182). HDAC2 was also expressed highly in all three *CM*$^{+}$ leukemia samples and in ME-1 cells, similar to HDAC1 (Figure 12B).

We next tested if HDAC1 and 2 can interact with CBFβ-SMMHC in COS-7 cells transfected with plasmids containing either HDAC1 or HDAC2 fused with a FLAG tag (*HDAC1-FLAG*, *HDAC2-FLAG*) and *CBFB-MYH11*, the gene encoding CBFβ-SMMHC. Using nuclear lysates, we performed co-immunoprecipitations (co-IP's). IP with an anti-SMMHC antibody resulted in the pulldown of HDAC1-FLAG in cells expressing both CBFβ-SMMHC and HDAC1-FLAG, but not in cells expressing HDAC1-FLAG alone (Figure 12C). In a reciprocal experiment, pulldown with an antibody against FLAG immunoprecipitated CBFβ-SMMHC in cells expressing HDAC1-FLAG and CBFβ-SMMHC, but not in cells expressing CBFβ-SMMHC only (Figure 12D). In contrast,

Figure 12. HDAC1 binds to CBFβ-SMMHC. (**A**) HDAC1, (**B**) HDAC2, or GAPDH protein expression was probed in wild-type mouse bone marrow, *CM*$^{+}$ mouse cells, and ME-1 cells by western blot. (**C**) COS-7 cells were transfected with plasmids expressing *CBFB-MYH11* or *HDAC1-FLAG* and IP's were performed on the lysates with anti-SMMHC or (**D**) anti-FLAG, followed by western blot. Total inputs are shown below. (**E**) COS-7 cells were transfected with plasmids containing *CBFB-MYH11* or *FLAG-HDAC2* and lysates were used for IP with SMMHC antibody followed by western blot for HDAC2. Total input is shown below. (**F**) COS-7 cells were transfected with plasmids expressing *CBFB-MYH11* or *HDAC1-FLAG,* and the lysates were evenly split into two reactions with one DNase-treated for 30 minutes (lane 1) and one without DNase added (lane 2). (**G**) Lysates from three independent *CM*$^{+}$ mice were separated into two equal fractions and incubated with either anti-SMMHC or anti-IgG, followed by western blot to probe for HDAC1. The dotted line indicates separation between two different gels. (**H**) Lysates from ME-1 cells or Kasumi-1 cells were subjected to IP with anti-SMMHC, followed by western blot for HDAC1. Arrows indicate HDAC1 at its expected size and a non-specific band observed in both lanes. Total input is shown below.

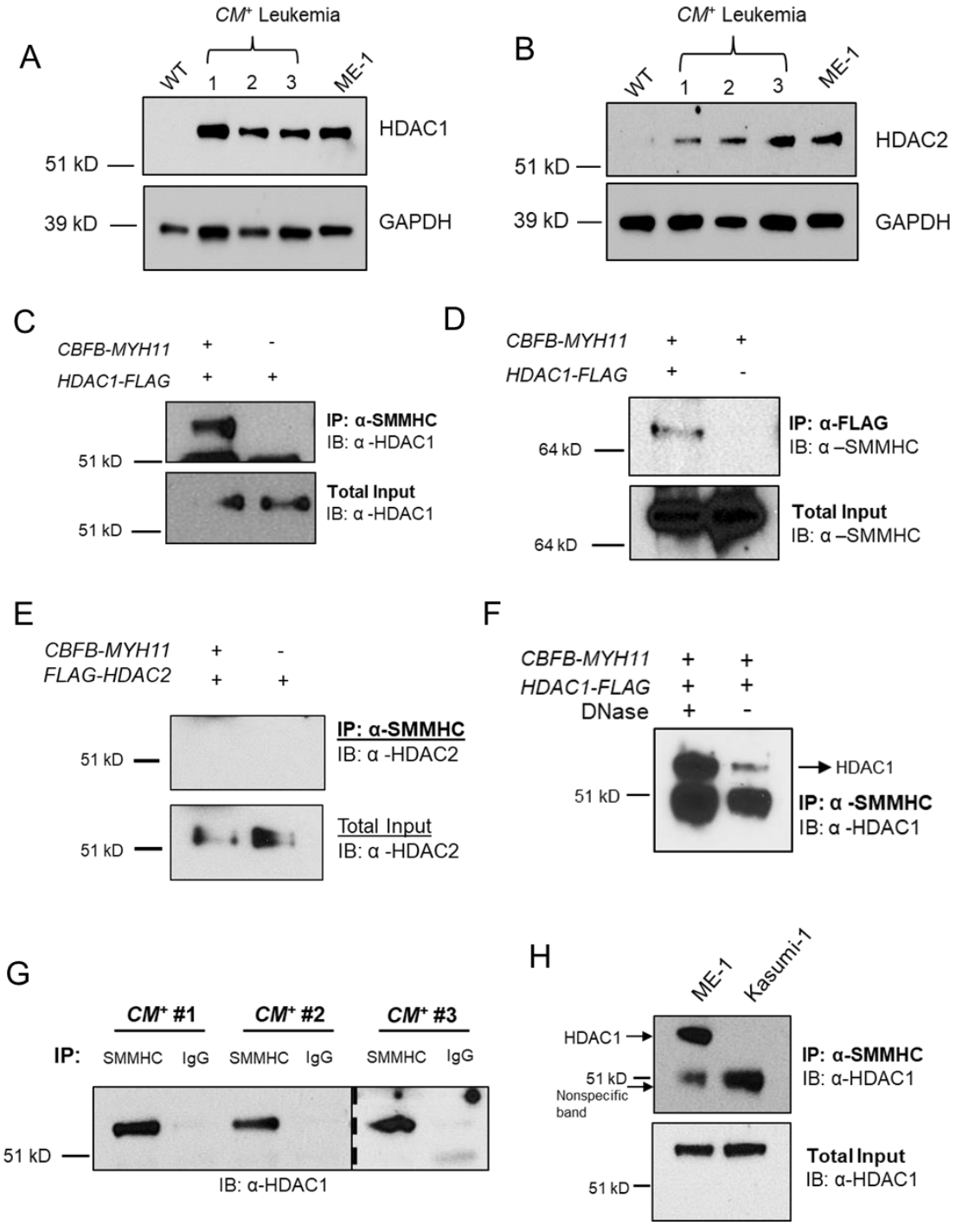
A
CM+ Leukemia
WT
1
2
3
ME-1
HDAC1
51 kD
GAPDH
39 kD
B
CM+ Leukemia
WT
1
2
3
ME-1
HDAC2
51 kD
GAPDH
39 kD
C
CBFB-MYH11 + -
HDAC1-FLAG + +
IP: α-SMMHC
IB: α -HDAC1
51 kD
Total Input
IB: α -HDAC1
51 kD
D
CBFB-MYH11 + +
HDAC1-FLAG + -
64 kD
IP: α-FLAG
IB: α –SMMHC
Total Input
IB: α –SMMHC
64 kD
E
CBFB-MYH11 + -
FLAG-HDAC2 + +
51 kD
IP: α-SMMHC
IB: α -HDAC2
51 kD
Total Input
IB: α -HDAC2
F
CBFB-MYH11 + +
HDAC1-FLAG + +
DNase + -
HDAC1
51 kD
IP: α -SMMHC
IB: α -HDAC1
G
CM+ #1
CM+ #2
CM+ #3
IP:
SMMHC
IgG
SMMHC
IgG
SMMHC
IgG
51 kD
IB: α-HDAC1
H
ME-1
Kasumi-1
HDAC1
51 kD
Nonspecific band
IP: α-SMMHC
IB: α-HDAC1
51 kD
Total Input
IB: α-HDAC1

immunoprecipitation with anti-SMMHC did not pull down HDAC2 (Figure 12E). These results suggest that CBFβ-SMMHC can interact with HDAC1, but not HDAC2.

To verify that the HDAC1:CBFβ-SMMHC interaction was not mediated through an indirect interaction with DNA, COS-7 cells were co-transfected with plasmids containing *HDAC1-FLAG* and *CBFB-MYH11*. Nuclear lysates were prepared and evenly split into two tubes. One tube was treated with DNase to degrade any DNA that was pulled down with the SMMHC antibody (Figure 12F, lane 1). The DNase treated sample pulled down more HDAC1 than the untreated sample, indicating that the CBFβ-SMMHC:HDAC1 interaction is not the result of an indirect interaction mediated by DNA (Figure 12F).

We next tested if endogenous CBFβ-SMMHC and HDAC1 form a complex. Nuclear lysates from leukemic cells from three independent CM^{+} mice were incubated with either anti-SMMHC or normal rabbit IgG. HDAC1 was immunoprecipitated with anti-SMMHC, but not with IgG, indicating that endogenous CBFβ-SMMHC and HDAC1 interact in mouse leukemia cells (Figure 12G). To confirm this interaction in human leukemia cells, we performed co-IPs using lysates from ME-1 cells and Kasumi-1 cells, a leukemia cell line which expresses HDAC1 but not CBFβ-SMMHC. HDAC1 and CBFβ-SMMHC co-IP'd in ME-1 cells but not in Kasumi-1 cells (Figure 12H). Together, these results indicate that endogenous CBFβ-SMMHC and HDAC1 interact in mouse and human leukemia cells.

HDAC1 is known to bind RUNX1, raising the possibility that RUNX1 mediates the interaction between HDAC1 and CBFβ-SMMHC (115). To test this, we performed IP's with mutant constructs of *CBFB-MYH11* with either reduced RUNX1 binding due to deletion of the high-affinity binding domain (HABD) (*CBFB-MYH11*$_{\Delta 179\text{-}221}$), or a complete loss of RUNX1 binding due to point mutations in the CBFβ domain as well as deletion of the HABD (*CBFB-MYH11*$_{N63K,\ N104K,\ \Delta 179\text{-}221}$) (Figure 13A) (255,256). In

Figure 13. HDAC1 binds to the SMMHC region in a RUNX1-independent manner. COS-7 cells were transfected with plasmids containing the indicated constructs and the nuclear lysates were subjected to IP's with (**A**) anti-RUNX1 or (**B/C**) anti-FLAG, followed by western blot for SMMHC (**A/B**) or CBFβ **(C)**. The dotted line indicates a division between two different regions of the same gel. Total input is shown below. (**D**) COS-7 cells were transfected as above and the nuclear lysates were subjected to IP with anti-CBFβ antibody followed by western blot for RUNX1 (left side of dotted line, first lane) or HDAC1 (right side of dotted line, first lane). The dotted line indicates where the membrane was cut. (**E**) *S. cerevisiae* was co-transformed with plasmids containing a fusion of the indicated gene to either the GAL4 DNA binding domain (bait) or the GAL4 activation domain (prey). Transformed yeast was plated on –Leu/-Trp/+His agar (+His) as a control and –Leu/-Trp/-His agar (-His) as a selection for protein interaction. (**F/G**) COS-7 cells were transfected with plasmids containing the indicated constructs and the nuclear lysates were subjected to IP with anti-FLAG followed by western blot for SMMHC. Total inputs are shown below. **(H)** Model of possible HDAC1 binding sites to SMMHC with tested regions in black and untested regions in red. Amino acid numbering is indicated.

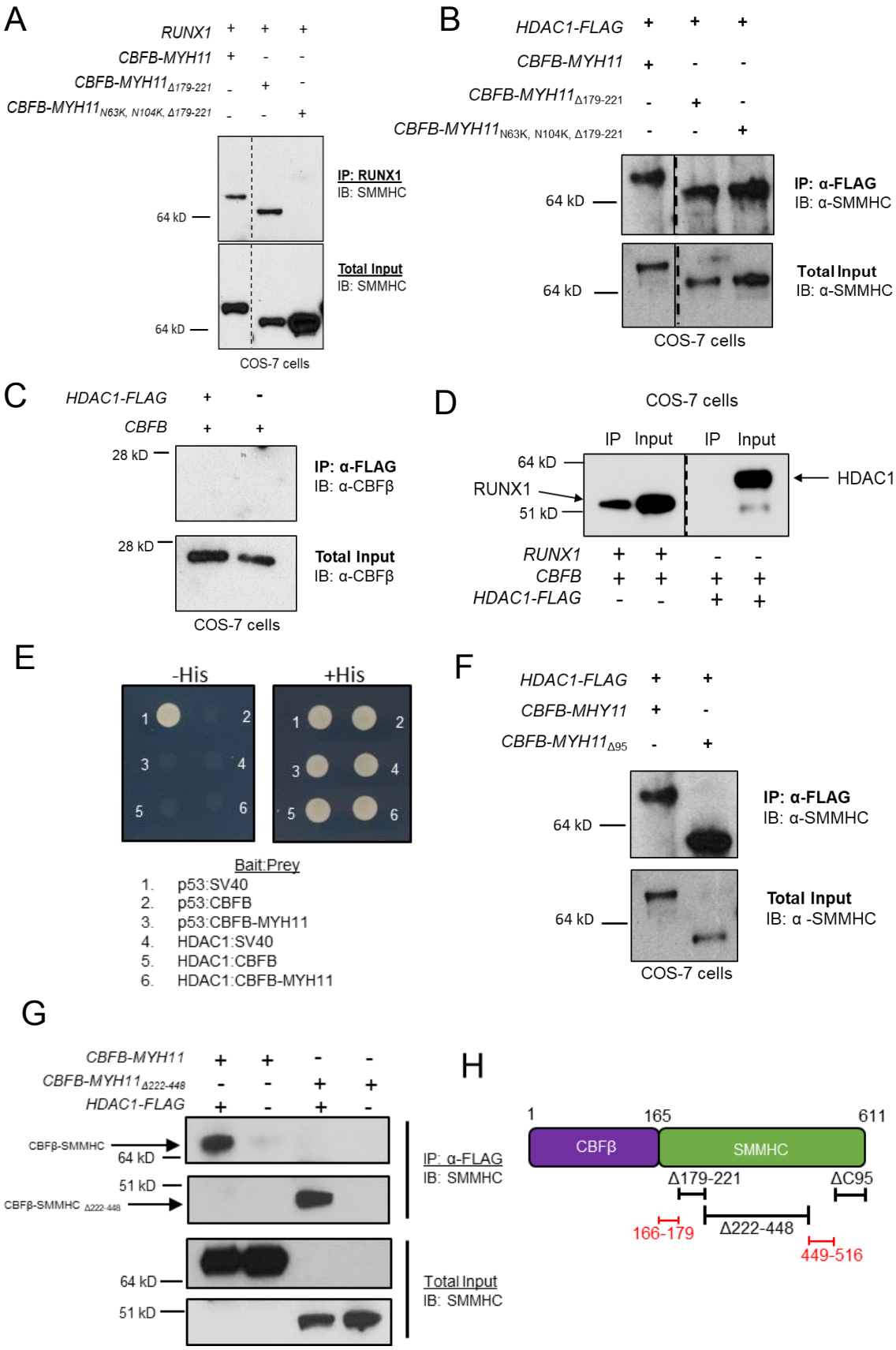
A
RUNX1 + + +
CBFB-MYH11 + - -
CBFB-MYH11Δ179-221 - + -
CBFB-MYH11N63K, N104K, Δ179-221 - - +
64 kD
IP: RUNX1
IB: SMMHC
64 kD
Total Input
IB: SMMHC
COS-7 cells
B
HDAC1-FLAG + + +
CBFB-MYH11 + - -
CBFB-MYH11Δ179-221 - + -
CBFB-MYH11N63K, N104K, Δ179-221 - - +
64 kD
IP: α-FLAG
IB: α-SMMHC
64 kD
Total Input
IB: α-SMMHC
COS-7 cells
C
HDAC1-FLAG + -
CBFB + +
28 kD
IP: α-FLAG
IB: α-CBFβ
28 kD
Total Input
IB: α-CBFβ
COS-7 cells
D
COS-7 cells
IP Input IP Input
64 kD
RUNX1
51 kD
HDAC1
RUNX1 + + - -
CBFB + + + +
HDAC1-FLAG - - + +
E
-His
+His
1 2 3 4 5 6
Bait:Prey
1. p53:SV40
2. p53:CBFB
3. p53:CBFB-MYH11
4. HDAC1:SV40
5. HDAC1:CBFB
6. HDAC1:CBFB-MYH11
F
HDAC1-FLAG + +
CBFB-MHY11 + -
CBFB-MYH11Δ95 - +
64 kD
IP: α-FLAG
IB: α-SMMHC
64 kD
Total Input
IB: α -SMMHC
COS-7 cells
G
CBFB-MYH11 + + - -
CBFB-MYH11Δ222-448 - - + +
HDAC1-FLAG + - + -
CBFβ-SMMHC
64 kD
51 kD
CBFβ-SMMHC Δ222-448
IP: α-FLAG
IB: SMMHC
64 kD
51 kD
Total Input
IB: SMMHC
H
1
165
611
CBFβ
SMMHC
Δ179-221
ΔC95
166-179
Δ222-448
449-516

transfected cells, IP with anti-FLAG was able to pull down both CBFβ-SMMHC mutants, indicating that RUNX1 is not required for the interaction between HDAC1 and CBFβ-SMMHC (Figure 13B).

We next tested the ability of HDAC1 to interact with two other important regions of the fusion protein: the CBFβ region and the c-terminal 95 amino acids, a part of the corepressor domain. In nuclear lysates from cells expressing HDAC1-FLAG and wild-type CBFβ, IP with anti-FLAG did not co-precipitate detectable CBFβ (Figure 13C), and neither did the reciprocal pulldown with anti-CBFβ, although the precipitation of the known CBFβ binding partner RUNX1 was readily apparent (Figure 13D). These findings indicate that HDAC1 and wild-type CBFβ do not form a complex.

To verify that there was no interaction between HDAC1 and CBFβ as well as determine if HDAC1 was binding directly to CBFβ-SMMHC, we performed a yeast two-hybrid assay. HDAC1 was cloned into the bait plasmid, resulting in HDAC1 fusion to the GAL4 DNA binding domain. *CBFB* or *CBFB-MYH11* were cloned into the prey plasmid, resulting in the separate fusion of each gene to the GAL4 activation domain. p53-GAL4 DNA binding domain and SV40 Large T Antigen-GAL4 activation domain were used as a positive control interaction. In this system, only proteins which interact directly will permit the synthesis of histidine in the cell, allowing yeast colonies to grow on plates lacking histidine. All combinations of bait:prey plasmids grew colonies on a plate with histidine (Figure 13E, right), indicating successful transformation and growth. However, only the p53:SV40 Large T Antigen positive control cells grew on a plate lacking histidine (Figure 13E, left). Confirming our IP results, HDAC1 did not directly interact with CBFβ in this assay. However, there was also no interaction detected between HDAC1 and CBFβ-SMMHC (Figure 13E). This result indicates that HDAC1 is likely not directly binding to CBFβ-SMMHC and possibly requires the presence of another unidentified protein to be recruited to the complex.

We next tested whether CBFβ-SMMHC's C-terminus is required for interaction with HDAC1. Nuclear lysates from cells transfected with *HDAC1-FLAG* and a C-terminal deletion mutant of *CBFB-MYH11* (*CBFB-MYH11*$_{\Delta C95}$) were immunoprecipitated with anti-FLAG. We found that IP of HDAC1 was able to pull down CBFβ-SMMHC$_{\Delta C95}$ (Figure 13F), indicating that the final 95 residues of SMMHC are not required to form a complex with HDAC1. This is in contrast to what has been shown for the interaction between CBFβ-SMMHC and HDAC8, implying that the fusion protein interacts with HDAC1 and HDAC8 through distinct domains (12).

In order to identify the region of SMMHC that binds to HDAC1, we made a large deletion in the middle region of MYH11 (*CBFB-MYH11*$_{\Delta 222-448}$) which we predicted would include the HDAC1 binding site. IP with anti-FLAG resulted in co-immunoprecipitation with CBFβ-SMMHC, as expected, but it also pulled down CBFβ-SMMHC$_{\Delta 222-448}$, indicating that this region is not required for HDAC1 binding (Figure 13G). There are several possible explanations for this finding, including that HDAC1 is binding to SMMHC in one of the regions which were not tested in any of our *CBFB-MYH11* mutant plasmids (Figure 13H) or that HDAC1 is recruited through multiple sites and therefore deletions of single regions are not sufficient to identify the binding site. For example, it is possible that HDAC1 is recruited by RUNX1 and Sin3A simultaneously.

3. HDAC1 is required for CBFβ-SMMHC target gene expression

In the inv(16) AML cell line ME-1, HDAC1 colocalizes with RUNX1 and CBFβ-SMMHC in the promoter regions of target genes (14). To confirm that HDAC1, CBFβ-SMMHC and RUNX1 colocalize in primary *CM*$^{+}$ mouse leukemia cells, we performed chromatin immunoprecipitation (ChIP) followed by quantitative real-time PCR for four known target genes: cyclin-dependent kinase inhibitor 1A (*CDKN1A*) which encodes

p21$^{Waf1/Cip1}$, myeloperoxidase (*MPO*), colony-stimulating factor 1 receptor (*CSF1R*), and CCAAT/enhancer binding protein delta (*CEBPD*) (239) as well as a negative control gene desert region (257). We found that HDAC1, CBFβ-SMMHC, and RUNX1 were each significantly enriched at the promoters of *Mpo*, *Csf1r*, and *Cebpd* as compared to control (Figure 14A). On the promoter of *Cdkn1a*, RUNX1 and HDAC1 were significantly enriched, and CBFβ-SMMHC showed a trend towards enrichment, although it did not reach the level of statistical significance (p=0.06).

To test if *Hdac1* activity is required for CBFβ-SMMHC-induced expression of these target genes, we used two different short hairpin RNA (shRNAs) to knockdown *Hdac1* in *CM*$^{+}$ mouse leukemia cells. Cells were transduced with lentiviral vectors expressing control or *Hdac1* shRNAs under an IPTG inducible promoter and expressing GFP from an internal ribosomal entry site. The cells were treated with IPTG to induce shRNA expression, and twenty-four hours later were sorted for GFP expression. Both shRNAs against *Hdac1* caused significant knockdown of *Hdac1* as compared to cells transduced with the control shRNA. (Figure 14B). Both shRNAs against HDAC1 also resulted in significant decreases in *Cdkn1a*, *Mpo*, *Csf1r*, and *Cebpd* expression (Figure 14B). Furthermore, expression of *Mpo*, *Csf1r*, and *Cebpd* appeared to show an *Hdac1* dose dependency. This suggests that *Hdac1* is required for expression of CBFβ-SMMHC target genes.

To determine if *Hdac1* is required for the CBFβ-SMMHC induced block in differentiation, we stained *Hdac1* knockdown and control *CM*$^{+}$ leukemia cells for expression of Gr-1 (Ly-6G) and Mac-1 (CD11b), which are both markers of mature myeloid cells. *Hdac1* knockdown in *CM*$^{+}$ cells showed increased expression of Gr-1 and to a lesser extent Mac-1, implying that HDAC1 is required for the CBFβ-SMMHC induced block in differentiation (Figure 14C). Cytospins of these cells showed smaller nuclei with lighter cytoplasm in the *Hdac1* knockdown cells compared to control,

Figure 14. HDAC1 colocalizes with CBFβ-SMMHC and RUNX1 and regulates target gene expression. (**A**) Chromatin immunoprecipitation (ChIP) was performed on cell lysates from at least three independent *CM*$^{+}$ mice with antibodies against normal rabbit IgG, RUNX1, SMMHC, or HDAC1. Quantitative real-time PCR was used to detect transcript levels of the indicated genes using beta-actin as a reference control. Data is plotted as fold enrichment compared to IgG. (**B**) Cells from three independent *CM*$^{+}$ mice were transduced with either a control shRNA with no target (shNT) or one of two different shRNA constructs targeting Hdac1 (shHDAC1). RNA/cDNA expression from sorted cells was analyzed using quantitative real-time PCR using beta-actin as a reference control. Data is plotted as relative gene expression compared to the control shRNA. (**C**) *CM*$^{+}$ cells were lentivirally transduced with control or Hdac1 shRNA constructs, and shRNA expression was induced after sorting. Twenty-four hours later, cells were analyzed for cell surface expression of Gr-1 or Mac-1 by flow cytometry. Data is plotted as fold change in staining compared to control shRNA. (**D**) Cells from (C) were used for cytospin before staining. Cells were stained with Wright-Giemsa and visualized at 100x magnification. (**E**) Cells from (C) were also stained with an antibody against annexin V, analyzed by flow cytometry, and plotted as fold change compared to control shRNA. (F) Cells from two *CM*$^{+}$ mice transduced with shHDAC1 were plated in methylcelluose with either PBS (Control) or 1 mM IPTG. Colonies were manually counted on day 14 and plotted as relative number compared to control. Error bars represent the standard error of the mean (SEM). ANOVA (A,B) or Student's t-test (C,E,F) was used to calculate statistical significance. * = $p \leq 0.05$, ** = $p \leq 0.01$, n.s. = not significant.

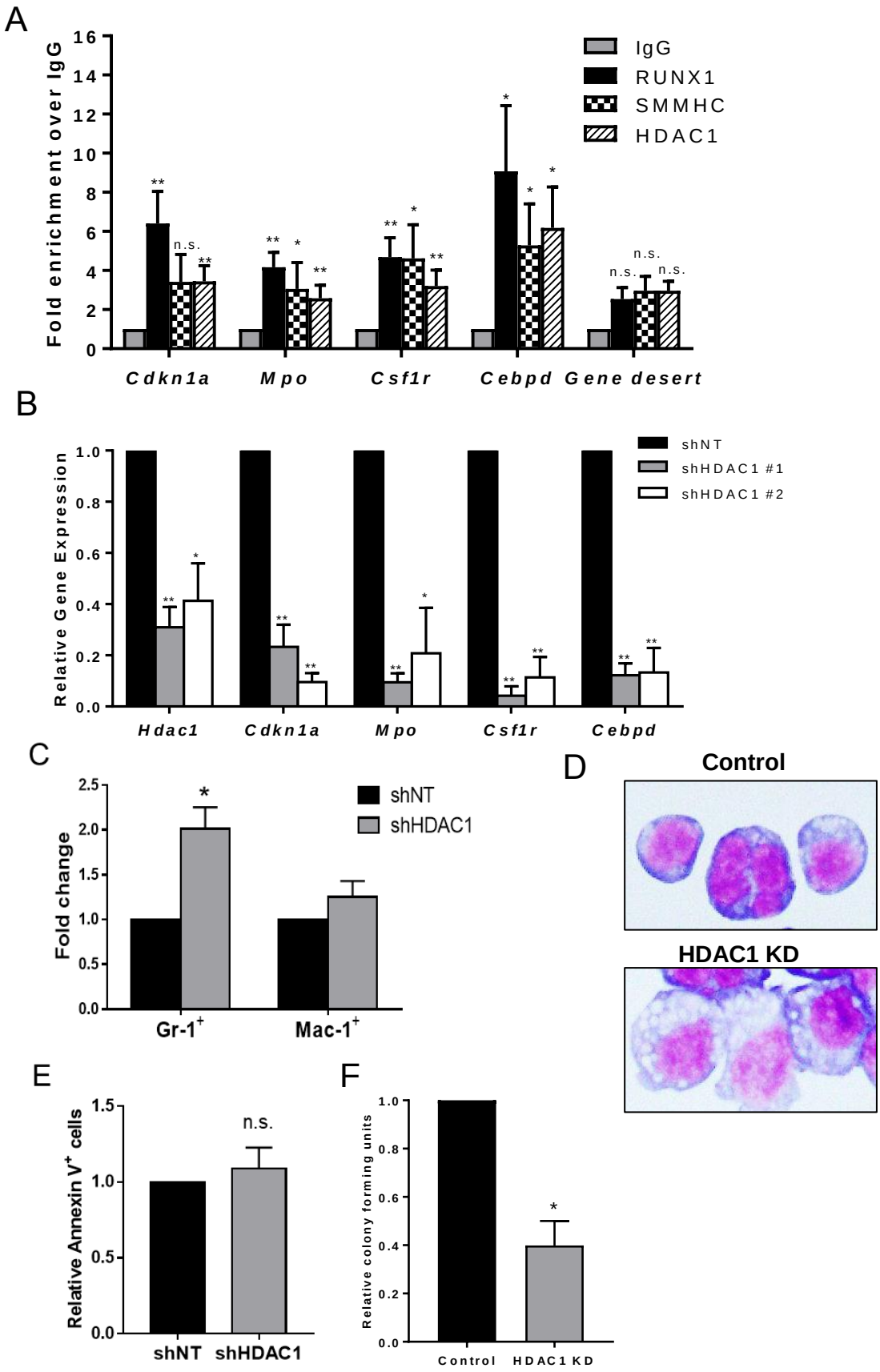
A
Fold enrichment over IgG
IgG
RUNX1
SMMHC
HDAC1
Cdkn1a
Mpo
Csf1r
Cebpd
Gene desert
n.s.
B
Relative Gene Expression
shNT
shHDAC1 #1
shHDAC1 #2
Hdac1
Cdkn1a
Mpo
Csf1r
Cebpd
C
Fold change
shNT
shHDAC1
Gr-1+
Mac-1+
D
Control
HDAC1 KD
E
Relative Annexin V+ cells
n.s.
shNT
shHDAC1
F
Relative colony forming units
Control
HDAC1 KD

indicating that loss of *Hdac1* increased morphological differentiation (Figure 14D). To test if loss of *Hdac1* affects the survival of *CM*$^+$ leukemia cells, we performed staining with annexin V, a marker of early apoptosis. In *Hdac1* knockdown cells, we did not observe a difference in annexin V staining compared to control, indicating that *Hdac1* is likely not directly regulating cell survival (Figure 14E). To test if knockdown of *Hdac1* affected colony forming ability, we induced *Hdac1* knockdown in transduced *CM*$^+$ leukemia cells for 24 hours, then sorted for live GFP positive cells and plated equal numbers of cells in methylcellulose containing vehicle or IPTG. After 14 days, we observed significantly fewer colonies in the *Hdac1* knockdown plates compared to control, suggesting that HDAC1 is important for leukemia stem cell activity (Figure 14F).

4. HDAC3 mimics HDAC1 binding to CBFβ-SMMHC and may also regulate gene expression in *CM*$^+$ cells

Because HDAC3 was recently shown to be a pharmacological target in other subtypes of hematological malignancies (258), we decided to also investigate whether HDAC3 could be important in inv(16) AML. We first tested whether HDAC3 was expressed by performing a western blot on lysates from wild-type bone marrow, three *CM*+ mice, and ME-1 cells (Figure 15A). HDAC3 was expressed at roughly equal levels in all samples tested, indicating its protein level may not be specifically increased in leukemia cells compared to normal bone marrow as we observed with HDAC1 and HDAC2. Next, we asked whether HDAC3 could bind to CBFβ-SMMHC. To test this, we performed immunoprecipitations on nuclear lysates from COS-7 cells transfected with expression plasmids containing *CBFB-MYH11* or *FLAG-HDAC3*. Pulldown with antibodies against SMMHC or HDAC3 resulted in a specific co-immunoprecipitation between CBFβ-SMMHC and HDAC3 (Figure 15B and C). To test whether the two

Figure 15. HDAC3 binds to CBFβ-SMMHC. (**A**) HDAC3 or GAPDH protein expression was probed in wild-type mouse bone marrow, *CM*$^{+}$ mouse cells, and ME-1 cells by western blot. COS-7 cells were transfected with plasmids expressing *CBFB-MYH11* or *FLAG-HDAC3* and IP's were performed on the lysates with (**B**) anti-SMMHC or (**C**) anti-HDAC3, followed by western blot. Total inputs are shown below. (**D**) Nuclear lysates from a *CM*$^{+}$ mouse (leukemia), normal bone marrow, ME-1 cells, or Jurkat cells was used for IP with anti-HDAC3 followed by western blot for CBFβ to detect CBFβ-SMMHC. Total input is shown below. (**E/F/G**) COS-7 cells were transfected with plasmids expressing the indicated constructs and the lysates were used for IP with anti-FLAG followed by western blot for anti-SMMHC (**E/G**) or anti-CBFβ (**F**). Total input is shown below. The dotted line indicates separation between different portions of the same gel. (**H**) Chromatin immunoprecipitation (ChIP) was performed on cell lysates from at least three independent *CM*$^{+}$ mice with antibodies against normal rabbit IgG, RUNX1, SMMHC, or HDAC3. Quantitative real-time PCR was used to detect transcript levels of the indicated genes using beta-actin as a reference control. Data is plotted as fold enrichment compared to IgG. Error bars represent the standard error of the mean (SEM). ANOVA was used to calculate statistical significance. * = $p \leq 0.05$, ** = $p \leq 0.01$, *** = $p \leq 0.001$, n.s. = not significant.

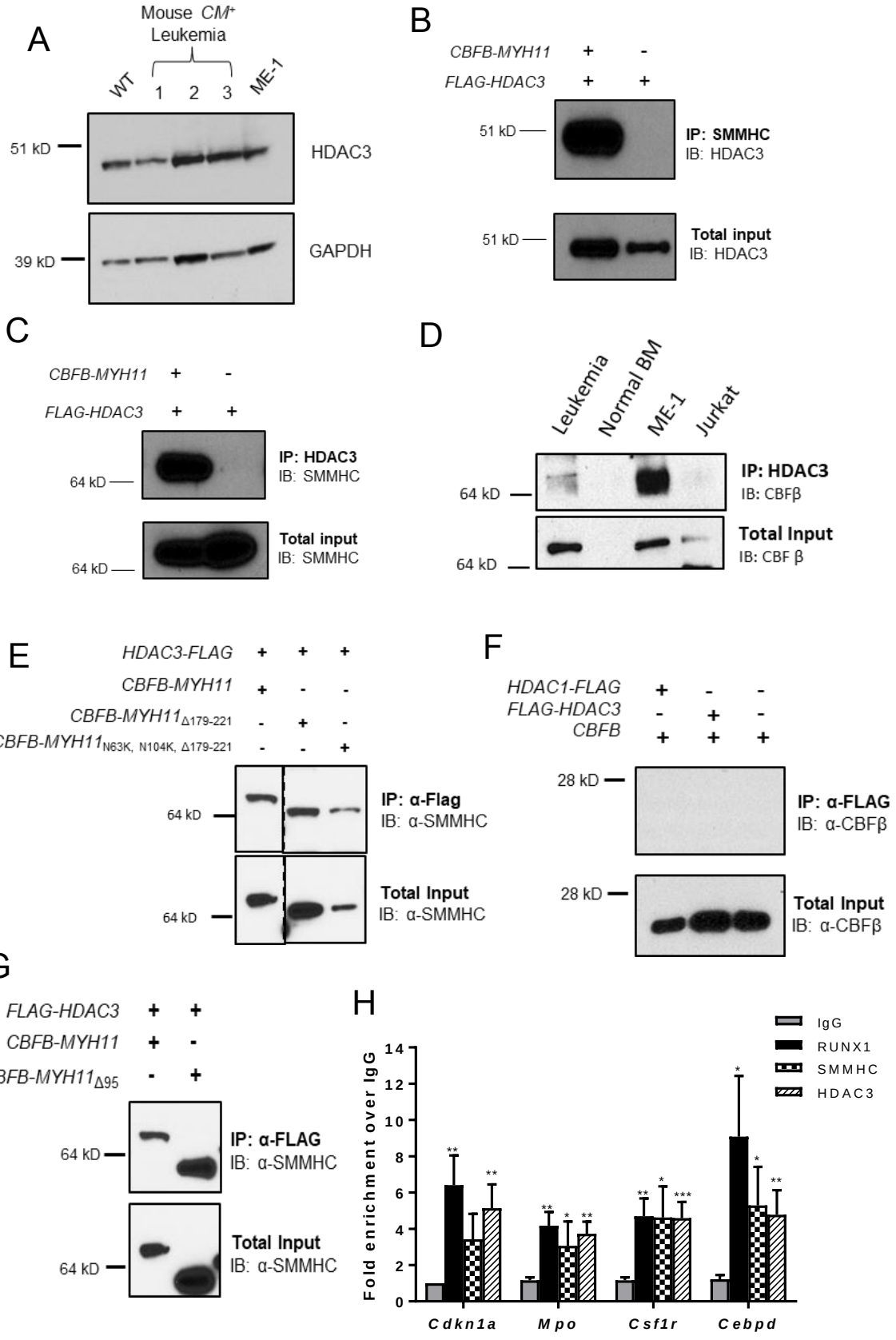
A
Mouse CM+ Leukemia
WT
1
2
3
ME-1
51 kD
HDAC3
39 kD
GAPDH
B
CBFB-MYH11 + -
FLAG-HDAC3 + +
51 kD
IP: SMMHC
IB: HDAC3
51 kD
Total input
IB: HDAC3
C
CBFB-MYH11 + -
FLAG-HDAC3 + +
64 kD
IP: HDAC3
IB: SMMHC
64 kD
Total input
IB: SMMHC
D
Leukemia
Normal BM
ME-1
Jurkat
64 kD
IP: HDAC3
IB: CBFβ
64 kD
Total Input
IB: CBF β
E
HDAC3-FLAG + + +
CBFB-MYH11 + - -
CBFB-MYH11Δ179-221 - + -
CBFB-MYH11N63K, N104K, Δ179-221 - - +
64 kD
IP: α-Flag
IB: α-SMMHC
64 kD
Total Input
IB: α-SMMHC
F
HDAC1-FLAG + - -
FLAG-HDAC3 - + -
CBFB + + +
28 kD
IP: α-FLAG
IB: α-CBFβ
28 kD
Total Input
IB: α-CBFβ
G
FLAG-HDAC3 + +
CBFB-MYH11 + -
CBFB-MYH11Δ95 - +
64 kD
IP: α-FLAG
IB: α-SMMHC
64 kD
Total Input
IB: α-SMMHC
H
IgG
RUNX1
SMMHC
HDAC3
Fold enrichment over IgG
0
2
4
6
8
10
12
14
Cdkn1a
Mpo
Csf1r
Cebpd

proteins interact when expressed at endogenous levels, we performed immunoprecipitation using an antibody against HDAC3 in *CM*$^{+}$ leukemia cells versus normal bone marrow, and ME-1 cells versus Jurkat cells, a human leukemia cell line which does not express CBFβ-SMMHC but does express HDAC3. Co-immunoprecipitation of HDAC3 and CBFβ-SMMHC was detected in *CM*$^{+}$ cells and ME-1 cells but not the corresponding negative controls, indicating that HDAC3 can bind to CBFβ-SMMHC in inv(16) AML cells (Figure 15D).

We next asked if HDAC3 binds to CBFβ-SMMHC through RUNX1, the CBFβ region of the fusion protein, or the C-terminal 95 amino acids of the fusion. We transfected COS-7 cells with plasmids containing *HDAC3-FLAG, CBFB-MYH11*, *CBFB-MYH11* $_{\Delta 179\text{-}221}$, or *CBFB-MYH11*$_{N63K,\ N104K,\ \Delta 179\text{-}221}$ to test if RUNX1 binding to CBFβ-SMMHC was required for the observed interaction. Nuclear lysates were subjected to IP with an antibody against FLAG followed by western blot for SMMHC. The interaction between HDAC3 and CBFβ-SMMHC was maintained even when CBFβ-SMMHC was deficient for RUNX1 binding, indicating that RUNX1 is not required for HDAC3 binding (Figure 15E). We next performed COS-7 transfections followed by IP with anti-FLAG to test if HDAC3 could be binding to the CBFβ portion of the fusion. No interaction between HDAC3 and CBFβ was detected (Figure 15F). COS-7 cells transfected with *FLAG-HDAC3* and *CBFB-MYH11*$_{\Delta C95}$ followed by IP with anti-FLAG and western blot for SMMHC demonstrated HDAC3 was pulled down in the absence of the C-terminal 95 amino acids of SMMHC. In summary, this data demonstrates that RUNX1 is not required for HDAC3 binding to CBFβ-SMMHC and the binding site is somewhere on the SMMHC tail prior to the C-terminal 95 amino acids. However, this does not rule out the possibility that RUNX1 contributes to HDAC3 binding or that HDAC3 binding occurs through multiple regions or protein partners. These are the same binding parameters found for

HDAC1, suggesting that HDAC1 and HDAC3 could be binding to CBFβ-SMMHC in the same region and through the same mechanism.

To explore the possibility that HDAC3 could be important for CBFβ-SMMHC leukemogenic activity, we performed ChIP on cells from three independent *CM*$^{+}$ mice with antibodies against total rabbit IgG, RUNX1, SMMHC, or HDAC3 followed by qRT-PCR for CBFβ-SMMHC target genes. HDAC3 was enriched at the CBFβ-SMMHC target gene promoters *Cdkn1a*, *Mpo*, *Csf1r*, and *Cebpd* and colocalizes with RUNX1 and CBFβ-SMMHC at these promoters (Figure 15H). This implies that HDAC3 may also contribute to gene regulation in inv(16) AML.

5. HDAC1 inhibitors impair growth of CBFβ-SMMHC^{+} leukemia cells *in vitro*

Our results indicate that HDAC1 is important for CBFβ-SMMHC activity, implying that inv(16) AML cells may be particularly sensitive to treatment with an HDAC1 inhibitor. To test this possibility, we performed colony assays in the presence of entinostat (MS-275), an HDAC1 selective inhibitor (206,225). Equal numbers of cells were plated in the presence of 1 μM entinostat or vehicle and cultured for 14 days. We observed significantly fewer colonies in entinostat treated plates compared to control plates (Figure 16A). The individual colonies also appeared smaller and more diffuse (Figure 16B). After culture, the cells were stained for Gr-1 and Mac-1 expression. There was a large increase in Mac-1^{+}Gr-1^{+} staining, indicating a more differentiated phenotype (Figure 16C). Cytospins of these cells after colony assay confirmed morphological differentiation, with entinostat treated cells exhibiting a greater number of cells with high granularity, which is consistent with a more differentiated phenotype (Figure 16D).

To test if HDAC inhibitors (HDACi) had a similar effect on gene expression as *Hdac1* knockdown, we treated *CM*$^{+}$ mouse leukemia cells with entinostat. Similar to the

Figure 16. HDAC1 inhibitor entinostat reduces the growth of *CM*$^+$ cells *in vitro*. (**A**) *CM*$^+$ cells from three independent mice were plated in triplicate in MethoCult mixed with either 1 µM entinostat or DMSO. Colonies were manually counted 14 days later and plotted as relative colony forming units compared to DMSO control. (**B**) Representative images of colonies from DMSO treated (top) or entinostat (bottom) plates. Scale bar represents 200 µm. (**C**) *CM*$^+$ cells were stained following the colony-forming assay for myeloid differentiation markers Gr-1 and Mac-1 and analyzed by flow cytometry. (**D**) Unstained cells from (C) were adhered to slides using a cytospin, stained with Wright-Giemsa, and imaged at 100x magnification. (**E**) *CM*$^+$ leukemia cells were treated with 1 µM entinostat for 24 hours. cDNA was analyzed by qRT-PCR using primers for the indicated genes. (**F**) ME-1 cells were treated with increasing doses of entinostat and cell viability was analyzed with PrestoBlue viability reagent. EC_{50} was calculated using GraphPad Prism. Error bars represent SEM. Student's t-test was used to calculate statistical significance. * = $p \leq 0.05$, *** = $p \leq 0.001$, n.s. = not significant.

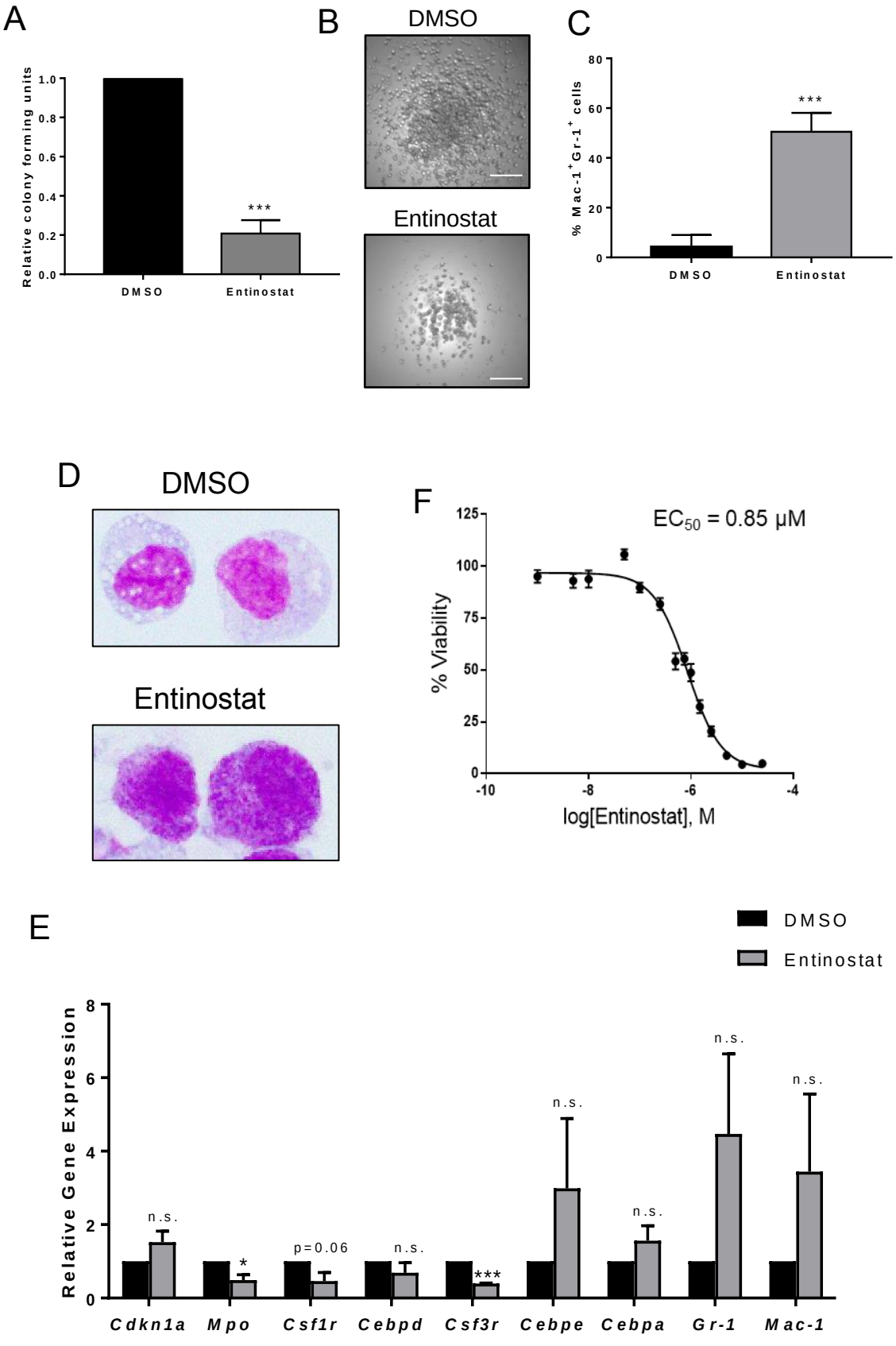
A
Relative colony forming units
1.0
0.8
0.6
0.4
0.2
0.0
***
DMSO
Entinostat
B
DMSO
Entinostat
C
% Mac-1+Gr-1+ cells
80
60
40
20
0
***
DMSO
Entinostat
D
DMSO
Entinostat
F
EC50 = 0.85 µM
% Viability
125
100
75
50
25
0
-10
-8
-6
-4
log[Entinostat], M
E
DMSO
Entinostat
Relative Gene Expression
8
6
4
2
0
n.s.
*
p=0.06
n.s.
***
n.s.
n.s.
n.s.
n.s.
Cdkn1a
Mpo
Csf1r
Cebpd
Csf3r
Cebpe
Cebpa
Gr-1
Mac-1

Hdac1 knockdown, we saw a trend of decreased gene expression for *Mpo*, *Csf1r*, and *Cebpd*, although not for *Cdk1na* (Figure 16E). We tested additional myeloid differentiation genes to determine if some genes were upregulated by HDAC1 inhibition, and found that *Cebpe*, *Cebpa*, *Gr-1* (*Ly6g*), and *Mac-1* (*Itgam*) mRNA expression showed a trend towards upregulation in entinostat treated cells, although not to levels of statistical significance, while the early granulopoiesis marker *Csf3r* was significantly downregulated. This data demonstrates that entinostat causes changes in gene expression similar to our results above with *Hdac1* knockdown and to previous findings with loss of CBFβ-SMMHC (14).

To test the effect of HDACi on human inv(16) AML cells, we treated ME-1 cells with increasing doses of entinostat and assayed for cell viability. ME-1 cells showed a dose-dependent decrease in viability over the range of concentrations tested, with an EC_{50} of 0.85 μM (Figure 16F). This indicates that human CBFβ-SMMHC-expressing cells are also sensitive to treatment with HDACi.

We next asked whether other HDACi have similar effects on *CM*$^+$ leukemia cells. To test this, we performed colony assays with cells from three *CM*$^+$ mice cultured in methylcellulose containing DMSO or 1 μM vorinostat. Vorinostat (SAHA) is an FDA-approved HDACi which targets HDAC1, 2, 3, 6, 8, and 10 (259). We saw a significant reduction in the number of colonies that grew on plates containing vorinostat, suggesting a decrease in *CM*$^+$ stem cell activity (Figure 17A). After colony assay, cells were stained for Gr-1 and Mac-1 expression. Vorinostat treated cells were significantly increased in Mac-1 staining and were enriched for Gr-1 and Gr-1/Mac-1 double-positive cells (Figure 17B). Because we found that HDAC3 also binds to CBFβ-SMMHC, we also tested the HDAC3 specific inhibitor RGFP966 on *CM*$^+$ leukemia cells (208). In colony assays, *CM*$^+$ cells cultured in methylcellulose with 1 μM RGFP966 did not have significantly fewer colonies compared to the control (Figure 17C). Staining for Mac-1 and Gr-1 expression

Figure 17. Other HDAC inhibitors have a negative effect on *CM*$^+$ cell growth. (**A**) *CM*$^+$ cells from three independent mice were plated in triplicate in MethoCult mixed with either 1 µM vorinostat or DMSO. Colonies were manually counted 14 days later and plotted as relative colony forming units compared to DMSO control. (**B**) *CM*+ cells were stained following the colony-forming assay for myeloid differentiation markers Gr-1, Mac-1, or double positive populations and analyzed by flow cytometry. (**C**) *CM*+ cells from three independent mice were plated in triplicate in MethoCult mixed with 1 µM of RGFP966 or DMSO. Colonies were manually counted 14 days later and plotted as relative colony forming units (CFU) compared to DMSO control. (**D**) Cells from (C) were stained and analyzed by flow cytometry for Mac-1 and Gr-1 expression after completion of colony assay.(**E**) ME-1 cells were treated with increasing doses of RGFP966 and cell viability was analyzed with PrestoBlue viability reagent. Error bars represent the standard error of the mean (SEM). Graphpad Prism software was used to calculate EC_{50} (D) and Student's t-test was used to calculate statistical significance (A,B,C). ** = p≤0.01, *** = p≤0.001, n.s. = not significant.

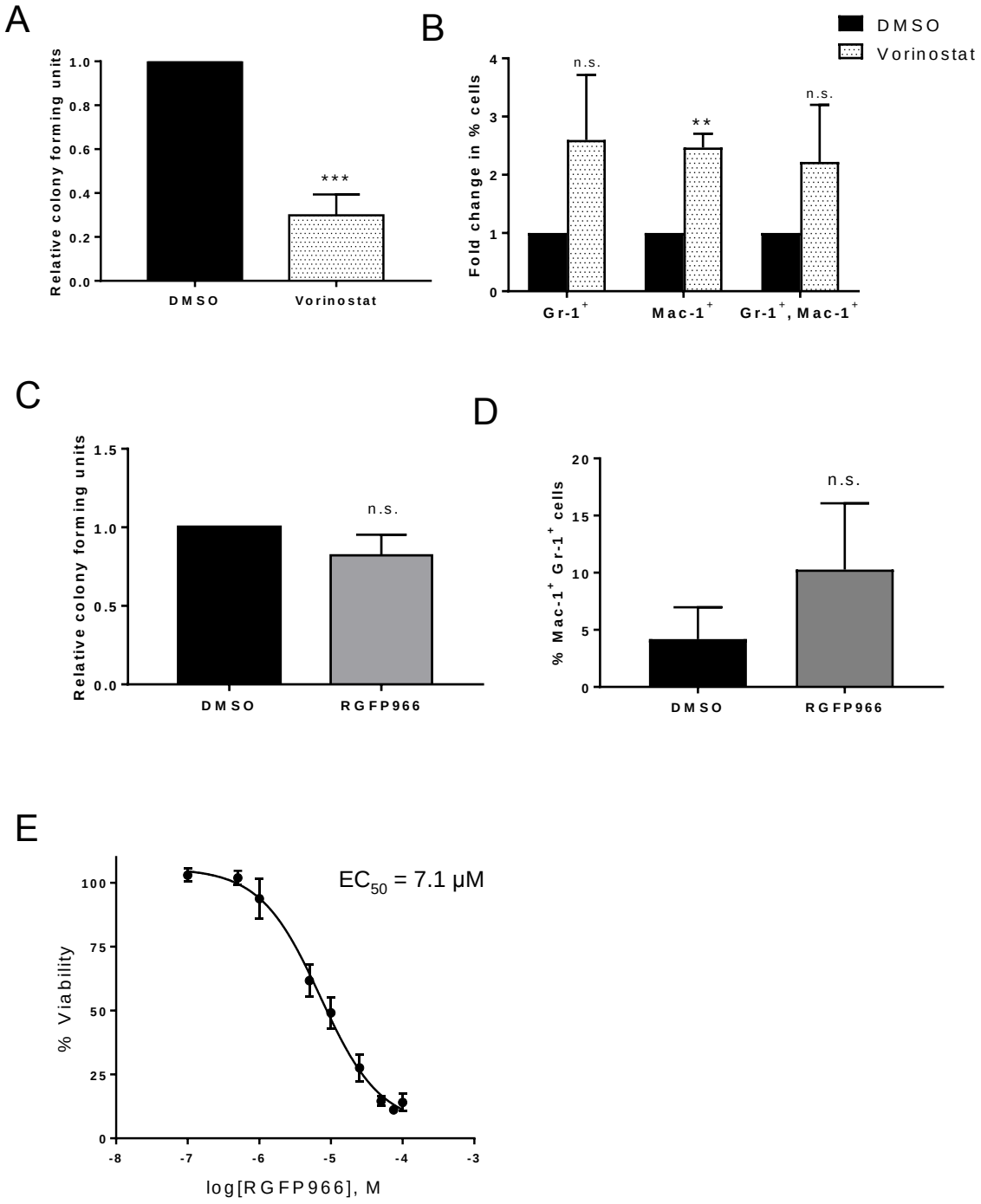
A
Relative colony forming units
1.0
0.8
0.6
0.4
0.2
0.0
***
DMSO
Vorinostat
B
DMSO
Vorinostat
Fold change in % cells
4
3
2
1
0
n.s.
**
n.s.
Gr-1+
Mac-1+
Gr-1+, Mac-1+
C
Relative colony forming units
1.5
1.0
0.5
0.0
n.s.
DMSO
RGFP966
D
% Mac-1+ Gr-1+ cells
20
15
10
5
0
n.s.
DMSO
RGFP966
E
EC50 = 7.1 μM
% Viability
100
75
50
25
0
-8
-7
-6
-5
-4
-3
log[RGFP966], M

after colony assay showed a modest enrichment in Mac-1^{+}Gr-1^{+} cells in RGFP966 treated cells (Figure 17D). ME-1 cells cultured with increasing doses of RGFP966 had dose-dependent viability and an EC_{50} of 7.1 μM, indicating that they were sensitive to treatment with an HDAC3 inhibitor, but less so than to entinostat (Figure 17E). Therefore, the 1 μM concentration used in the colony assay may not have been close enough to the EC_{50} to see a significant decrease in colonies compared to control. Overall, this data suggests that inhibitors which target HDACs known to bind to CBFβ-SMMHC have a negative effect on *CM*$^{+}$ leukemia cell growth.

To test the effect of HDACi's on normal hematopoiesis, we performed colony-forming assays with bone marrow cells from healthy wild-type mice. Importantly, there was no significant difference in the growth of any type of colony in the presence of either entinostat or vorinostat, as compared to DMSO (Figure 18A and B). These results indicate CBFβ-SMMHC-expressing leukemia cells are more sensitive to the effects of HDAC inhibitors than normal hematopoietic cells.

Our data indicates that HDAC1 is required for CBFβ-SMMHC induced gene expression, implying that HDAC1 and RUNX1 are acting in the same pathway. To test this, we treated leukemia cells with either entinostat, the RUNX1 inhibitor Ro5-3335, or both entinostat and Ro5-3335 (11). Either Ro5-3335 or entinostat alone significantly reduced colony growth, as compared to control (Figure 19A). The combination of Ro5-3335 and entinostat significantly reduced the number of colonies compared to DMSO and Ro5-3335 alone but did not further inhibit colony growth compared to entinostat alone, suggesting that these drugs are inhibiting the same pathway (Figure 19A). Neither drug, alone or in combination, had any significant effect on the colony growth of normal bone marrow cells, indicating that CBFβ-SMMHC-expressing leukemia cells are more sensitive to loss of either RUNX1 or HDAC1 activity than normal blood cells (Figure 19B).

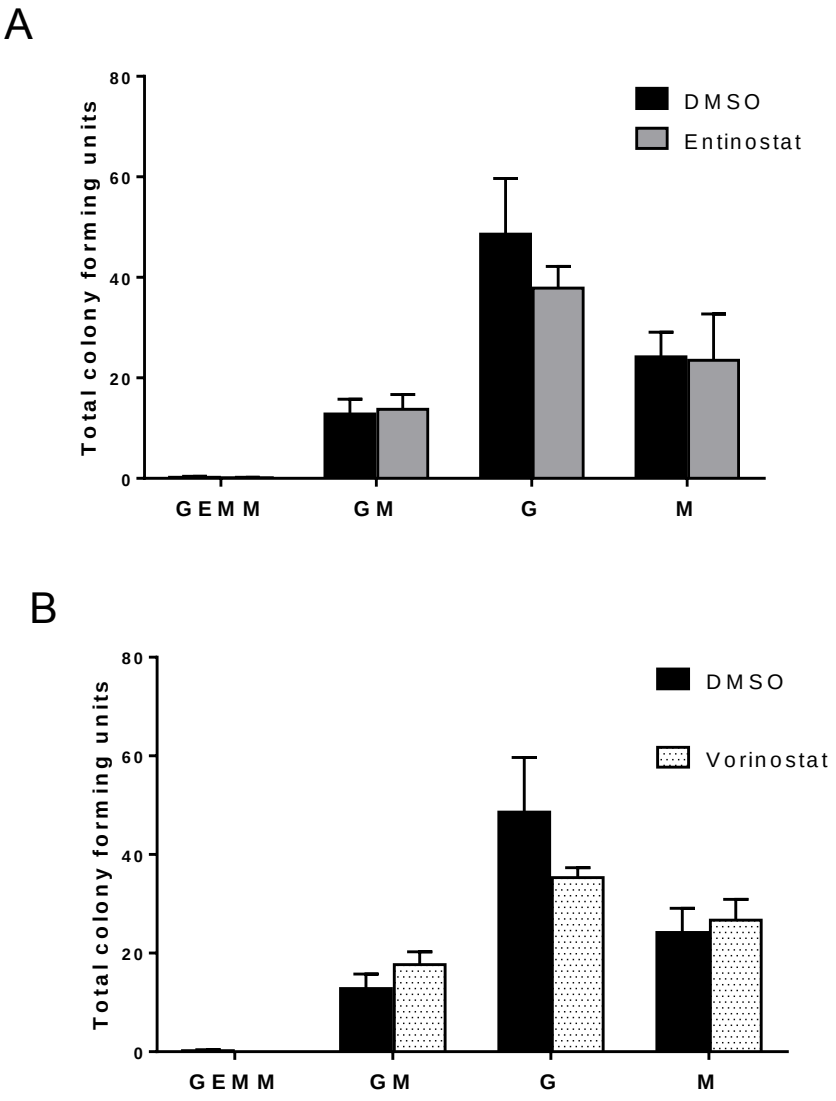

Figure 18. HDACi are not toxic to stem cells in healthy bone marrow. Bone marrow from three different healthy wild-type mice was plated in triplicate in MethoCult with 1 μM (**A**) entinostat or (**B**) vorinostat or DMSO control. Colonies were manually counted 14 days later and classified according to their constituent cells. Data is plotted as total colony forming units (CFU) for each type of colony. All comparisons between DMSO and treatment are non-significant for each colony type using Student's t-test. Abbreviations: GEMM, granulocyte-erythrocyte-monocyte-megakaryocyte; GM, granulocyte-macrophage; G, granulocyte; M, macrophage.

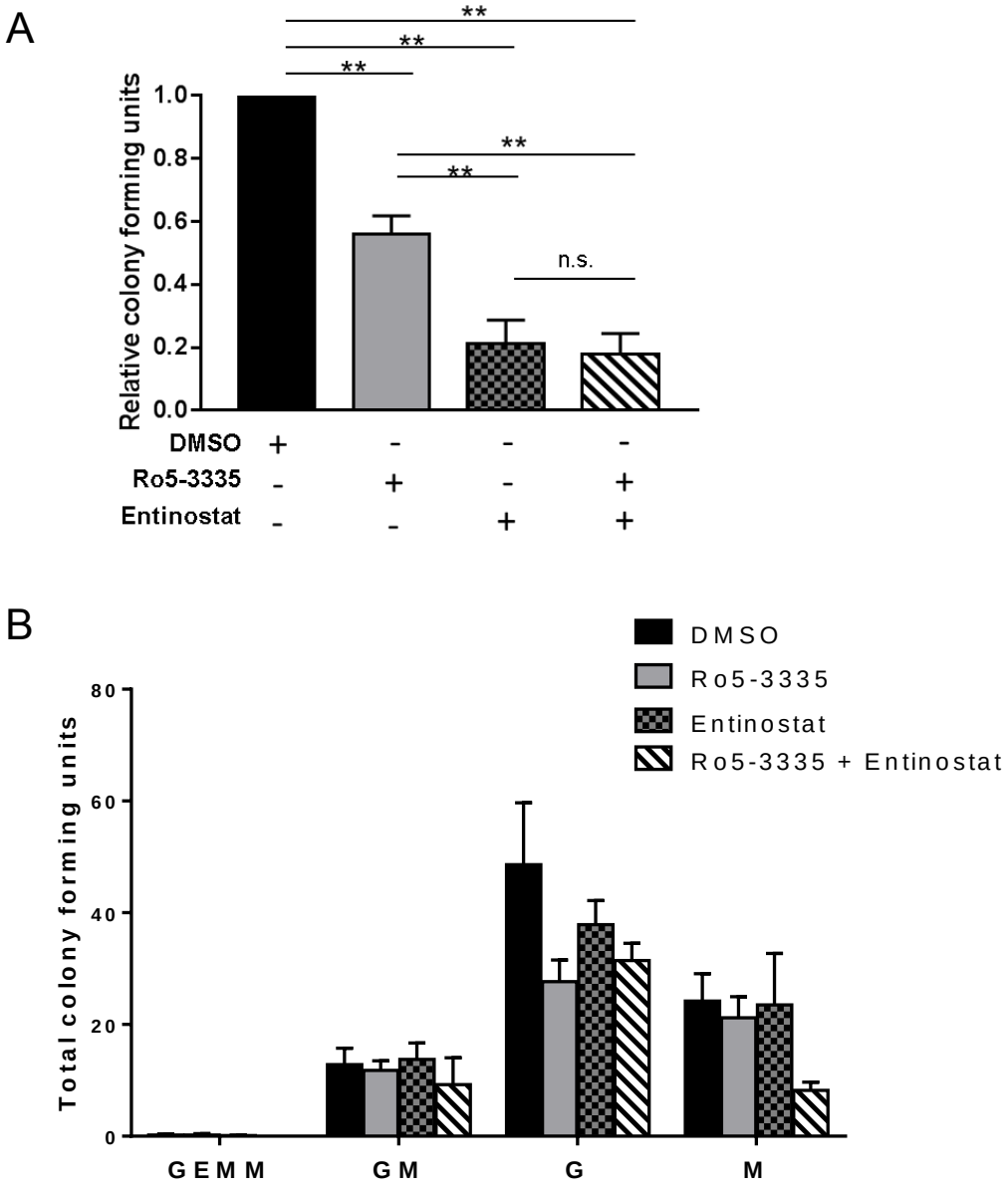

Figure 19. RUNX1 and HDAC1 inhibition likely target an overlapping pathway in *CM*$^+$ cells. (**A**) *CM*$^+$ cells from three independent mice were plated in triplicate in MethoCult mixed with 1 μM of the indicated combinations of Ro5-3335, entinostat, or DMSO. Colonies were manually counted 14 days later and plotted as relative colony forming units (CFU) compared to DMSO control. (**B**) Wild-type mouse bone marrow was plated as in (A) and colonies were counted and classified according to their constituent cells. Data is plotted as total CFU's for each type of colony. Error bars represent SEM. ANOVA was used to calculate statistical significance. ** = p≤0.01, n.s = not significant. Abbreviations: GEMM, granulocyte-erythrocyte-monocyte-megakaryocyte; GM, granulocyte-macrophage; G, granulocyte; M, macrophage.

6. Entinostat decreases leukemic burden *in vivo*

Entinostat treatment reduced *CM*$^{+}$ colony growth *in vitro*, suggesting that it may be effective against *CM*$^{+}$ leukemia *in vivo*. Before we tested entinostat treatment on mice with leukemia, we performed a toxicity study in healthy wild-type mice. Three mice were treated with 30 mg/kg/day entinostat or vehicle control by IP injection for 5 days. There were no observed complications during treatment. The day after the last treatment, tissues were harvested for histology and peripheral blood was collected for complete blood counts. In the peripheral blood, entinostat treatment decreased the white blood cell count below the normal range, specifically by depleting the monocyte population (Table 6). Histological analysis of the bone marrow showed mild erythroid hypoplasia in entinostat treated mice but comparable cellularity between the two groups (Figure 20). In the spleens, histological analysis showed expanded red pulp with focal extramedullary hematopoiesis in entinostat treated mice compared to controls (Figure 20). Overall, the results show that *in vivo* treatment with entinostat causes mild effects in normal cells in the bone marrow, spleens, and peripheral blood of healthy mice but that the treatment is relatively well tolerated. Therefore, we proceeded to test entinostat in leukemic mice. We predicted that entinostat would target the leukemic cells because HDAC1 expression was higher in *CM*$^{+}$ leukemic cells versus normal bone marrow and because we predict HDAC2 can compensate for loss of HDAC1 in normal cells but not in *CM*$^{+}$ leukemic cells.

We transplanted *CM*$^{+}$ primary mouse leukemia samples that also express GFP from the Rosa26 locus (*Cbfb*$^{+/56M}$*, Mx1-Cre*$^{+}$*, Rosa26*$^{tdT/GFP}$) into sub-lethally irradiated congenic recipient mice (237). This system allows us to analyze the effects of drug treatment on both the transplanted, GFP^{+} leukemia cells, and the recipient mouse's GFP^{-}, normal blood cells. Two to three weeks later, peripheral blood was analyzed to

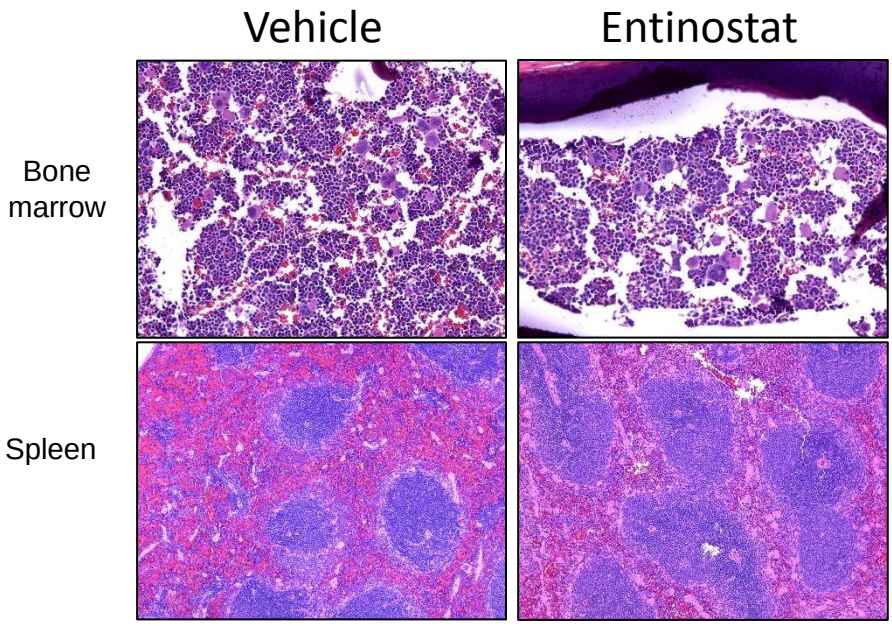

Figure 20. Entinostat treatment is not overtly toxic to wild-type mice. Mice were treated with 30 mg/kg/day entinostat or vehicle by IP injection for five consecutive days. Representative H&E stained tissue sections from bone marrow and spleen taken at 10x magnification are shown.

Table 6. Results from complete blood counts after entinostat treatment in wild-type mice. Results which are outside of the normal range are in red. Abbreviations: RBC, red blood cells. WBC, white blood cells. Hgb, hemoglobin. Hct, hematocrit. MCV, mean corpuscular volume.

	Vehicle	Entinostat	Normal Range (C57/Bl6 Charles River)
RBC (M/uL)	10.79	9.9	7.14 - 12.2
WBC (K/uL)	5.3	1.07	4.45 - 13.96
Hgb (g/dL)	16.17	14.4	10.8 - 19.2
Hct (%)	49.37	45.53	37.3 - 58.0
MCV (fL)	46	46	42.7 - 56.0
Neutrophils (%)	18.9	14.8	7.36 -28.59
Lymphocytes (%)	75.57	80.26	61.26 - 87.18
Monocytes (%)	3.63	0	2.18 - 11.02
Eosinophils (%)	2.43	2.06	0.13 - 4.42
Basophils (%)	0.013	1.43	0.01 - 1.24

confirm leukemia engraftment, and mice were treated for 7 days with 10 mg/kg/day entinostat or vehicle. The day after the last treatment, mice were sacrificed, and blood and tissue were harvested (Figure 21A). Mice treated with entinostat showed significant reductions in the number of leukemia cells in the peripheral blood, as determined by GFP or Kit expression (Figure 21B-D). In the entinostat treated mice, the remaining GFP^+ leukemia cells in the peripheral blood showed increased expression of both Mac-1 and Gr-1, consistent with our *in vitro* data (Figure 21E). There was a trend towards increased annexin V^+ staining in the GFP^+ leukemia cells in the peripheral blood, although this difference did not achieve statistical significance (Figure 21F). There was a parallel decrease in GFP^+ cells in the lineage-depleted (lin^-) bone marrow of entinostat treated mice (Figure 22A). The remaining GFP^+ cells in the bone marrow showed a small, but statistically significant increase in annexin V^+ staining (Figure 22B). Cell cycle analysis of lin^- bone marrow showed no differences between vehicle and entinostat treated mice (Figure 22C).

Entinostat treated mice also had smaller spleens and significantly decreased spleen weights (Figure 23A). Histological examination showed decreased leukemic infiltration in the spleen (Figure 23B). As a control for entinostat activity in the mice, western blot was performed on whole cell lysates made from spleen tissue. Acetyl-histone H4 expression was increased relative to total histone H4 in entinostat treated mice compared to controls, indicating that entinostat inhibited HDAC activity *in vivo* (Figure 24).

Entinostat treatment did not cause an increase in annexin V, Mac-1, or Gr-1 staining in the GFP^- cells, indicating that entinostat does not induce apoptosis or differentiation of normal blood cells (Figure 25A and B). These findings indicate that entinostat specifically targets CBFβ-SMMHC-expressing leukemia cells and promotes their differentiation *in vivo*.

Figure 21. Entinostat treatment decreases leukemic burden in the peripheral blood of mice with *CM*$^{+}$ leukemia. (**A**) Representative plots from flow cytometry analysis of Kit and GFP in peripheral blood. (**B**) Flow cytometry analysis on peripheral blood for GFP (leukemia cell population) after treatment (left) and GFP cells in each mouse pre-treatment (pre) with DMSO or entinostat and post-treatment (post) (right). Each line represents one individual mouse. (**C**) Percentage of Kit^{+} cells in peripheral blood (left) and percentage of Kit^{+} cells pre- and post-treatment (right). Each line represents one individual mouse. (**D**) Flow cytometry analysis of the percentage of Mac-1^{+}Gr-1^{+} cells within the GFP^{+} cell compartment. (**E**) Flow cytometry analysis of the percentage of annexin V^{+} cells within the GFP^{+} cell compartment. Each dot on bar graphs represents one individual mouse. Error bars represent SEM. Student's t-test was used to calculate statistical significance. * = p≤0.05, ** = p≤0.01, *** = p≤0.001, n.s. = not significant.

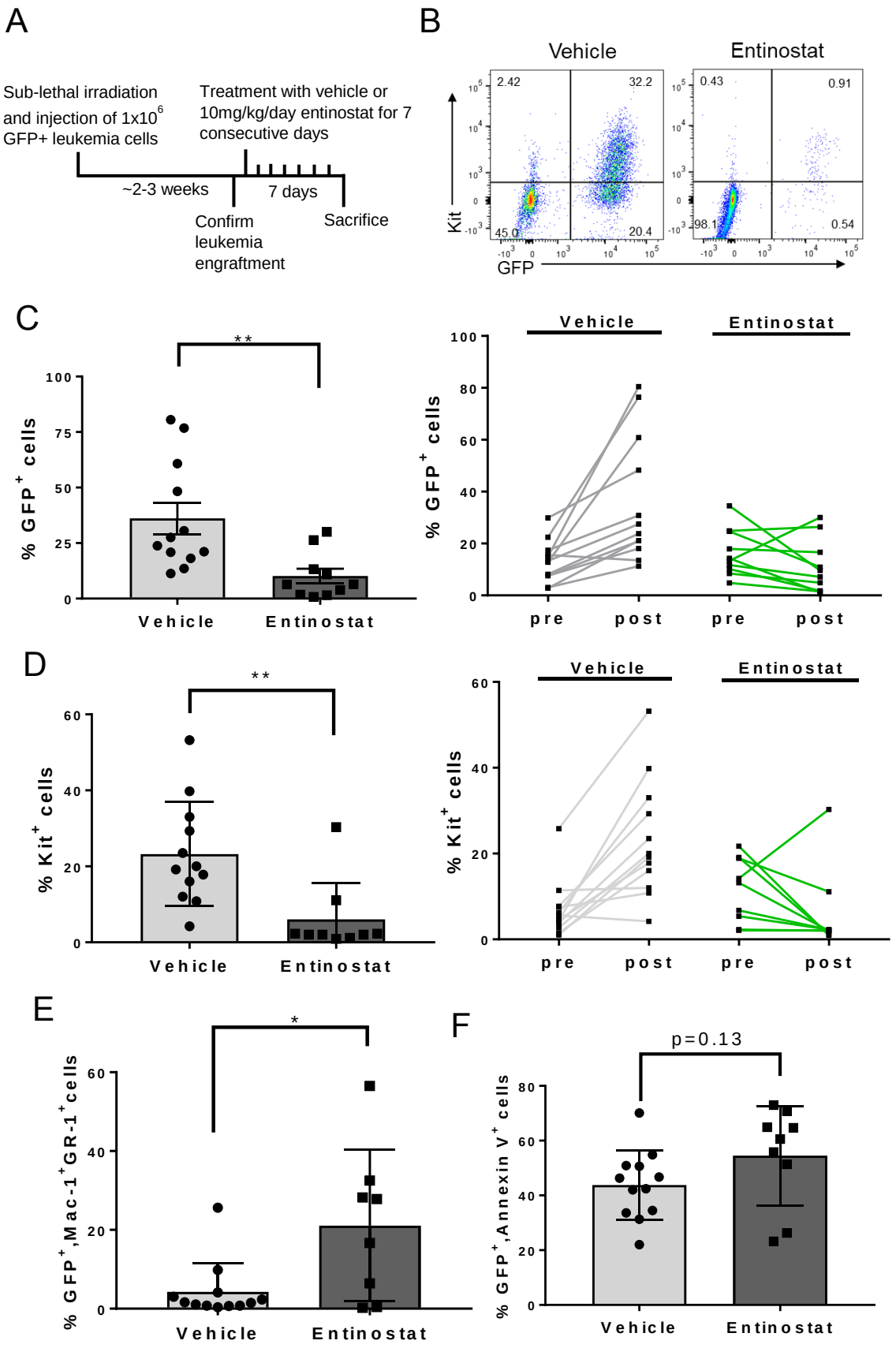
A
Sub-lethal irradiation and injection of 1x10^6 GFP+ leukemia cells
Treatment with vehicle or 10mg/kg/day entinostat for 7 consecutive days
~2-3 weeks
7 days
Confirm leukemia engraftment
Sacrifice
B
Vehicle
Entinostat
2.42
32.2
45.0
20.4
0.43
0.91
98.1
0.54
Kit
GFP
C
% GFP+ cells
Vehicle
Entinostat
pre
post
D
% Kit+ cells
E
% GFP+,Mac-1+GR-1+cells
F
p=0.13
% GFP+,Annexin V+ cells

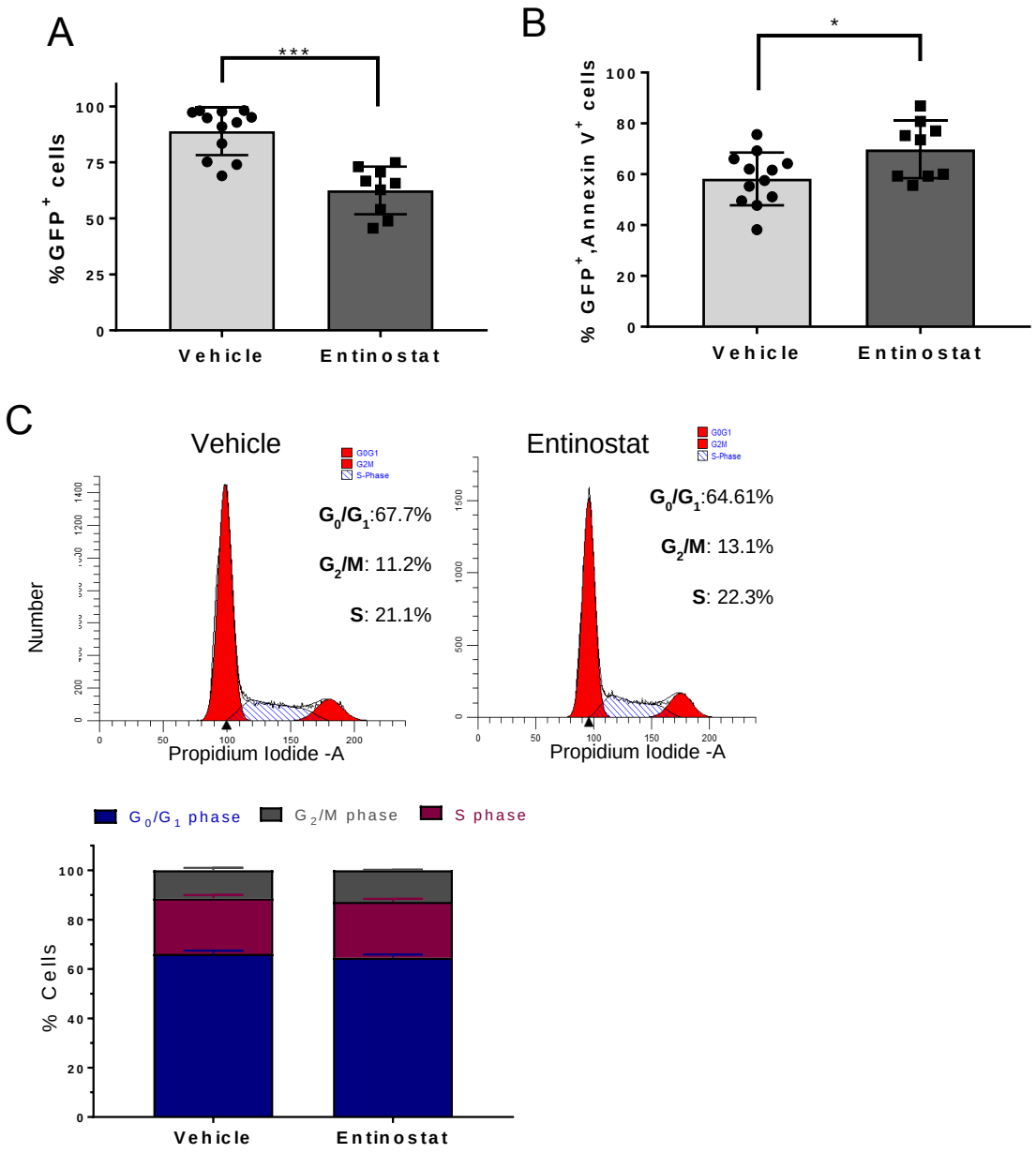

Figure 22. Entinostat treatment decreases leukemic burden and increases apoptosis of leukemia cells in bone marrow of mice with *CM*$^+$ leukemia. (A) Flow cytometry analysis of the percentage of GFP$^+$ cells in lin$^-$ bone marrow. (**B)** Flow cytometry analysis of the percentage of annexin V$^+$ cells in the GFP$^+$ compartment of the lin$^-$ bone marrow. (**C**) Flow cytometry analysis of cell cycle in lin$^-$ bone marrow fixed and stained with Telford Reagent. Representative images obtained with ModFit and quantification of cell cycle analysis. Each dot on bar graphs represents one individual mouse. Error bars represent SEM. Student's t-test was used to calculate statistical significance. * = p≤0.05, *** = p≤0.001.

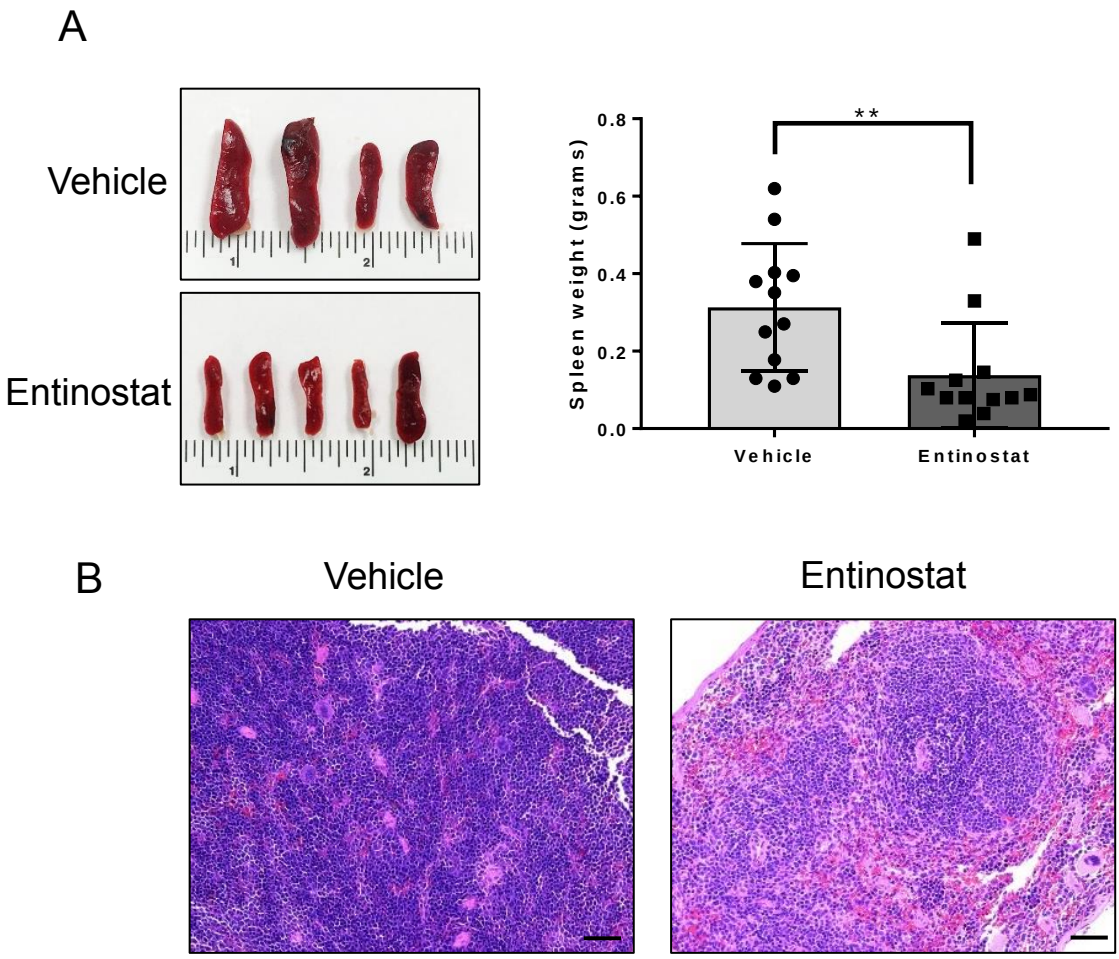

Figure 23. Entinostat treatment decreases leukemic burden in the spleens of mice with *CM*$^{+}$ leukemia. (**A)** Representative images of DMSO or entinostat treated spleens (left) and quantification of spleen weights (right). (**B**) Representative H&E stained images of spleen sections after treatment taken at 20x magnification. Scale bar = 50 μm. Each dot on bar graphs represents one individual mouse. Error bars represent SEM. Student's t-test was used to calculate statistical significance. ** = p≤0.01

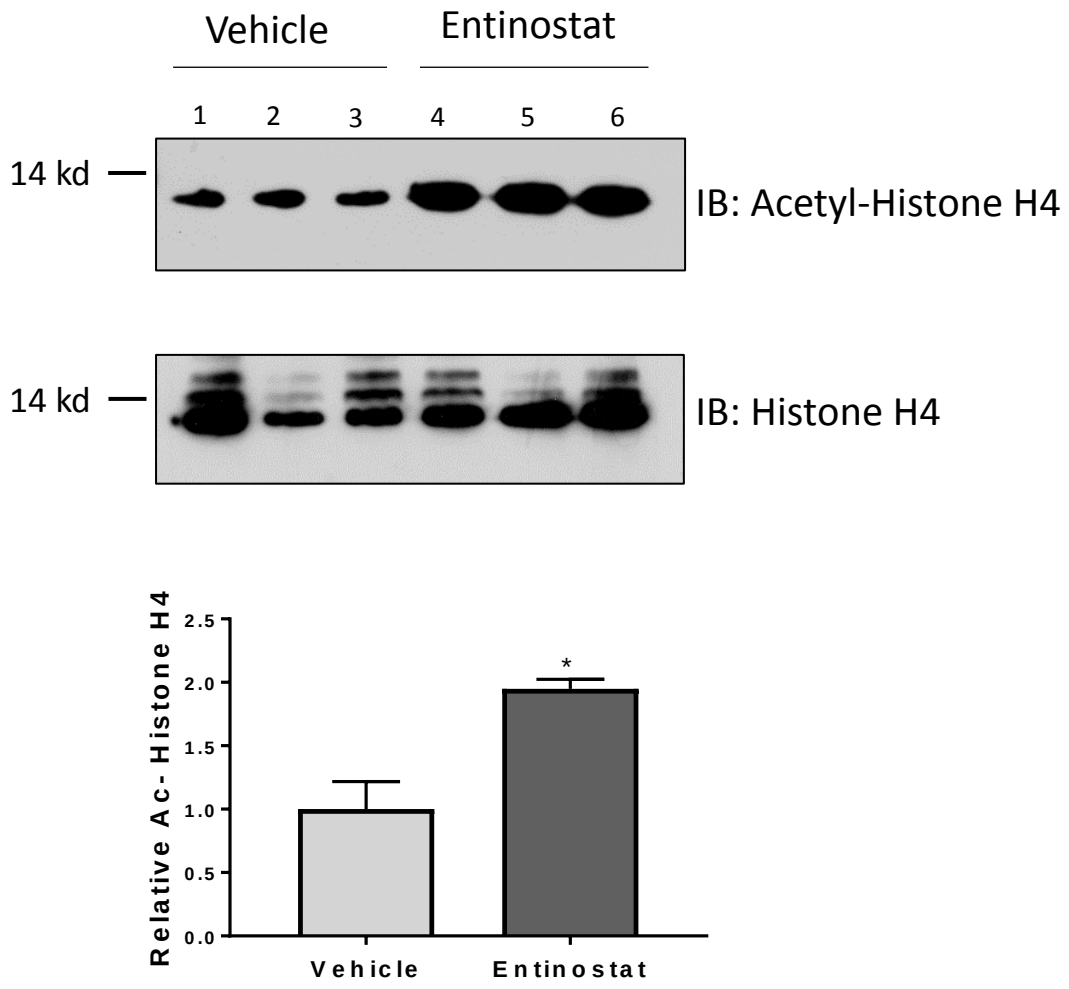

Figure 24. Histone acetylation levels are increased in the spleen cells of entinostat treated mice. Whole cell lysates were made from spleens of three vehicle control and three entinostat treated mice. Western blots were performed and blots were probed for acetylated histone H4 (Ac-histone H4), followed by stripping and reprobing for total histone H4. Quantification of band intensity is shown below. ImageJ was used for densitometry analysis. Student's t-test was used to calculate statistical significance. Error bars represent the SEM. * = $p \leq 0.05$

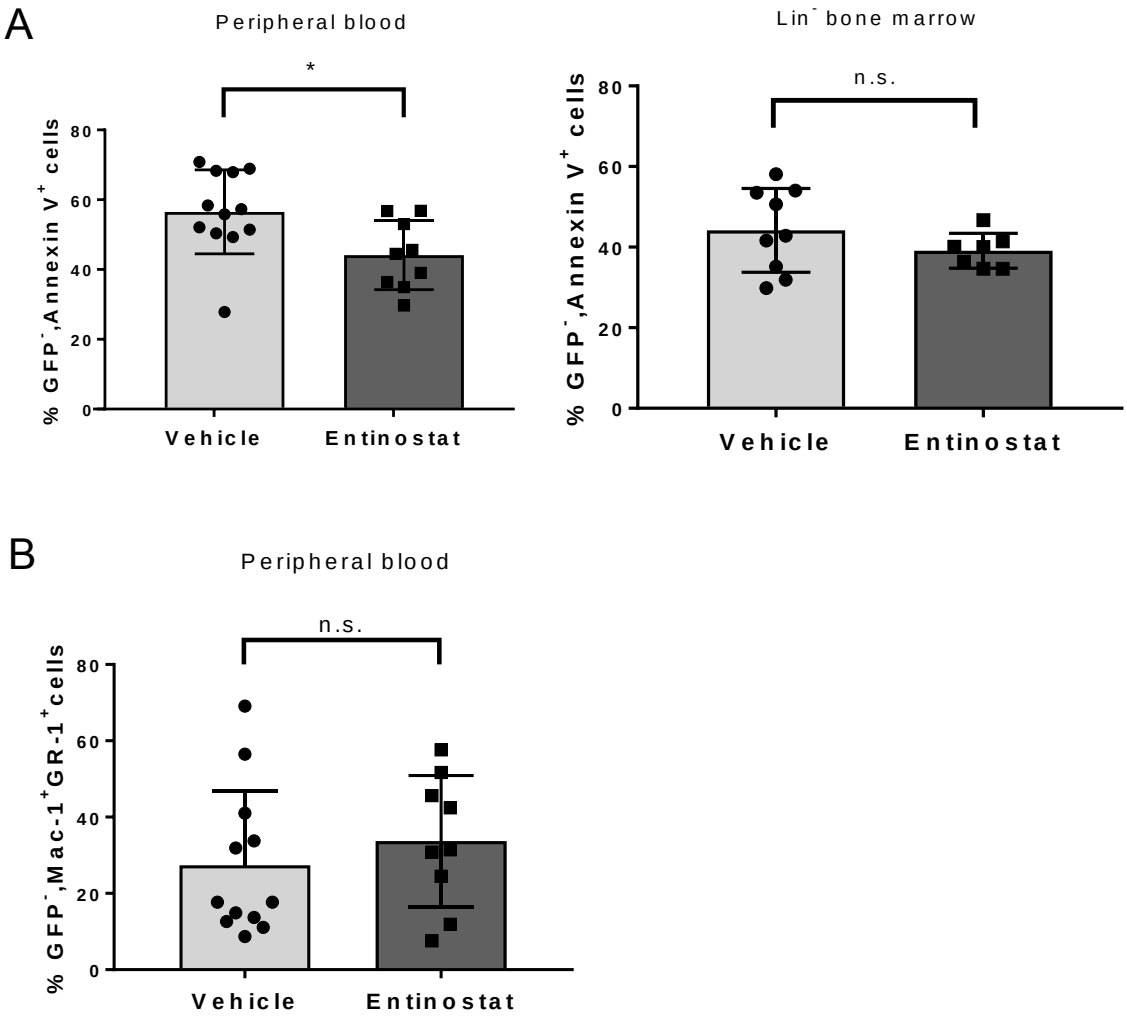

Figure 25. Entinostat does not affect normal blood cells. (**A**) Flow cytometry analysis of the percentage of annexin V^+ cells within the GFP^- cell compartment in the peripheral blood (left) or bone marrow (right). (**B**) Flow cytometry analysis of the percentage of $Mac\text{-}1^+Gr\text{-}1^+$ cells within the GFP^- cell compartment in the peripheral blood. Student's t-test was used to calculate statistical significance. Error bars represent the SEM. * = $p \leq 0.05$, n.s.= not significant.

7. Entinostat treatment increases survival only in certain samples of *CM*$^+$ leukemia

Because entinostat treatment had major effects on *CM*$^+$ leukemia cells analyzed immediately after cessation of treatment, we asked whether this treatment scheme would also impact long-term survival of mice with *CM*$^+$ leukemia. We performed three independent experiments, each with a separate sample of *CM*$^+$ leukemia that originated from an independent mouse, and monitored the mice by retro-orbital eye bleeds and visual assessment for signs of leukemia. The combined data for the three samples showed no difference in survival time between vehicle and entinostat treated mice (Figure 26A). However, each individual sample had a different effect on survival. One had a significant increase in survival with entinostat treatment (Figure 26B), one had a trend towards increased survival (Figure 26C), and one had a trend towards decreased survival with entinostat treatment (Figure 26D).

We also monitored GFP in the peripheral blood during the experiment and found that the percentage of GFP$^+$ cells tended to increase over time, indicating that the remaining leukemia cells continue to proliferate after cessation of treatment. The third clone had a strange pattern of expression in which the GFP$^+$ cell percentage decreased over time for both the vehicle and entinostat treated mice (Figure 26D). This could indicate that there were non-GFP$^+$ leukemia cells that got missorted and eventually outcompeted the GFP$^+$ counterparts for growth or that there was selective pressure to turn off GFP expression. Altogether, this data suggests that there may be inherent differences between leukemia samples that determine their susceptibility to entinostat treatment. In addition, a short course of entinostat treatment is not sufficient to prevent the outgrowth of residual leukemia cells.

Figure 26. Entinostat treatment increases overall survival only in mice with leukemia from certain samples of *CM*$^+$ cells. (A) Kaplan-Meier survival curve combining data from three independent *CM*$^+$ leukemia samples. (**B, C, D)** Kaplan-Meier survival curve for each individual sample of *CM*$^+$ leukemia (left) and flow cytometry analysis of GFP$^+$ cell percentage in the peripheral blood monitored during the survival experiment (right). Error bars represent the SEM. Statistical significance for survival was calculated in GraphPad Prism using the Log-Rank test. ** = p≤0.01

A

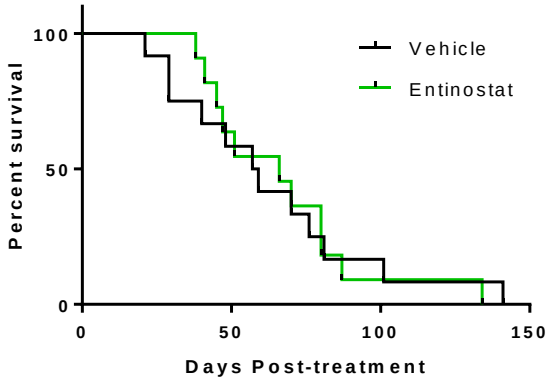
Percent survival
100
50
0
0
50
100
150
Days Post-treatment
Vehicle
Entinostat

B

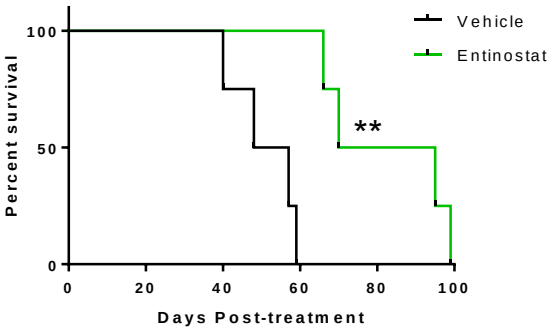
Percent survival
100
50
0
0
20
40
60
80
100
Days Post-treatment
Vehicle
Entinostat
**

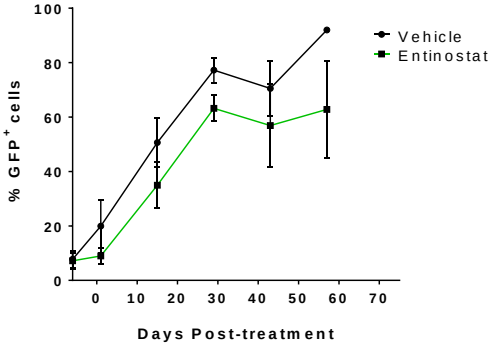
% GFP+ cells
100
80
60
40
20
0
0
10
20
30
40
50
60
70
Days Post-treatment
Vehicle
Entinostat

C

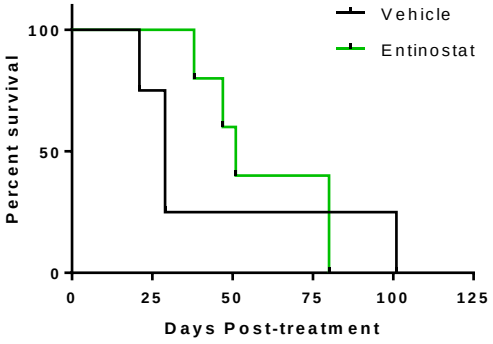
Percent survival
100
50
0
0
25
50
75
100
125
Days Post-treatment
Vehicle
Entinostat

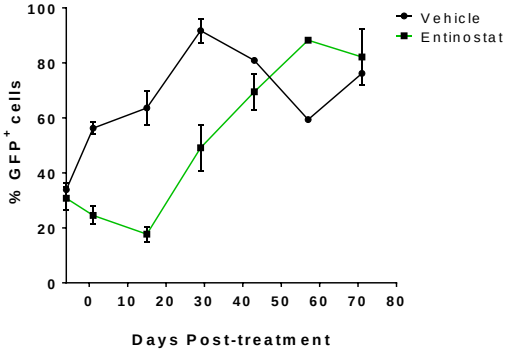
% GFP+ cells
100
80
60
40
20
0
0
10
20
30
40
50
60
70
80
Days Post-treatment
Vehicle
Entinostat

D

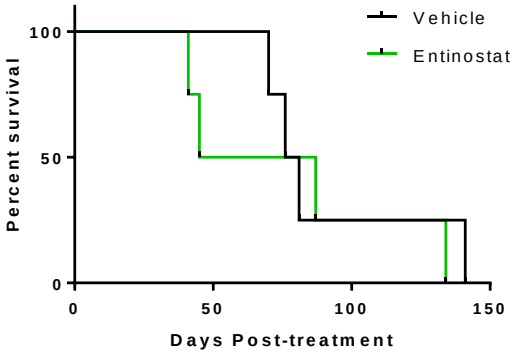
Percent survival
100
50
0
0
50
100
150
Days Post-treatment
Vehicle
Entinostat

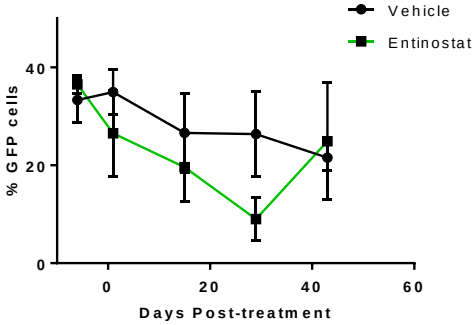
% GFP cells
40
20
0
0
20
40
60
Days Post-treatment
Vehicle
Entinostat

8. *Hdac1* knockdown *in vivo* mimics entinostat treatment in mice with *CM*$^+$ leukemia

We next asked whether the effects of entinostat treatment in mice with *CM*$^+$ leukemia were specifically caused by HDAC1 inhibition rather than off-target effects. To test this, we generated a *CM*$^+$ leukemia sample with stable integration of an IPTG-inducible shRNA targeting *Hdac1* and GFP expressed from an IRES. These cells were injected into sub-lethally irradiated wild-type mice and monitored for leukemia development as above. Leukemic mice were treated with or without 10 mM IPTG in the water bag for seven days. Treated mice had inconsistent knockdown of *Hdac1* (Figure 27A). However, mice which did have successful knockdown showed decreased GFP$^+$ cells in the peripheral blood (Figure 27B), smaller spleen sizes (Figure 27C), and a reduction of infiltrating leukemic cells in the spleen (Figure 27D). The overall implications of this experiment are that HDAC1 is required for *CM*$^+$ leukemia *in vivo* and that HDAC1 is the critical target for entinostat in *CM*$^+$ leukemia. It is also notable that this experiment genetically depletes *Hdac1* specifically in the leukemia cell compartment of sick mice, implying that it is HDAC1 in leukemia cells and not the leukemia-supporting microenvironment that is critical for the survival of *CM*$^+$ cells.

Figure 27. *Hdac1* knockdown *in vivo* mimics the effects of entinostat treatment. (A) After exposure to 10 mM IPTG for seven days in the water bag, spleen tissue was collected, sorted for GFP^+ cells, and analyzed for *Hdac1* mRNA expression by qRT-PCR. Expression was normalized to beta-actin. Data is plotted as relative level of *Hdac1* mRNA compared to control mice. **(B)** At the time of sacrifice, peripheral blood was collected and analyzed by flow cytometry for GFP. **(C)** Representative images of control or IPTG treated spleens (left) and quantification of spleen weights (right). (**D**) Representative H&E stained images of spleen sections after treatment taken at 10x (scale bar = 100 um) or 20x (scale bar = 50 um) magnification. Each dot on bar graphs represents one individual mouse. Error bars represent SEM. Student's t-test was used to calculate statistical significance. * = $p \leq 0.05$, n.s.=not significant.

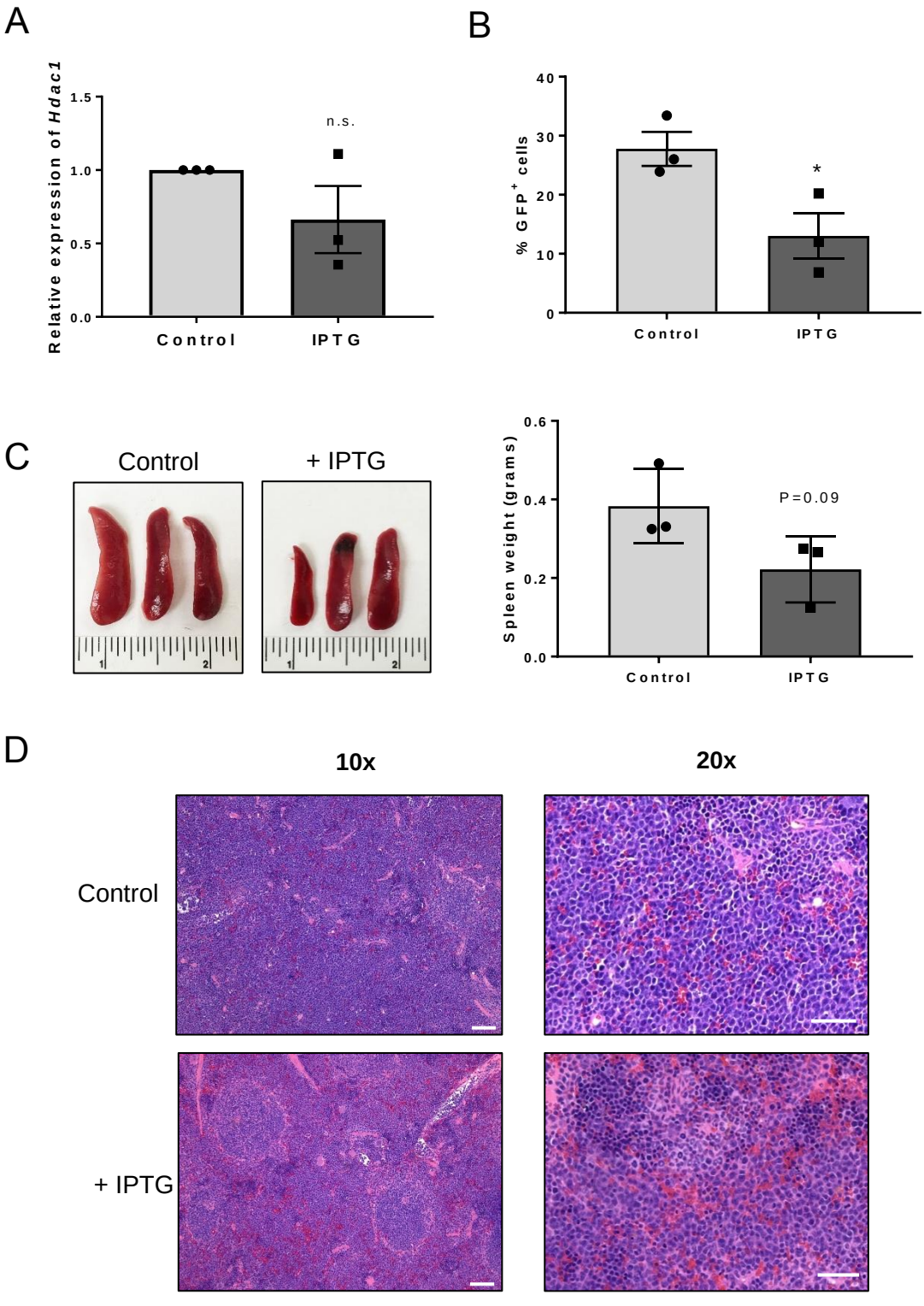
A
Relative expression of Hdac1
1.5
1.0
0.5
0.0
n.s.
Control
IPTG
B
% GFP+ cells
40
30
20
10
0
*
Control
IPTG
C
Control
+ IPTG
Spleen weight (grams)
0.6
0.4
0.2
0.0
P=0.09
Control
IPTG
D
10x
20x
Control
+ IPTG

Chapter IV

Discussion

CBFβ-SMMHC expression is known to be the initiating event in inv(16) AML, but it is less clear what role the fusion protein has after leukemic transformation. Early models suggested that CBFβ-SMMHC acts as a repressor of RUNX1 by outcompeting CBFβ for binding (31,39,106,117). More recent work indicates that CBFβ-SMMHC has a direct role in gene expression, likely acting as part of a transcription factor complex requiring RUNX1 (14,18,120). This raises the possibility that other transcriptional regulators may be recruited to the RUNX1:CBFβ-SMMHC complex and be required for the gene expression changes associated with inv(16) AML. Indeed, the chromatin remodeling factor Chromodomain Helicase DNA Binding Protein 7 (CHD7) is recruited to the RUNX1:CBFβ-SMMHC complex through an interaction with RUNX1 and plays a role in the transactivation activity of the complex in the context of leukemia initiation (128). HDAC8 also binds to CBFβ-SMMHC, although through the c-terminal 95 amino acids of the SMMHC tail, and deacetylates p53 bound to CBFβ-SMMHC (12). Deacetylation inactivates p53 and prevents induction of apoptosis, collaborating with CBFβ-SMMHC to induce leukemia. Our work expands this model, demonstrating that the RUNX1:CBFβ-SMMHC complex includes the epigenetic modifiers HDAC1 and HDAC3.

1. Interaction of HDAC1/3, and lack of interaction of HDAC2, with CBFβ-SMMHC

We show here previously unrecognized interactions between HDAC1, HDAC3 and the fusion protein CBFβ-SMMHC in mouse and human leukemia cells. Previous work by others failed to detect these interactions, likely due to the use of whole cell lysates rather than nuclear extracts, as were used in this study (12,115). In fact, we were unable to detect co-IP of HDAC1 and CBFβ-SMMHC from whole cell extracts, possibly because HDAC1 is only expressed in the nucleus, whereas CBFβ-SMMHC can localize

to the cytoplasm when overexpressed (39). In addition, using a yeast-two hybrid assay we found that the interaction between HDAC1 and CBFβ-SMMHC is not direct, and therefore may be more difficult to detect in co-immunoprecipitations.

This implies that HDAC1 requires one or more proteins to mediate the interaction with CBFβ-SMMHC. One candidate is Sin3A, which is already known to bind to CBFβ-SMMHC (115). Sin3A is associated with transcriptional repressor complexes and acts as a scaffold to unite transcription factors with HDAC1 and HDAC2 which are recruited as a homo- or heterodimer (126,127). We tested many *CBFB-MYH11* deletion mutants for HDAC1 binding, including elimination of aa 179-221, 222-448, and 517-611 (ΔC95), which all retained the ability to bind to HDAC1. Sin3A binding occurs somewhere between aa 514-542 (115), so it was likely eliminated by the ΔC95 mutant. This implies that Sin3A is not required for HDAC1 binding but does not rule out the possibility that Sin3A is helping to mediate the interaction.

Because RUNX1 is an established binding partner of HDAC1 and HDAC3 (15,115), we checked whether RUNX1 was responsible for their recruitment to the fusion protein complex. Elimination of RUNX1 binding to the fusion with the *CBFB-MYH11*$_{N63K,\ N104K,\ \Delta 179\text{-}221}$ mutation retained the ability to bind both HDAC1 and HDAC3, demonstrating that, like Sin3A, RUNX1 is not required for the interaction with CBFβ-SMMHC. However, our results do not exclude the possibility that HDAC1 could be recruited by both Sin3A and RUNX1 simultaneously. Further mutagenesis studies should be able to answer this question. It is clearly also possible that HDAC1 is recruited through interactors of CBFβ-SMMHC that have not yet been identified.

Sin3A does not bind to HDAC3, so the potential mechanism of HDAC3 binding is less clear. Although HDAC3 binds to RUNX1, elimination of RUNX1 binding to CBFβ-SMMHC did not eliminate the interaction with HDAC3. Therefore, HDAC3 must be binding through at least one additional mechanism. NCoR/SMRT, which recruit HDAC3

to a corepressor complex, have not been tested for binding to CBFβ-SMMHC. However, NCoR/SMRT and HDAC3 have been implicated in the molecular pathogenesis of other types of AML caused by fusion proteins, including PML-RARα and RUNX1-RUNX1T1 (260,261). Therefore, it is possible that HDAC3 is recruited to the CBFβ-SMMHC fusion through similar mechanisms, and future studies of CBFβ-SMMHC binding partners should determine whether NCoR/SMRT are present in the complex.

Due to the potential involvement of Sin3A in HDAC1 binding, the high homology between HDAC1 and HDAC2, and the observed protein expression of HDAC2 in mouse and human inv(16) AML samples, it is surprising that we did not find HDAC2 to be pulled down with CBFβ-SMMHC using the same IP conditions. However, there are reports of HDAC1 being preferred in Sin3A complexes over HDAC2. In T-cells, Sin3A/HDAC2 interaction can only be observed following knockout of HDAC1 (262). Mass spectrometry in embryonic stem cells indicated that HDAC1 is the major HDAC component of Sin3A complexes rather than HDAC2, which is only found to be associated with Sin3A in more differentiated cell types (263). Therefore, it is possible that there is specificity for HDAC1 in the context of the CBFβ-SMMHC complex. The lack of involvement of HDAC2 in CBFβ-SMMHC-induced leukemogenesis could be exploited for therapeutic purposes. Because there is some redundancy in function between HDAC1 and HDAC2 and they can compensate for each other when depleted in normal hematopoietic cells (181), it may be possible to target CBFβ-SMMHC by inhibiting HDAC1 with less toxic effects towards normal blood cells. This could be a major reason why entinostat treatments did not harm non-leukemic cells in our mouse leukemia model, as will be discussed below.

2. HDAC1 regulation of CBFβ-SMMHC target genes

Previous work demonstrated that HDAC1 colocalizes with RUNX1 and CBFβ-SMMHC on chromatin in ME-1 cells (14). We have extended this finding by showing their colocalization in primary mouse *CM*$^{+}$ cells on the promoters of genes that are regulated by CBFβ-SMMHC (14). We also found that HDAC3 was enriched at the same gene promoters in the same experiments, raising the possibility that it could be colocalizing to promoters simultaneously with HDAC1. While these results suggest that HDAC3 could have an important role in inv(16) AML, we largely focused our study on HDAC1's specific role on CBFβ-SMMHC activity. The role of HDAC3 on CBFβ-SMMHC activity and any convergent or divergent activity compared to HDAC1 should be the subject of future studies.

To proceed with the investigation of the role of HDAC1 in *CM*$^{+}$ cells, we performed knockdowns of *Hdac1* using shRNA. Knockdown of HDAC1 resulted in a 2-fold or greater downregulation of *Cdkn1a*, *Mpo*, and *Cebpd* in *CM*$^{+}$ leukemia cells, suggesting cooperation between HDAC1 and CBFβ-SMMHC in regulating gene expression changes (14). This data is consistent with the previous finding that knockdown of CBFβ-SMMHC decreased expression of *MPO*, *CDKN1A*, and *CEBPD* in ME-1 cells (14). While a decrease in expression of myeloid genes seems paradoxical to the observed myeloid differentiation induced by HDAC1 knockdown or inhibition, the maturation of myeloid cells consists of multiple phases of gene expression and repression. The *MPO*, *CSF1R*, and *CSF3R* genes are all expressed during the initial steps of myelopoiesis, but their expression decreases with further differentiation. In contrast, *CEBPE*, *GR-1* and *MAC-1* expression is restricted to more mature myeloid cells (48). Therefore, it is not necessarily surprising that loss of *MPO* and *CSF1R* expression would accompany terminal myeloid differentiation.

Our findings also support the model of the RUNX1:CBFβ-SMMHC complex acting as an active transcription factor complex in inv(16) AML. It is noteworthy that

knockdown of HDAC1 resulted in decreased expression of target genes, since HDACs are traditionally thought to function only as transcriptional corepressors. However, this assumption is challenged in recent reports showing HDAC1 is associated with the promoters of highly expressed genes, and that genetic depletion or inhibition of HDAC activity results in decreased gene expression (164,253). These findings suggest that HDACs may have non-canonical roles in transcriptional activation as well. Currently, the mechanism of HDACs' role in transcriptional activation is unclear, but has been proposed to involve deacetylation of non-histone proteins or the turnover of acetylation marks between rounds of transcription (164,253).

3. Use of HDAC inhibitors *in vitro* for treatment of *CM*$^{+}$ leukemia

The requirement of HDAC1 for CBFβ-SMMHC activity implies that HDAC inhibitors may be able to inhibit the fusion protein indirectly. In fact, we observed that treatment with either entinostat, which is selective for HDAC1, or the pan-HDAC inhibitor vorinostat significantly reduced the growth of CBFβ-SMMHC-expressing leukemia cells. Notably, entinostat treatment mirrored the effects of HDAC1 knockdown in colony assays, differentiation analysis, and gene expression analysis, indicating that entinostat treatment is likely working through targeting HDAC1. However, our results do not rule out the possibility that entinostat is targeting HDAC3 to some extent as well. Use of an HDAC3 specific inhibitor, RGFP966, resulted in a dose-dependent decrease in ME-1 cell viability, similar to HDAC1. However, the EC_{50} was about 8x higher with RGFP966, possibly indicating that the drug is not as potent as entinostat or that HDAC3 is not as critical in inv(16) leukemia. This is in contrast to MLL-rearranged leukemias which are more sensitive to HDAC3 depletion than HDAC1 (258). In colony assays using 1 μM RGFP966 we did not see significant decreases in colony formation or significant

increases in cell differentiation. However, based on our dose response curve, it is possible that the concentration we tested was not set high enough to see statistical significance of these effects. Therefore, further studies should investigate whether RGFP966 at higher doses could also inhibit CBFβ-SMMHC activity as we would expect based on our viability assay data. In addition, combination treatment with entinostat and RGFP966 could be tested as a way to determine if HDAC1 and HDAC3 have different roles in mediating CBFβ-SMMHC activity based on whether there are synergistic effects.

An important experiment to determine the feasibility of this approach would be performing colony assay on normal bone marrow with RGFP966. Entinostat and vorinostat treatment in colony assays with normal bone marrow did not result in any significant changes in colony formation indicating that the doses used were specifically toxic to leukemia cells and not toxic to normal bone marrow. This could be due to HDAC1 protein levels being greatly upregulated in mouse *CM*$^{+}$ cells and human ME-1 cells compared to normal bone marrow, or because HDAC2 could be compensating for HDAC1 loss in normal bone marrow but not in *CM*$^{+}$ cells. HDAC3 protein levels, conversely, were roughly equal in normal bone marrow compared to leukemia cells, and so HDAC3-specific inhibitors may cause considerable toxicity to normal cells at levels that target leukemia cells. Consequently, it is possible that HDAC3 will not be a desirable target to inhibit the fusion protein's activity therapeutically.

We also tested the RUNX1 inhibitor Ro5-3335 in combination with HDAC1 in colony forming assays. Ro5-3335 inhibits transcriptional activity of RUNX1:CBFβ and results in a dose-dependent decrease in ME-1 cell viability with an EC_{50} of 1.1 μM (11). It is significant that the combination of entinostat and the RUNX1 inhibitor Ro5-3335 did not have an increased effect as compared to treatment with entinostat alone. This is consistent with a model in which HDAC1 and RUNX1 are both required for CBFβ-SMMHC's ability to regulate gene expression. While much work has focused on finding

an inhibitor of the RUNX1:CBFβ or RUNX1:CBFβ-SMMHC interaction, our results indicate that HDAC1 inhibitors, which are already in use clinically, can have a similar effect on CBFβ-SMMHC activity.

4. Use of entinostat *in vivo* for treatment of mice with *CM*$^{+}$ leukemia

As strong support for this hypothesis, entinostat treatment of mice with *CM*$^{+}$ leukemia had a strong anti-leukemic effect, reducing the number of leukemic cells and promoting their differentiation. Other studies examining cell differentiation agents on leukemia cells have found that differentiation to more mature blood cells is proceeded by apoptosis (264–266). In support of this specific timeline for cell differentiation and death, we found an increase in apoptosis in the peripheral blood and bone marrow after our seven day entinostat treatment, in contrast to our findings after twenty-four hour knockdown of *Hdac1 in vitro*. Studies in various cancers have also found HDACi to act through cell cycle arrest (267). However, our analysis of bone marrow cells indicated there was no difference in the cell cycle profiles between control or entinostat treated mice.

If entinostat is acting exclusively through a differentiation-to-apoptosis pathway in our model, it could have important implications for combining treatment with other chemotherapeutic agents. Although tested here as a monotherapy, HDACi have historically been ineffective at treating cancer as a monotherapy and because of their relatively low toxicity they can be combined with chemotherapeutic agents to achieve a maximal effect (200). Specifically, entinostat treatment could be combined with the commonly used leukemia chemotherapy agents cytarabine and doxorubicin, which both incorporate into DNA during S-phase and thus require rapidly proliferating cells to exert an anti-cancer effect. However, the timing of entinostat administration would need to be

considered since differentiation is likely to halt proliferation of the cells and thus inhibit the anti-cancer activity of DNA intercalating agents. In future studies, we plan to treat with entinostat following a course of chemotherapy. Entinostat would act as a consolidation therapy to target non-proliferating cells that were missed by the initial chemotherapy. Our hypothesis is that specifically targeting CBFβ-SMMHC activity with entinostat in combination with chemotherapy to target proliferating cells will have an added benefit compared to either treatment alone.

Because our short-term entinostat treatments showed substantial *in vivo* activity against leukemia cells, we also tested the same treatment scheme and monitored long-term survival. However, our results largely indicate that the leukemia cells continue to grow as soon as the treatment is discontinued and consequently no significant improvement in survival time is observed. Therefore, our treatment scheme may need to be optimized to increase the eradication of leukemia stem cells *in vivo*. A higher dose or a different dosing schedule may improve upon our current protocol and improve both short and long-term outcomes.

Another interesting observation from our survival studies is that there is a sample-dependent response to entinostat treatment. Each original transgenic *Cbfb*$^{+/56M}$*, Mx1-Cre*$^{+}$*, Rosa26*$^{tdT/GFP}$ mouse which is treated to induce the expression of *CBFB-MYH11* and drive leukemia formation develops its own unique leukemia clone. Because *CBFB-MYH11* expression is not sufficient to develop leukemia (130), there are additional spontaneous mutations that occur in order for the mouse to develop frank leukemia. A limitation of this model is that we do not know which additional mutations are present in each sample. In the future, we would like to do sequencing to determine the mutational profiles of our leukemia samples to test if different clones have a unique mutational spectrum that influences its susceptibility to drug treatment. It is possible that the sample-dependent increase in survival (which also corresponds with increased response

in the short-term assay) is a product of this mutational variability. Because these differences have major implications for clinical translation, determining whether secondary mutations influence the efficacy of entinostat will be an important future direction.

5. HDACs and leukemia fusion proteins: exploiting a common characteristic for treatment

Interestingly, many of the most common AML fusion proteins bind to HATs and/or HDACs including RUNX1-RUNX1T1, CBFβ-SMMHC, MLL-AF9, and PML-RARα (268–270). Even less common AML fusions such as NUP98-HOXA9, RUNX1-CBFA2T3, RUNX1-EVI1, or PLZF-RARα, have been shown to bind to HATs/HDACs (271,272) or complexes which recruit HDACs (273,274). In other AML fusion proteins such as MOZ-CREBBP, MOZ-p300, and MOZ-TIF2, one or both of the fused proteins is an acetyltransferase itself (275). There are reports of non-AML fusion proteins recruiting HATs/HDACs as well, such as the ALL-associated fusion ETV6-RUNX1 which binds to HDACs and HDAC containing complexes (270). This commonality has led us to postulate that there must be a requirement for HATs/HDACs in many subtypes of leukemia.

Of keen interest to the work shown here are similarities with other core binding factor-related fusion proteins. Our data parallels what has been shown in the related CBF leukemia defined by the t(8;21) rearrangement. The resultant fusion protein, RUNX1-RUNX1T1, is known to bind HDAC1, HDAC2, HDAC3, Sin3A, NCoR, and SMRT (193,194,276–278). RUNX1-RUNX1T1 disrupts the normal gene regulation of RUNX1 by recruitment of HATs, HDACs, and other epigenetic regulators to regulatory regions of RUNX1 target genes. While most RUNX1-RUNX1T1 activity is centered

around the repression of genes involved in cell growth or differentiation, the fusion is also involved in gene activation, much like CBFβ-SMMHC (68).

Treatment with HDACi's has been beneficial in several models of RUNX1-RUNX1T1 leukemia. Valproic acid (VPA), trichostatin A (TSA), or phenylbutyrate treatments have rescued expression of genes repressed by RUNX1-RUNX1T1 *in vitro* (215,264,276,279). Relieving the RUNX1-RUNX1T1-mediated repression of target genes was always followed by increased differentiation of the RUNX1-RUNX1T1^{+} cells (215,264,279,280). Romidepsin, VPA, vorinostat, and phenylbutyrate all caused an increase in apoptosis in cell line models of RUNX1-RUNX1T1 which were usually preceded by an increase in differentiation (221,264,279,281). In a mouse model of RUNX1-RUNX1T1, panobinostat treated mice had a profound survival advantage over non-treated mice and panobinostat treatment phenocopied knockdown of the fusion protein, implying that HDACi can indirectly inhibit fusion protein activities (282), similar to what we established in this study with CBFβ-SMMHC and entinostat. HDACi treatment has also worked clinically for treatment of patients with RUNX1-RUNX1T1^{+} leukemia. A phase II clinical trial of romidepsin in relapsed or refractory AML patients showed anti-leukemic effects in three out of five patients with t(8;21) (283). Overall, it is clear that RUNX1-RUNX1T1 requires HDACs for its activity and HDACi's are beneficial in treating t(8;21) AML.

Examining all of the leukemia-associated fusion proteins which bind to and rely on HDACs to exert leukemogenic activity is beyond the scope of this discussion. However, it is clear that exploiting the functions of epigenetic regulators is a common mechanism particularly in the pathogenesis of CBF fusion proteins. Our discovery of HDAC1 and HDAC3 binding to CBFβ-SMMHC and HDAC1 being required for its activity is the latest addition to this body of research and firmly establishes a common theme

among core binding factor leukemia fusion proteins. Because these molecular subtypes of AML share a common requirement for HDACs, future clinical trials should focus on testing HDAC inhibitors in these patients, rather than including AML patients regardless of subtype. Applying what we know about the molecular pathogenesis of these diseases will inform the design of better clinical trials in the future.

6. Future directions: Determining how HDAC1 regulates gene expression in inv(16) AML

The results of this study have left us with many interesting follow-up questions which will be part of the future directions of this study, many of which were commented on above such as: 1) What is the role of HDAC3 in inv(16) leukemia, 2) Can we improve upon entinostat treatment by combining it with other therapeutic agents, and 3) Do the secondary mutations in leukemia cells contribute to their susceptibility to HDACi treatment? Another major overarching question that results from this work is how is HDAC1 mechanistically responsible for regulating gene expression along with CBFβ-SMMHC in inv(16) AML?

Previous models have assumed that leukemia fusion proteins act as corepressors by recruiting HDACs to suppress gene expression by deacetylating histones at gene promoters (107,193,215,277,284–286). More recent work analyzing fusion protein binding and acetylation on a genome-wide scale has shown that histone acetylation is still present at or surrounding fusion protein binding sites (14,287–289), implying that deacetylation of histones may not be the sole activity of HDACs recruited by the fusion proteins. This is especially true for CBFβ-SMMHC, which had much higher levels of histone acetylation at its binding sites compared to RUNX1-RUNX1T1 or PML-RARα (289). Because knockdown or inhibition of HDAC1 in our study resulted in a decrease of expression of many of the genes tested, implying HDAC1 is required for the

active expression of these genes, we postulated that HDAC1 is playing a role in inv(16) AML beyond its canonical role in histone deacetylation.

6.A. Altering RUNX1 activity as a mechanism

RUNX1 has two acetylation sites which regulate its activity, lysines 24 and 43 of the RUNX1b isoform (62,290). Two acetyltransferases, p300 and MOZ, have been shown to acetylate RUNX1 (60,61). Although histone deacetylases are known to interact with RUNX1 (15,291), to date no publications have identified deacetylases involved in the specific deacetylation of RUNX1. Acetylation of RUNX1 increases its binding affinity for DNA thereby stimulating transcriptional activation *in vitro* (62). RUNX1 acetylation is also critical for the leukemogenic activity of the t(8;21) AML fusion RUNX1-RUNX1T1 (290). We hypothesized that the regulation of RUNX1 acetylation is critical for leukemogenic activity of CBFβ-SMMHC and that HDAC1 can deacetylate RUNX1 when they are complexed with CBFβ-SMMHC.

We have begun the process of testing this hypothesis by making acetylation mutants in our RUNX1c-containing plasmids, which have a slightly longer N-terminus compared to RUNX1b. Consequently the numbering is shifted compared to the published acetylation sites in RUNX1b, and the corresponding lysines are aa 51 and 70. To test if these acetylation mutants would affect RUNX1's transactivation of gene expression, we co-expressed plasmids containing *RUNX1, RUNX1*$_{K51,70Q}$*, or RUNX1*$_{K51,70R}$ together with plasmids containing the RUNX binding region of the M-CSFR promoter fused to firefly luciferase and a renilla luciferase control plasmid in HEK293 cells. RUNX1 did not have much transactivation ability on its own but co-expression of a *CBFB*-containing plasmid resulted in a large increase in luciferase activity, as reported previously (Appendix A, Figure A.1 and A.2) (62,292). Addition of *HDAC1-FLAG* resulted in a significant decrease in luciferase activity, implying that

HDAC1 can regulate RUNX1 activity. However, addition of *HDAC1-FLAG* to either of the *RUNX1* acetylation mutants with *CBFB* did not have a significant effect on RUNX1 activity. This suggests that HDAC1 affects RUNX1 activity through deacetylation and that lysines 51 and 70 are the relevant HDAC1 target sites in the RUNX1c isoform.

To test if RUNX1 acetylation status affects its activity in the context of the inv(16) fusion protein, we transfected an inducible CBFβ-SMMHC^{+} cell line with WT or acetylation mutant RUNX1 plasmids and examined expression of the CBFβ-SMMHC target gene *Mpo*. In CBFβ-SMMHC^{+} cells overexpressing WT RUNX1, we found similar changes as untransfected cells. However, expression of either of the acetylation mimetics blocked the CBFβ-SMMHC-induced changes in gene expression (Appendix A, Figure A.3). Both the acetylated and non-acetylated mimetic prevented *Mpo* expression, perhaps indicating that it is the physical presence of the acetyl group that impacts transcription and that this function cannot be properly mimicked with substitution of similar amino acids. Overall, this implies that regulation of RUNX1 acetylation is important for the transcriptional activity of the RUNX1:CBFβ-SMMHC complex.

Because acetylation is important for RUNX1 binding to DNA *in vitro*, we tested if localization of the CBFβ-SMMHC:RUNX1 complex to gene promoters would be *affected* by inhibition of HDAC1 activity. To test this, we performed ChIP in *CM*$^{+}$ cells with stable incorporation of an inducible shRNA against HDAC1 or in entinostat treated *CM*$^{+}$ cells. Our preliminary results suggest that the complex of CBFβ-SMMHC, RUNX1, and HDAC1 are no longer enriched on the promoters of target genes after HDAC1 is inhibited (Appendix B, Figure B.1) or knocked down (Appendix B, Figure B.2). This suggests that HDAC1 is required for the localization of the entire complex to target genes. Because the same trend is observed whether there is a decrease in total protein level or just inhibition of its enzymatic activity, it implies that the activity of HDAC1 is the

important factor in the localization of the complex rather than the physical presence of HDAC1.

Taken together, our preliminary data clearly demonstrates that HDAC1 can regulate RUNX1 activity and that deacetylation of RUNX1 is a potential mechanism to explain this activity. While the role of RUNX1 deacetylation in inv(16) AML is not clear at this time, our preliminary data suggests that regulation of RUNX1 acetylation may be critical for the gene expression changes induced by expression of CBFβ-SMMHC. RUNX1 acetylation may be necessary for DNA binding and RUNX1 deacetylation for resetting the transcriptional machinery for elongation or subsequent rounds of transcription. Future experiments are needed to determine if this model can explain the requirement of HDAC1 in gene activation in inv(16) AML.

To address the role of RUNX1 acetylation in inv(16) AML in the future, we will perform immunoprecipitations for SMMHC in *CM*$^{+}$ cells with or without HDAC1 KD or entinostat treatment, and probe for acetylated RUNX1 to determine if HDAC1 is deacetylating RUNX1 when it is part of the fusion protein complex. When we previously attempted this approach, we found that the RUNX1 acetylation band was obscured by a more highly expressed acetylated protein running at close to the same molecular weight. We now believe this protein to be tubulin, which was unknowingly present in our pulldowns. Intriguingly, our experiments consistently demonstrated that HDAC1 was capable of deacetylating tubulin (Appendix C, Figures C.1-4). Previous work has shown HDAC6 to be the major tubulin deacetylase (293) while HDAC3 may indirectly regulate tubulin acetylation (294). Our observations have possible implications for the localization of RUNX1. RUNX2 was found to be translocated from the nucleus to the cytoplasm upon tubulin stabilization (295). As acetylation turnover influences tubulin stability (296,297), it is possible that blocking HDAC1 could stabilize tubulin and induce the translocation of

RUNX1, which could explain why blocking HDAC1 resulted in less binding of RUNX1 and CBFβ-SMMHC to promoters.

6.B. Repression of CBFβ as a mechanism

Another possible mechanism for HDAC1's role in inv(16) AML gene expression is through the repression of wild-type CBFβ expression. While performing experiments in which HDAC1 was inhibited or knocked down, we noticed a pattern in which CBFβ protein levels were consistently increased. In ME-1 cells or mouse *CM*$^{+}$ cells, entinostat treatment led to an increase in CBFβ levels (Appendix D, Figures D.1-2). A 32% knockdown of HDAC1 protein level in *CM*$^{+}$ cells resulted in a small increase in total CBFβ but a substantially increased amount of RUNX1 binding to CBFβ (Appendix D, Figure D.3). Overexpression of HDAC1 with RUNX1 and CBFβ in COS-7 cells had the opposite effect, slightly decreasing total CBFβ but substantially decreasing binding of RUNX1 to CBFβ. Substitution of the enzymatically inactive $HDAC1_{H141A}$ mutant rescued the expression of CBFβ and the binding of CBFβ to RUNX1 (Appendix D, Figure D.4). Furthermore, inducing CBFβ-SMMHC expression in the zinc-inducible 32d INV cell line (238) led to a decrease in CBFβ mRNA expression and protein expression in both whole cell and nuclear lysates (Appendix D, Figures D.5-7).

This data suggests that CBFβ-SMMHC and HDAC1 are negatively regulating the expression of *CBFB*. Analysis of a ChiP-Seq data repository from ME-1 cells revealed that CBFβ-SMMHC was present on the promoter of *CBFB* (14). To confirm whether CBFβ-SMMHC was binding to the promoter of *CBFB* and determine which regions were bound, we performed ChIP in ME-1 cells with anti-SMMHC antibody followed by qRT-PCR with primers against five different *CBFB* promoter regions (298). We found that CBFβ-SMMHC localization was enriched at each of the five promoter regions (Appendix D, Figure D.8). Entinostat treatment upregulated CBFβ-SMMHC binding at two specific

promoter regions, with no change at the others. The significance of this observation is unknown at this time and warrants further investigation.

Altogether, this data forms the beginning of a model in which HDAC1 and CBFβ-SMMHC act in concert to suppress wild-type CBFβ in inv(16) AML cells (Appendix D, Figure D.9). HDAC1 and the CBFβ-SMMHC complex may be localizing to the promoter of *CBFB* in leukemia cells and preventing its transcription, while entinostat relieves this repression causing an increase in CBFβ mRNA and protein. This could tip the balance of wild-type CBFβ and CBFβ-SMMHC competing for binding to RUNX1, resulting in more CBFβ:RUNX1 complexes. Finally, the CBFβ:RUNX1 complexes can revert the cells to a more normal pattern of gene expression leading to differentiation and finally apoptosis of the leukemia cells.

This preliminary model is an exciting possibility which could delineate a novel mechanism of CBFβ-SMMHC activity in inv(16) AML. However, much work still needs to be done to determine if the re-expression of CBFβ is responsible for the downstream effects of entinostat treatment. Because inv(16) AML cells have one allele of CBFβ-SMMHC and one allele of wild-type CBFβ, it is hard to explain why these effects would be occurring at one allele and not the other, as the promoter regions are expected to be the same at both alleles. We have not noticed a consistent increase in CBFβ-SMMHC protein expression with entinostat treatment as with wild-type CBFβ, which would indicate that allele specific gene regulation is occurring, or that the major effect of treatment is in protein stabilization rather than transcriptional regulation. It is possible that epigenetic mechanisms are selectively repressing the allele that expresses *CBFB* while maintaining *CBFB-MYH11* expression in CBFβ-SMMHC^{+} cells. The future directions of this project will explore the answers to these questions in order to form a more complete model of CBFβ-SMMHC and HDAC1 activity in inv(16) AML.

7. Summary

In this study, we have identified HDAC1 and HDAC3 as novel interacting partners of CBFβ-SMMHC. We have determined that they are recruited by CBFβ-SMMHC and that they colocalize with the fusion protein complex at gene promoters. In addition, CBFβ-SMMHC^{+} cells are sensitive to treatment with both HDAC1- and HDAC3-selective inhibitors, implying that these proteins are critical for the survival of the leukemia cells. We further tested the role of HDAC1 in inv(16) AML by knockdown in CBFβ-SMMHC^{+} cells and determined that HDAC1 is required for gene expression and maintenance of the differentiation block in these cells. Treatment of a mouse model of inv(16) leukemia with the HDAC1-selective inhibitor entinostat significantly decreased leukemic burden by causing differentiation and apoptosis in leukemia cells while sparing normal blood cells. However, survival was not improved with treatment indicating that HDAC1 must be continually repressed to prevent repopulation of leukemia and that future studies should focus on improving the eradication of leukemia stem cells.

Our study demonstrates that HDAC1 is required for CBFβ-SMMHC activity and therefore can be used as a proxy for therapeutic targeting of the fusion protein complex. The significance of this discovery is that HDAC inhibitors are already FDA approved for other hematological malignancies and therefore can be rapidly translated into treatment for inv(16) AML. Furthermore, the relatively low toxicity of HDAC inhibitors allows for combination with other treatments or alternatively it could be considered for use as a monotherapy in patients that cannot tolerate high dose chemotherapy. Our results contribute to the growing body of literature indicating that HDACs are required in core binding factor leukemias and HDAC inhibitors may be uniquely efficacious in these specific AML subtypes.

Bibliography

1. Liu P, Tarlé S a, Hajra a, Claxton DF, Marlton P, Freedman M, et al. Fusion between transcription factor CBF beta/PEBP2 beta and a myosin heavy chain in acute myeloid leukemia. Science. 1993;261(5124):1041–4.

2. Byrd JC, Mro K, Dodge RK, Carroll AJ, Edwards CG, Arthur DC, et al. Pretreatment cytogenetic abnormalities are predictive of induction success, cumulative incidence of relapse, and overall survival in adult patients with de novo acute myeloid leukemia: results from Cancer and Leukemia Group B (CALGB 8461). Blood. 2002;100(13):4325–36.

3. Slovak ML, Kopecky KJ, Cassileth P a, Harrington DH, Theil KS, Paietta E, et al. Karyotypic analysis predicts outcome of preremission and postremission therapy in adult acute myeloid leukemia : a Southwest Oncology Group / Eastern Cooperative Oncology Group study Karyotypic analysis predicts outcome of preremission and postremission t. Blood. 2000;96(13):4075–83.

4. Kihara R, Nagata Y, Kiyoi H, Kato T, Yamamoto E, Suzuki K, et al. Comprehensive analysis of genetic alterations and their prognostic impacts in adult acute myeloid leukemia patients. Leukemia. 2014;28(8):1586–95.

5. Paschka P, Döhner K. Core-binding factor acute myeloid leukemia: can we improve on HiDAC consolidation? Hematol Am Soc Hematol Educ Progr. 2013;2013:209–19.

6. Billström R, Ahlgren T, Békássy AN, Malm C, Olofsson T, Höglund M, et al. Acute myeloid leukemia with inv(16)(p13q22): Involvement of cervical lymph nodes and tonsils is common and may be a negative prognostic sign. Am J Hematol.

2002;71(1):15–9.

7. Marcucci G, Mrózek K, Ruppert AS, Maharry K, Kolitz JE, Moore JO, et al. Prognostic factors and outcome of core binding factor acute myeloid leukemia patients with t(8;21) differ from those of patients with inv(16): A Cancer and Leukemia Group B study. J Clin Oncol. 2005;23(24):5705–17.

8. Appelbaum FR, Kopecky KJ, Tallman MS, Slovak ML, Gundacker HM, Kim HT, et al. The clinical spectrum of adult acute myeloid leukaemia associated with core binding factor translocations. Br J Haematol. 2006;135:165–73.

9. Solh M, Yohe S, Weisdorf D, Ustun C. Core-binding factor acute myeloid leukemia: Heterogeneity, monitoring, and therapy. Am J Hematol. 2014;89(12):1121–31.

10. Khan M, Cortes J, Qiao W, Alzubaidi MA, Pierce SA, Ravandi F, et al. Outcomes of Patients With Relapsed Core Binding Factor-Positive Acute Myeloid Leukemia. Clin Lymphoma Myeloma Leuk. 2018 Jan;18(1):e19–25.

11. Cunningham L, Finckbeiner S, Hyde RK, Southall N, Marugan J, Yedavalli VRK, et al. Identification of benzodiazepine Ro5-3335 as an inhibitor of CBF leukemia through quantitative high throughput screen against RUNX1-CBF interaction. Proc Natl Acad Sci. 2012;109(36):14592–7.

12. Qi J, Singh S, Hua W-K, Cai Q, Chao S-W, Li L, et al. HDAC8 Inhibition Specifically Targets Inv(16) Acute Myeloid Leukemic Stem Cells by Restoring p53 Acetylation. Cell Stem Cell. 2015;17(16):1–14.

13. Illendula A, Pulikkan JA, Zong H, Grembecka J, Xue L, Sen S, et al. A small-molecule inhibitor of the aberrant transcription factor CBFβ-SMMHC delays

leukemia in mice. Science. 2015 Feb 13;347(6223):779–84.

14. Mandoli a, Singh a a, Jansen PWTC, Wierenga a TJ, Riahi H, Franci G, et al. CBFB-MYH11/RUNX1 together with a compendium of hematopoietic regulators, chromatin modifiers and basal transcription factors occupies self-renewal genes in inv(16) acute myeloid leukemia. Leukemia. 2014;28(4):770–8.

15. Guo H, Friedman AD. Phosphorylation of RUNX1 by cyclin-dependent kinase reduces direct interaction with HDAC1 and HDAC3. J Biol Chem. 2011 Jan 7;286(1):208–15.

16. Ogawa E, Inuzuka M, Maruyama M, Satake M, Naito-Fujimoto M, Ito Y, et al. Molecular cloning and characterization of pebp2β, the heterodimeric partner of a novel drosophila runt-related dna binding protein pebp2α. Vol. 194, Virology. 1993. p. 314–31.

17. Liu P, Seidel N, Bodine D, Speck N, Tarle S, Collins FS. Acute myeloid leukemia with Inv(16) produces a chimeric transcription factor with a myosin heavy chain tail. In: Cold Spring Harbor Symposia on Quantitative Biology. 1994.

18. Hyde RK, Zhao L, Alemu L, Liu PP. Runx1 is required for hematopoietic defects and leukemogenesis in Cbfb-MYH11 knock-in mice. Leukemia. 2015;29(8):1771–8.

19. Tavian M, Péault B. The changing cellular environments of hematopoiesis in human development in utero. Exp Hematol. 2005 Sep;33(9):1062–9.

20. Jagannathan-Bogdan M, Zon LI. Hematopoiesis. Development. 2013;140(12):2463–7.

21. Kim C. Homeostatic and pathogenic extramedullary hematopoiesis. J Blood Med.

2010;13.

22. Wilson NK, Calero-Nieto FJ, Ferreira R, Göttgens B. Transcriptional regulation of haematopoietic transcription factors. Stem Cell Res Ther. 2011;2(1):2–9.

23. Levanon D, Glusman G, Bangsow T, Ben-Asher E, Male DA, Avidan N, et al. Architecture and anatomy of the genomic locus encoding the human leukemia-associated transcription factor RUNX1/AML1. Gene. 2001;262(1–2):23–33.

24. Bee T, Liddiard K, Swiers G, Bickley SRB, Vink CS, Jarratt A, et al. Alternative Runx1 promoter usage in mouse developmental hematopoiesis. Blood Cells, Mol Dis. 2009;43(1):35–42.

25. de Bruijn MF, Speck NA. Core-binding factors in hematopoiesis and immune function. Oncogene. 2004;23(24):4238–48.

26. Sasaki K, Yagi H, Bronson RT, Tominaga K, Matsunashi T, Deguchi K, et al. Absence of fetal liver hematopoiesis in mice deficient in transcriptional coactivator core binding factor beta. Proc Natl Acad Sci U S A. 1996;93(22):12359–63.

27. Wang Q, Stacy T, Binder M, Marin-Padilla M, Sharpe a H, Speck N a. Disruption of the Cbfa2 gene causes necrosis and hemorrhaging in the central nervous system and blocks definitive hematopoiesis. Proc Natl Acad Sci U S A. 1996;93(8):3444–9.

28. Okuda T, Van Deursen J, Hiebert SW, Grosveld G, Downing JR. AML1, the target of multiple chromosomal translocations in human leukemia, is essential for normal fetal liver hematopoiesis. Cell. 1996;84:321–30.

29. Meyers S, Downing JR, Hiebert SW. Identification of AML-1 and the (8;21) translocation protein (AML-1/ETO) as sequence-specific DNA-binding proteins:

the runt homology domain is required for DNA binding and protein-protein interactions. Mol Cell Biol. 1993;13(10):6336–45.

30. Wang S, Wang Q, Crute BE, Melnikova IN, Keller SR, Speck NA. Cloning and characterization of subunits of the T-cell receptor and murine leukemia virus enhancer core-binding factor. Mol Cell Biol. 1993;13(6):3324–39.

31. Huang G, Shigesada K, Ito K, Wee HJ, Yokomizo T, Ito Y. Dimerization with PEBP2beta protects RUNX1/AML1 from ubiquitin-proteasome-mediated degradation. EMBO J. 2001 Feb 15;20(4):723–33.

32. Hajra A, Collins FS. Structure of the leukemia-associated human CBFB gene. Genomics. 1995;

33. Adya N, Castilla LH, Liu PP. Function of CBFbeta/Bro proteins. Semin Cell Dev Biol. 2000 Oct;11(5):361–8.

34. Levanon D, Negreanu V, Bernstein Y, Bar-Am I, Avivi L, Groner Y. Aml1, aml2, and aml3, the human members of the runt domain gene-family: Cdna structure, expression, and chromosomal localization. Genomics. 1994;23(2):425–32.

35. Kagoshima H, Akamatsu Y, Ito Y, Shigesada K. Functional dissection of the alpha and beta subunits of transcription factor PEBP2 and the redox susceptibility of its DNA binding activity. J Biol Chem. 1996;271(51):33074–82.

36. Huang X, Peng JW, Speck N a, Bushweller JH. Solution structure of core binding factor beta and map of the CBF alpha binding site. Nat Struct Biol. 1999;6(7):624–7.

37. Warren a J, Bravo J, Williams RL, Rabbitts TH. Structural basis for the heterodimeric interaction between the acute leukaemia-associated transcription

factors AML1 and CBFbeta. EMBO J. 2000;19(12):3004–15.

38. Tahirov TH, Inoue-bungo T, Morii H, Fujikawa A, Sasaki M, Kimura K, et al. Structural Analyses of DNA Recognition by the AML1/Runx-1 Runt Domain and Its Allosteric Control by CBFβ. Cell. 2001;105(2):291–291.

39. Adya N, Stacy T, Speck N a, Liu PP. The leukemic protein core binding factor beta (CBFbeta)-smooth-muscle myosin heavy chain sequesters CBFalpha2 into cytoskeletal filaments and aggregates. Mol Cell Biol. 1998;18(12):7432–43.

40. Lu JIE, Maruyama M, Satake M, Bae S, Ogawa E, Kagoshima H, et al. Subcellular Localization of the α and β Subunits of the Acute Myeloid Leukemia-Linked Transcription Factor PEBP2 / CBF. Mol Cell Biol. 1995;15(3):1651–61.

41. Wang Q, Stacy T, Miller JD, Lewis a F, Gu TL, Huang X, et al. The CBFbeta subunit is essential for CBFalpha2 (AML1) function in vivo. Cell. 1996;87:697–708.

42. Levanon D, Glusman G, Bettoun D, Ben-Asher E, Negreanu V, Bernstein Y, et al. Phylogenesis and regulated expression of the RUNT domain transcription factors RUNX1 and RUNX3. Blood Cells, Mol Dis. 2003;30(2):161–3.

43. Inoue K, Shiga T, Ito Y. Runx transcription factors in neuronal development. Neural Dev. 2008 Aug 26;3(1):20.

44. Westendorf JJ, Hiebert SW. Mammalian runt-domain proteins and their roles in hematopoiesis, osteogenesis, and leukemia. J Cell Biochem. 1999;75(S32):51–8.

45. Miyoshi H, Shimizu K, Kozu T, Maseki N, Kaneko Y, Ohki M. t(8;21) breakpoints on chromosome 21 in acute myeloid leukemia are clustered within a limited region of a single gene, AML1. Proc Natl Acad Sci U S A. 1991 Dec 1;88(23):10431–4.

46. North TE, Stacy T, Matheny CJ, Speck NA, de Bruijn MFTR. Runx1 is expressed in adult mouse hematopoietic stem cells and differentiating myeloid and lymphoid cells, but not in maturing erythroid cells. Stem Cells. 2004;22(2):158–68.

47. Lorsbach RB, Moore J, Ang SO, Sun W, Lenny N, Downing JR. Role of RUNX1 in adult hematopoiesis: Analysis of RUNX1-IRES-GFP knock-in mice reveals differential lineage expression. Blood. 2004;103(7):2522–9.

48. Friedman AD. Transcriptional regulation of granulocyte and monocyte development. Oncogene. 2002 May 13;21(21):3377–90.

49. Otto F, Lübbert M, Stock M. Upstream and downstream targets of RUNX proteins. J Cell Biochem. 2003;89(1):9–18.

50. Ichikawa M, Asai T, Saito T, Yamamoto G, Seo S, Yamazaki I, et al. AML-1 is required for megakaryocytic maturation and lymphocytic differentiation, but not for maintenance of hematopoietic stem cells in adult hematopoiesis. Nat Med. 2004;10(3):299–304.

51. Ichikawa M, Goyama S, Asai T, Kawazu M, Nakagawa M, Takeshita M, et al. AML1/Runx1 Negatively Regulates Quiescent Hematopoietic Stem Cells in Adult Hematopoiesis. J Immunol. 2008;180(7):4402–8.

52. Growney JD, Shigematsu H, Li Z, Lee BH, Adelsperger J, Rowan R, et al. Loss of Runx1 perturbs adult hematopoiesis and is associated with a myeloproliferative phenotype. Blood. 2005;106(2):494–504.

53. Putz G, Rosner A, Nuesslein I, Schmitz N, Buchholz F. AML1 deletion in adult mice causes splenomegaly and lymphomas. Oncogene. 2006 Feb 10;25(6):929–39.

54. Cai X, Gaudet JJ, Mangan JK, Chen MJ, De Obaldia ME, Oo Z, et al. Runx1 loss minimally impacts long-term hematopoietic stem cells. PLoS One. 2011;6(12):e28430.

55. Bae S, Lee YH. Phosphorylation , acetylation and ubiquitination : The molecular basis of RUNX regulation. 2003;366(2006):58–66.

56. Wang L, Huang G, Zhao X, Hatlen MA, Vu L, Liu F, et al. Post-translational modifications of Runx1 regulate its activity in the cell. Blood Cells, Mol Dis. 2009;43(1):30–4.

57. Goyama S, Huang G, Kurokawa M, Mulloy JC. Posttranslational modifications of RUNX1 as potential anticancer targets. Oncogene. 2015;34(27):3483–92.

58. Wang L, Gural A, Sun X-J, Zhao X, Perna F, Huang G, et al. The leukemogenicity of AML1-ETO is dependent on site-specific lysine acetylation. Science. 2011 Aug 5;333(6043):765–9.

59. Leong WY, Guo H, Ma O, Huang H, Cantor AB, Friedman AD. Runx1 Phosphorylation by Src Increases Trans-activation via Augmented Stability, Reduced Histone Deacetylase (HDAC) Binding, and Increased DNA Affinity, and Activated Runx1 Favors Granulopoiesis. J Biol Chem. 2016 Jan 8;291(2):826–36.

60. Kitabayashi I, Yokoyama A, Shimizu K, Ohki M. Interaction and functional cooperation of the leukemia- associated factors AML1 and p300 in myeloid cell differentiation. EMBO J. 1998;17(11):2994–3004.

61. Kitabayashi I, Aikawa Y, Nguyen LA, Yokoyama A, Ohki M. Activation of AML1-mediated transcription by MOZ and inhibition by the MOZ-CBP fusion protein. EMBO J. 2002;20(24):7184–96.

62. Yamaguchi Y, Kurokawa M, Imai Y, Izutsu K, Asai T, Ichikawa M, et al. AML1 Is Functionally Regulated through p300-mediated Acetylation on Specific Lysine Residues. J Biol Chem. 2004;279(15):15630–8.

63. Sood R, Kamikubo Y, Liu P. Role of RUNX1 in hematological malignancies. Blood. 2017;129(15):2070–82.

64. Downing JR. The AML1-ETO chimaeric transcription factor in acute myeloid leukaemia: biology and clinical significance. Br J Haematol. 1999 Aug;106(2):296–308.

65. Licht JD. AML1 and the AML1-ETO fusion protein in the pathogenesis of t(8;21) AML. Oncogene. 2001 Sep 8;20(40):5660–79.

66. Lam K, Zhang D-E. RUNX1 and RUNX1-ETO: roles in hematopoiesis and leukemogenesis. Front Biosci (Landmark Ed. 2012 Jan 1;17(1):1120–39.

67. Davis JN, McGhee L, Meyers S. The ETO (MTG8) gene family. Gene. 2003;303(1–2):1–10.

68. Li J, Guo C, Steinauer N, Zhang J. New insights into transcriptional and leukemogenic mechanisms of AML1-ETO and E2A fusion proteins. Front Biol (Beijing). 2016 Aug;11(4):285–304.

69. Kampen KR. The discovery and early understanding of leukemia. Leuk Res. 2012;36(1):6–13.

70. Peloquin GL, Chen Y-B, Fathi AT. The evolving landscape in the therapy of acute myeloid leukemia. Protein Cell. 2013;4(10):735–46.

71. Jordan CT. Unique molecular and cellular features of acute myelogenous leukemia stem cells. Leukemia. 2002;16(4):559–62.

72. Jan M, Majeti R. Clonal evolution of acute leukemia genomes. Oncogene. 2013;32(2):135–40.

73. Desai P, Mencia-Trinchant N, Savenkov O, Simon MS, Cheang G, Lee S, et al. Somatic mutations precede acute myeloid leukemia years before diagnosis. Nat Med. 2018;24(7):1015–23.

74. Welch JS, Ley TJ, Link DC, Miller C a, Larson DE, Koboldt DC, et al. The origin and evolution of mutations in acute myeloid leukemia. Cell. 2012 Jul 20;150(2):264–78.

75. Grove CS, Vassiliou GS. Acute myeloid leukaemia: a paradigm for the clonal evolution of cancer? Dis Model Mech. 2014;7(8):941–51.

76. Chang HY, Rodriguez V, Narboni G, Bodey GP, Luna MA, Freireich EJ. Causes of death in adults with acute leukemia. Medicine (Baltimore). 1976 May;55(3):259–68.

77. Surveillance, Epidemiology, and End Results (SEER) Program (www.seer.cancer.gov) Research Data (1973-2011), National Cancer Institute, DCCPS, Surveillance Research Program, Surveillance Systems Branch, released April 2014, based on the November 2013 submi.

78. Tamamyan G, Kadia T, Ravandi F, Borthakur G, Cortes J, Jabbour E, et al. Frontline treatment of acute myeloid leukemia in adults. Crit Rev Oncol Hematol. 2017;110:20–34.

79. Belson M, Kingsley B, Holmes A. Risk factors for acute leukemia in children: A review. Environ Health Perspect. 2007;115(1):138–45.

80. Ganser A, Heuser M. Therapy-related myeloid neoplasms. Curr Opin Hematol.

2017 Sep;24(2):152–8.

81. Godley LA, Larson RA. Therapy-related myeloid leukemia. Semin Oncol. 2008 Aug;35(4):418–29.

82. Siegel RL, Miller KD, Jemal A. Cancer statistics, 2018. CA Cancer J Clin. 2018;65(1):5–29.

83. Siegel RL, Miller KD, Jemal A. Cancer statistics, 2016. CA Cancer J Clin. 2016 Jan;66(1):7–30.

84. Davis AS, Viera AJ, Mead MD. Leukemia: an overview for primary care. Am Fam Physician. 2014 May 1;89(9):731–8.

85. Shephard EA, Hamilton W, Neal RD, Rose PW, Walter FM. Symptoms of adult chronic and acute leukaemia before diagnosis: Large primary care case-control studies using electronic records. Br J Gen Pract. 2016;66(644):e182–8.

86. Heim S, Mitelman F. Cytogenetic analysis in the diagnosis of acute leukemia. Cancer. 1992;70(4 S):1701–9.

87. Grigoropoulos NF, Petter R, Van ’t Veer MB, Scott MA, Follows GA. Leukaemia update. Part 1: diagnosis and management. BMJ. 2013 Mar 28;346:f1660.

88. Sorensen JT, Gerald K, Bodensteiner D, Holmes FF. Effect of age on survival in acute leukemia. Cancer. 1993;72(5):1602–6.

89. Eleni LD, Nicholas ZC, Alexandros S. Challenges in treating older patients with acute myeloid leukemia. J Oncol. 2010;2010:943823.

90. Dombret H, Gardin C. An update of current treatments for adult acute myeloid leukemia. Blood. 2016 Jan 7;127(1):53–61.

91. Tawfik B, Sliesoraitis S, Lyerly S, Klepin HD, Lawrence J, Isom S, et al. Efficacy of the hypomethylating agents as frontline, salvage, or consolidation therapy in adults with acute myeloid leukemia (AML). Ann Hematol. 2014;93(1):47–55.

92. Parkin B, Ouillette P, Li Y, Keller J. Clonal evolution and devolution after chemotherapy in adult acute myelogenous leukemia. Blood. 2013;121(2):369–77.

93. Duval M, Klein JP, He W, Cahn JY, Cairo M, Camitta BM, et al. Hematopoietic stem-cell transplantation for acute leukemia in relapse or primary induction failure. J Clin Oncol. 2010;28(23):3730–8.

94. Walker A, Marcucci G. Molecular prognostic factors in cytogenetically normal acute myeloid leukemia. Expert Rev Hematol. 2012;5(5):547–58.

95. Reilly JT. Pathogenesis of acute myeloid leukaemia and inv(16)(p13;q22): a paradigm for understanding leukaemogenesis? Br J Haematol. 2005 Jan;128(1):18–34.

96. Liu PP, Hajra a, Wijmenga C, Collins FS. Molecular pathogenesis of the chromosome 16 inversion in the M4Eo subtype of acute myeloid leukemia. Blood. 1995;85:2289–302.

97. Wessels HW, Dauwerse HG, Breuning MH, Beverstock GC. Inversion 16 and translocation (16;16) in ANLL M4eo break in the same subregion of the short arm of chromosome 16. Cancer Genet Cytogenet. 1991;57(2):225–8.

98. Larson RA, Williams SF, Le Beau MM, Bitter MA, Vardiman JW, Rowley JD. Acute myelomonocytic leukemia with abnormal eosinophils and inv(16) or t(16;16) has a favorable prognosis. Blood. 1986 Dec;68(6):1242–9.

99. Eghtedar A, Borthakur G, Ravandi F, Jabbour E, Cortes J, Pierce S, et al.

Characteristics of translocation (16;16)(p13;q22) acute myeloid leukemia. Am J Hematol. 2012 Mar;87(3):317–8.

100. Delaunay J, Vey N, Leblanc T, Fenaux P, Rigal-Huguet F, Witz F, et al. Prognosis of inv(16)/t(16;16) acute myeloid leukemia (AML): A survey of 110 cases from the French AML intergroup. Blood. 2003;102(2):462–9.

101. Park TS, Lee ST, Song J, Lee KA, Lee JH, Kim J, et al. Detection of a novel CBFB/MYH11 variant fusion transcript (K-type) showing partial insertion of exon 6 of CBFB gene using two commercially available multiplex RT-PCR kits. Cancer Genet Cytogenet. 2009;189(2):87–92.

102. Schwind S, Edwards CG, Nicolet D, Mrózek K, Maharry K, Wu YZ, et al. Inv(16)/t(16;16) acute myeloid leukemia with non-type A CBFB-MYH11 fusions associate with distinct clinical and genetic features and lack KIT mutations. Blood. 2013;121(2):385–91.

103. Stulberg J, Kamel-Reid S, Chun K, Tokunaga J, Wells RA. Molecular analysis of a new variant of the CBF beta-MYH11 gene fusion. Leuk Lymphoma. 2002 Oct;43(10):2021–6.

104. van der Reijden B a, Dauwerse HG, Giles RH, Jagmohan-Changur S, Wijmenga C, Liu PP, et al. Genomic acute myeloid leukemia-associated inv(16)(p13q22) breakpoints are tightly clustered. Oncogene. 1999;18:543–50.

105. Weckerle, Allison B., Santra, Madhumita, Ng, Maggie C.Y., Koty, Patrick P., Wang Y-H. CBFB and MYH11 in inv(16)(p13q22) of Acute Myeloid Leukemia Display Close Spatial Proximity in Interphase Nuclei of Human Hematopoietic Stem Cells. Genes Chromosom Cancer. 2011;50(9):746–55.

106. Lukasik SM, Zhang L, Corpora T, Tomanicek S, Li Y, Kundu M, et al. Altered affinity of CBF beta-SMMHC for Runx1 explains its role in leukemogenesis. Nat Struct Biol. 2002 Sep;9(9):674–9.

107. Lutterbach B, Hou Y, Durst KL, Hiebert SW. The inv(16) encodes an acute myeloid leukemia 1 transcriptional corepressor. Proc Natl Acad Sci U S A. 1999;96(16):12822–7.

108. Kummalue T, Lou J, Friedman a D. Multimerization via its myosin domain facilitates nuclear localization and inhibition of core binding factor (CBF) activities by the CBFbeta-smooth muscle myosin heavy chain myeloid leukemia oncoprotein. Mol Cell Biol. 2002;22(23):8278–91.

109. Zhang L, D'Costa J, Kummalue T, Civin CI, Friedman a D. Identification of a region on the outer surface of the CBFbeta-SMMHC myeloid oncoprotein assembly competence domain critical for multimerization. Oncogene. 2006;25(55):7289–96.

110. Van der Reijden B a, de Wit L, van der Poel S, Luiten EB, Lafage-Pochitaloff M, Dastugue N, et al. Identification of a novel CBFB-MYH11 transcript: implications for RT-PCR diagnosis. Hematol J. 2001;2(3):206–9.

111. Kamikubo Y, Zhao L, Wunderlich M, Corpora T, Hyde RK, Paul T a., et al. Accelerated Leukemogenesis by Truncated CBFβ-SMMHC Defective in High-Affinity Binding with RUNX1. Cancer Cell. 2010;17(5):455–68.

112. D'Costa J, Chaudhuri S, Civin CI, Friedman AD. CBFβ-SMMHC slows proliferation of primary murine and human myeloid progenitors. Leukemia. 2005;19(6):921–9.

113. Kim H-G, LeGrand J, Swindle CS, Nick HJ, Oster RA, Chen D, et al. The assembly competence domain is essential for inv(16)-associated acute myeloid leukemia. Leukemia. 2017;31(10):2267–71.

114. Zhao L, Alkadi H, Kwon EM, Zhen T, Lichtenberg J, Alemu L, et al. The C-Terminal multimerization domain is essential for leukemia development by CBFβ-SMMHC in a mouse knockin model. Leukemia. 2017;31(12):2841–4.

115. Durst KL, Lutterbach B, Kummalue T, Friedman AD, Hiebert SW. The inv (16) Fusion Protein Associates with Corepressors via a Smooth Muscle Myosin Heavy-Chain Domain. Mol Cell Biol. 2003;23(2):607–19.

116. Kamikubo Y, Hyde RK, Zhao L, Alemu L, Rivas C, Garrett LJ, et al. The C-terminus of CBFβ-SMMHC is required to induce embryonic hematopoietic defects and leukemogenesis. Blood. 2013 Jan 24;121(4):638–42.

117. Huang G, Shigesada K, Wee H-J, Liu PP, Osato M, Ito Y. Molecular basis for a dominant inactivation of RUNX1/AML1 by the leukemogenic inversion 16 chimera. Blood. 2004;103(8):3200–7.

118. Castilla LH, Wijmenga C, Wang Q, Stacy T, Speck N a., Eckhaus M, et al. Failure of embryonic hematopoiesis and lethal hemorrhages in mouse embryos heterozygous for a knocked-in leukemia gene CBFB-MYH11. Cell. 1996;87:687–96.

119. Zhao W, Claxton DF, Jeffrey Medeiros L, Lu D, Vadhan-Raj S, Kantarjian HM, et al. Immunohistochemical analysis of CBFβ-SMMHC protein reveals a unique nuclear localization in acute myeloid leukemia with inv(16)(p13q22). Am J Surg Pathol. 2006;30(11):1436–44.

120. Hyde RK, Kamikubo Y, Anderson S, Kirby M, Alemu L, Zhao L, et al. Cbfb/Runx1 repression-independent blockage of differentiation and accumulation of Csf2rb-expressing cells by Cbfb-MYH11. Blood. 2010;115(7):1433–43.

121. Hyde RK, Liu P, Friedman AD. RUNX1 and CBFβ mutations and activities of their wild-type alleles in AML. In: RUNX Proteins in Development and Cancer Advances in Experimental Medicine and Biology. 2017. p. 265–82.

122. Wang Y, Xie Y, Williams J, Hang Y, Richter L, Becker M, et al. Use of polymeric CXCR4 inhibitors as siRNA delivery vehicles for the treatment of acute myeloid leukemia. Cancer Gene Ther. 2019.

123. Ben-Ami O, Friedman D, Leshkowitz D, Goldenberg D, Orlovsky K, Pencovich N, et al. Addiction of t(8;21) and inv(16) Acute Myeloid Leukemia to Native RUNX1. Cell Rep. 2013;4(6):1131–43.

124. Tang J, Hou H, Chen C, Liu C, Chou W, Tseng M, et al. AML1 / RUNX1 mutations in 470 adult patients with de novo acute myeloid leukemia : prognostic implication and interaction with other gene alterations. Blood. 2009;114(26):5352–61.

125. Schnittger S, Dicker F, Kern W, Wendland N, Sundermann J, Alpermann T, et al. RUNX1 mutations are frequent in de novo AML with noncomplex karyotype and confer an unfavorable prognosis. Blood. 2011 Feb 24;117(8):2348–57.

126. Kadamb R, Mittal S, Bansal N, Batra H, Saluja D. Sin3: Insight into its transcription regulatory functions. Eur J Cell Biol. 2013;92(8–9):237–46.

127. Silverstein RA, Ekwall K. Sin3: A flexible regulator of global gene expression and genome stability. Curr Genet. 2005;47(1):1–17.

128. Zhen T, Kwon EM, Zhao L, Hsu J, Hyde RK, Lu Y, et al. Chd7 deficiency delays

leukemogenesis in mice induced by Cbfb-MYH11. Blood. 2017;130(22):2431–42.

129. Conway O'Brien E, Prideaux S, Chevassut T. The epigenetic landscape of acute myeloid leukemia. Adv Hematol. 2014;103175.

130. Castilla LH, Garrett L, Adya N, Orlic D, Dutra A, Anderson S, et al. The fusion gene Cbfb-MYH11 blocks myeloid differentiation and predisposes mice to acute myelomonocytic leukaemia. Nat Genet. 1999 Oct;23(2):144–6.

131. Pulikkan JA, Castilla LH. Preleukemia and Leukemia-Initiating Cell Activity in inv(16) Acute Myeloid Leukemia. Front Oncol. 2018;8(APR):129.

132. Müller AMS, Duque J, Shizuru JA, Lübbert M. Complementing mutations in core binding factor leukemias: From mouse models to clinical applications. Oncogene. 2008;27(44):5759–73.

133. Paschka P, Du J, Schlenk RF, Gaidzik VI, Bullinger L, Corbacioglu A, et al. Secondary genetic lesions in acute myeloid leukemia with inv (16) or t (16 ; 16): a study of the German-Austrian AML Study Group (AMLSG). Blood. 2013;121(1):170–7.

134. Haferlach C, Dicker F, Kohlmann A, Schindela S, Weiss T, Kern W, et al. AML with CBFB-MYH11 rearrangement demonstrate RAS pathway alterations in 92% of all cases including a high frequency of NF1 deletions. Leukemia. 2010 May;24(5):1065–9.

135. Boissel N, Leroy H, Brethon B, Philippe N, de Botton S, Auvrignon A, et al. Incidence and prognostic impact of c-Kit, FLT3, and Ras gene mutations in core binding factor acute myeloid leukemia (CBF-AML). Leukemia. 2006;20(6):965–70.

136. Care RS, Valk PJM, Goodeve AC, Abu-Duhier FM, Geertsma-Kleinekoort WMC,

Wilson G a., et al. Incidence and prognosis of c-KIT and FLT3 mutations in core binding factor (CBF) acute myeloid leukaemias. Br J Haematol. 2003;121(1999):775–7.

137. Castilla LH, Perrat P, Martinez NJ, Landrette SF, Keys R, Oikemus S, et al. Identification of genes that synergize with Cbfb-MYH11 in the pathogenesis of acute myeloid leukemia. Proc Natl Acad Sci U S A. 2004;101(14):4924–9.

138. Zhao L, Melenhorst JJ, Alemu L, Kirby M, Anderson S, Kench M, et al. KIT with D816 mutations cooperates with CBFB-MYH11 for leukemogenesis in mice. Blood. 2012;119(6):1511–21.

139. Xue L, Pulikkan J a, Valk PJM, Castilla LH. NrasG12D oncoprotein inhibits apoptosis of preleukemic cells expressing Cbfβ-SMMHC via activation of MEK/ERK axis. Blood. 2014 Jul 17;124(3):426–36.

140. Schlenk RF, Benner a., Krauter J, Büchner T, Sauerland C, Ehninger G, et al. Individual patient data-based meta-analysis of patients aged 16 to 60 years with core binding factor acute myeloid leukemia: A survey of the German acute myeloid leukemia intergroup. J Clin Oncol. 2004;22(18):3741–50.

141. Andersen MK, Larson RA, Mauritzson N, Schnittger S, Jhanwar SC, Pedersen-Bjergaard J. Balanced chromosome abnormalities inv(16) and t(15;17) in therapy-related myelodysplastic syndromes and acute leukemia: Report from an international workshop. Genes Chromosom Cancer. 2002;33(4):395–400.

142. Grimwade D, Hills RK, Moorman A V, Walker H, Chatters S, Goldstone AH, et al. Refinement of cytogenetic classification in acute myeloid leukemia: determination of prognostic significance of rare recurring chromosomal abnormalities among 5876 younger adult patients treated in the United Kingdom Medical Research

Council trials. Blood. 2010 Jul 22;116(3):354–65.

143. Sinha C, Cunningham LC, Liu PP. Core Binding Factor Acute Myeloid Leukemia: New Prognostic Categories and Therapeutic Opportunities. Semin Hematol. 2015 Jul;52(3):215–22.

144. Roboz GJ. Current treatment of acute myeloid leukemia. Curr Opin Oncol. 2012;24:711–9.

145. Koreth J, Schlenk R, Kopecky KJ, Honda S, Sierra J, Djulbegovic BJ, et al. Allogeneic stem cell transplantation for acute myeloid leukemia in first complete remission: Systematic review and meta-analysis of prospective clinical trials. JAMA - J Am Med Assoc. 2009;301(22):2349–61.

146. Kurosawa S, Miyawaki S, Yamaguchi T, Kanamori H, Sakura T, Moriuchi Y, et al. Prognosis of patients with core binding factor acute myeloid leukemia after first relapse. Haematologica. 2013;98(10):1525–31.

147. Goldman SL, Hassan C, Khunte M, Soldatenko A, Jong Y, Afshinnekoo E, et al. Epigenetic modifications in acute myeloid leukemia: Prognosis, treatment, and heterogeneity. Front Genet. 2019;10(MAR).

148. Wingelhofer B, Somervaille TCP. Emerging Epigenetic Therapeutic Targets in Acute Myeloid Leukemia. Front Oncol. 2019;9.

149. Glozak M a., Sengupta N, Zhang X, Seto E. Acetylation and deacetylation of non-histone proteins. Gene. 2005;363(1–2):15–23.

150. Aksnes H, Drazic A, Marie M, Arnesen T. First Things First: Vital Protein Marks by N-Terminal Acetyltransferases. Trends Biochem Sci. 2016;41(9):746–60.

151. Drazic A, Myklebust LM, Ree R, Arnesen T. The world of protein acetylation.

Biochim Biophys Acta - Proteins Proteomics. 2016;1864(10):1372–401.

152. Allfrey VG, Mirsky AE. Structural Modifications of Histones and their Possible Role in the Regulation of RNA Synthesis. Science. 1964 May 1;144(3618):559.

153. Lee DY, Hayes JJ, Pruss D, Wolffe AP. A positive role for histone acetylation in transcription factor access to nucleosomal DNA. Cell. 1993;72(1):73–84.

154. Grunstein M. Histone acetylation in chromatin structure and transcription. Nature. 1997;389(6649):349–52.

155. Cary PD, Crane-Robinson C, Bradbury EM, Dixon GH. Effect of acetylation on the binding of N-terminal peptides of histone H4 to DNA. Eur J Biochem. 1982 Sep;127(1):137–43.

156. Hong L, Schroth GP, Matthews HR, Yau P, Bradbury EM. Studies of the DNA binding properties of histone H4 amino terminus. Thermal denaturation studies reveal that acetylation markedly reduces the binding constant of the H4 “tail” to DNA. J Biol Chem. 1993;268(1):305–14.

157. Smith SG, Zhou MM. The Bromodomain as an Acetyl-Lysine Reader Domain. Chromatin Signal Dis. 2016;97–110.

158. Gu W, Roeder RG. Activation of p53 sequence-specific DNA binding by acetylation of the p53 C-terminal domain. Cell. 1997;90(4):595–606.

159. Imhof A, Yang XJ, Ogryzko V V, Nakatani Y, Wolffe AP, Ge H. Acetylation of general transcription factors by histone acetyltransferases. Curr Biol. 1997 Sep 1;7(9):689–92.

160. Lundby A, Lage K, Weinert BT, Bekker-Jensen DB, Secher A, Skovgaard T, et al. Proteomic Analysis of Lysine Acetylation Sites in Rat Tissues Reveals Organ

Specificity and Subcellular Patterns. Cell Rep. 2012;2(2):419–31.

161. Allis CD, Berger SL, Cote J, Dent S, Jenuwien T, Kouzarides T, et al. New Nomenclature for Chromatin-Modifying Enzymes. Cell. 2007;131(4):633–6.

162. Covault J, Chalkley R. The identification of distinct populations of acetylated histone. J Biol Chem. 1980;255(19):9110–6.

163. Yamagoe S, Kanno T, Kanno Y, Sasaki S, Siegel RM, Lenardo MJ, et al. Interaction of histone acetylases and deacetylases in vivo. Mol Cell Biol. 2003;23(3):1025–33.

164. Wang Z, Zang C, Cui K, Schones DE, Barski A, Peng W, et al. Genome-wide Mapping of HATs and HDACs Reveals Distinct Functions in Active and Inactive Genes. Cell. 2009;138(5):1019–31.

165. Kurdistani SK, Tavazoie S, Grunstein M. Mapping global histone acetylation patterns to gene expression. Cell. 2004;117(6):721–33.

166. Smith CL. A shifting paradigm: Histone deacetylases and transcriptional activation. BioEssays. 2008;30(1):15–24.

167. Lee KK, Workman JL. Histone acetyltransferase complexes: One size doesn't fit all. Nat Rev Mol Cell Biol. 2007;8(4):284–95.

168. Seto E, Yoshida M. Erasers of histone acetylation: the histone deacetylase enzymes. Cold Spring Harb Perspect Biol. 2014 Apr 1;6(4):a018713.

169. Taunton J, Hassig C a, Schreiber SL. A mammalian histone deacetylase related to the yeast transcriptional regulator Rpd3p. Science. 1996;272(5260):408–11.

170. Bartl S, Taplick J, Lagger G, Khier H, Kuchler K, Seiser C. Identification of mouse

histone deacetylase 1 as a growth factor-inducible gene. Mol Cell Biol. 1997;17(9):5033–43.

171. Yang WM, Yao YL, Sun JM, Davie JR, Seto E. Isolation and characterization of cDNAs corresponding to an additional member of the human histone deacetylase gene family. J Biol Chem. 1997;272(44):28001–7.

172. Taplick J, Kurtev V, Kroboth K, Posch M, Lechner T, Seiser C. Homo-oligomerisation and nuclear localisation of mouse histone deacetylase 1. J Mol Biol. 2001;

173. Brunmeir R, Lagger S, Seiser C. Histone deacetylase 1 and 2-controlled embryonic development and cell differentiation. Int J Dev Biol. 2009;53(2–3):275–89.

174. Hassig CA, Tong JK, Fleischer TC, Owa T, Grable PG, Ayer DE, et al. A role for histone deacetylase activity in HDAC1-mediated transcriptional repression. Proc Natl Acad Sci U S A. 1998;95(7):3519–24.

175. Li J, Staver MJ, Curtin ML, Holms JH, Frey RR, Edalji R, et al. Expression and functional characterization of recombinant human HDAC1 and HDAC3. Life Sci. 2004;74(22):2693–705.

176. Huang G, Zhao X, Wang L, Elf S, Xu H, Zhao X, et al. The ability of MLL to bind RUNX1 and methylate H3K4 at PU . 1 regulatory regions is impaired by MDS / AML-associated RUNX1 / AML1 mutations. Blood. 2011;118(25):6544–53.

177. Lagger G, O'Carroll D, Rembold M, Khier H, Tischler J, Weitzer G, et al. Essential function of histone deacetylase 1 in proliferation control and CDK inhibitor repression. EMBO J. 2002;21(11):2672–81.

178. Dovey OM, Foster CT, Cowley SM. Histone deacetylase 1 (HDAC1), but not HDAC2, controls embryonic stem cell differentiation. Proc Natl Acad Sci U S A. 2010;107(18):8242–7.

179. Zupkovitz G, Tischler J, Posch M, Sadzak I, Ramsauer K, Egger G, et al. Negative and Positive Regulation of Gene Expression by Mouse Histone Deacetylase 1. Mol Cell Biol. 2006;26(21):7913–28.

180. Wada T, Kikuchi J, Nishimura N, Shimizu R, Kitamura T, Furukawa Y. Expression levels of histone deacetylases determine the cell fate of hematopoietic progenitors. J Biol Chem. 2009;284(44):30673–83.

181. Heideman MR, Lancini C, Proost N, Yanover E, Jacobs H, Dannenberg J-H. Sin3a-associated Hdac1 and Hdac2 are essential for hematopoietic stem cell homeostasis and contribute differentially to hematopoiesis. Haematologica. 2014 Aug;99(8):1292–303.

182. Wilting RH, Yanover E, Heideman MR, Jacobs H, Horner J, van der Torre J, et al. Overlapping functions of Hdac1 and Hdac2 in cell cycle regulation and haematopoiesis. EMBO J. 2010;29(15):2586–97.

183. Zimmermann S, Kiefer F, Prudenziati M, Spiller C, Hansen J, Floss T, et al. Reduced body size and decreased intestinal tumor rates in HDAC2-mutant mice. Cancer Res. 2007;67(19):9047–54.

184. Yang WM, Tsai SC, Wen Y Der, Fejé G, Seto E. Functional domains of histone deacetylase-3. J Biol Chem. 2002;277(11):9447–54.

185. You SH, Lim HW, Sun Z, Broache M, Won KJ, Lazar MA. Nuclear receptor co-repressors are required for the histone-deacetylase activity of HDAC3 in vivo. Nat

Struct Mol Biol. 2013;20(2):182–7.

186. Karagianni P, Wong J. HDAC3: Taking the SMRT-N-CoRrect road to repression. Oncogene. 2007;26(37):5439–49.

187. Montgomery RL, Potthoff MJ, Haberland M, Qi X, Matsuzaki S, Humphries KM, et al. Maintenance of cardiac energy metabolism by histone deacetylase 3 in mice. J Clin Invest. 2008;118(11):3588–97.

188. Buggy JJ, Sideris ML, Mak P, Lorimer DD, McIntosh B, Clark JM. Cloning and characterization of a novel human histone deacetylase, HDAC8. Biochem J. 2000 Aug 15;350 Pt 1(1):199–205.

189. Wolfson N a., Ann Pitcairn C, Fierke C a. HDAC8 substrates: Histones and beyond. Biopolymers. 2013;99(2):112–26.

190. Chakrabarti A, Oehme I, Witt O, Oliveira G, Sippl W, Romier C, et al. HDAC8: A multifaceted target for therapeutic interventions. Trends Pharmacol Sci. 2015;36(7):481–92.

191. Haberland M, Mokalled MH, Montgomery RL, Olson EN. Epigenetic control of skull morphogenesis by histone deacetylase 8. Genes Dev. 2009;23(14):1625–30.

192. David G, Alland L, Hong SH, Wong CW, DePinho R a, Dejean a. Histone deacetylase associated with mSin3A mediates repression by the acute promyelocytic leukemia-associated PLZF protein. Oncogene. 1998;16:2549–56.

193. Wang J, Hoshino T, Redner RL, Kajigaya S, Liu JM. ETO, fusion partner in t(8;21) acute myeloid leukemia, represses transcription by interaction with the human N-CoR/mSin3/HDAC1 complex. Proc Natl Acad Sci U S A. 1998;95(September):10860–5.

194. Amann JM, Nip J, Strom DK, Lutterbach B, Harada H, Lenny N, et al. ETO, a target of t(8;21) in acute leukemia, makes distinct contacts with multiple histone deacetylases and binds mSin3A through its oligomerization domain. Mol Cell Biol. 2001;21(19):6470–83.

195. Bradbury C a, Khanim FL, Hayden R, Bunce CM, White D a, Drayson MT, et al. Histone deacetylases in acute myeloid leukaemia show a distinctive pattern of expression that changes selectively in response to deacetylase inhibitors. Leukemia. 2005 Oct;19(10):1751–9.

196. Huang Y, Chen J, Lu C, Han J, Wang G, Song C, et al. HDAC1 and Klf4 interplay critically regulates human myeloid leukemia cell proliferation. Cell Death Dis. 2014;5(10):1–12.

197. Marks P a, Richon VM, Breslow R, Rifkind R a. Histone deacetylase inhibitors as new cancer drugs. Curr Opin Oncol. 2001;13:477–83.

198. Melnick A, Licht JD. Histone deacetylases as therapeutic targets in hematologic malignancies. Curr Opin Hematol. 2002;9:322–32.

199. Durst KL, Hiebert SW. Role of RUNX family members in transcriptional repression and gene silencing. Oncogene. 2004;23:4220–4.

200. Suraweera A, O'Byrne KJ, Richard DJ. Combination Therapy With Histone Deacetylase Inhibitors (HDACi) for the Treatment of Cancer: Achieving the Full Therapeutic Potential of HDACi. Front Oncol. 2018;8(March):1–15.

201. Halsall JA, Turner BM. Histone deacetylase inhibitors for cancer therapy: An evolutionarily ancient resistance response may explain their limited success. BioEssays. 2016;38(11):1102–10.

202. Salvador LA, Luesch H. Discovery and mechanism of natural products as modulators of histone acetylation. Curr Drug Targets. 2012 Jul;13(8):1029–47.

203. Dashwood RH, Ho E. Dietary agents as histone deacetylase inhibitors: Sulforaphane and structurally related isothiocyanates. Nutr Rev. 2008 Aug;66:S36-8.

204. Halsall JA, Turan N, Wiersma M, Turner BM. Cells adapt to the epigenomic disruption caused by histone deacetylase inhibitors through a coordinated, chromatin-mediated transcriptional response. Epigenetics and Chromatin. 2015;8(1):1–16.

205. Kim H-J, Bae S-C. Histone deacetylase inhibitors: molecular mechanisms of action and clinical trials as anti-cancer drugs. Am J Transl Res. 2011 Feb;3(2):166–79.

206. Xu WS, Parmigiani RB, Marks P. Histone deacetylase inhibitors: molecular mechanisms of action. Oncogene. 2007;26:5541–52.

207. Bieliauskas A V, Pflum MKH. Isoform-selective histone deacetylase inhibitors. Chem Soc Rev. 2008 Jul;37(7):1402–13.

208. Malvaez M, McQuown SC, Rogge GA, Astarabadi M, Jacques V, Carreiro S, et al. HDAC3-selective inhibitor enhances extinction of cocaine-seeking behavior in a persistent manner. Proc Natl Acad Sci. 2013;110(7):2647–52.

209. Huang WJ, Wang YC, Chao SW, Yang CY, Chen LC, Lin MH, et al. Synthesis and Biological Evaluation of ortho-Aryl N-Hydroxycinnamides as Potent Histone Deacetylase (HDAC) 8 Isoform-Selective Inhibitors. ChemMedChem. 2012;7(10):1815–24.

210. Balasubramanian S, Ramos J, Luo W, Sirisawad M, Verner E, Buggy JJ. A novel histone deacetylase 8 (HDAC8)-specific inhibitor PCI-34051 induces apoptosis in T-cell lymphomas. Leukemia. 2008 May;22(5):1026–34.

211. Deschamps N, Simões-Pires CA, Carrupt PA, Nurisso A. How the flexibility of human histone deacetylases influences ligand binding: An overview. Drug Discov Today. 2015;20(6):736–42.

212. Bantscheff M, Hopf C, Savitski MM, Dittmann A, Grandi P, Michon A-M, et al. Chemoproteomics profiling of HDAC inhibitors reveals selective targeting of HDAC complexes. Nat Biotechnol. 2011;29(3):255–65.

213. Millard CJ, Watson PJ, Fairall L, Schwabe JWR. Targeting Class I Histone Deacetylases in a “Complex” Environment. Trends Pharmacol Sci. 2017;38(4):363–77.

214. Stankov M V, El Khatib M, Kumar Thakur B, Heitmann K, Panayotova-Dimitrova D, Schoening J, et al. Histone deacetylase inhibitors induce apoptosis in myeloid leukemia by suppressing autophagy. Leukemia. 2014;28(3):577–88.

215. Liu S, Klisovic RB, Vukosavljevic T, Yu J, Paschka P, Huynh L, et al. Targeting AML1 / ETO-Histone Deacetylase Repressor Complex : A Novel Mechanism for Valproic Acid-Mediated Gene Expression and Cellular Differentiation in AML1 / ETO-Positive Acute Myeloid Leukemia Cells. J Pharmacol Exp Ther. 2007;321(3):953–60.

216. Bots M, Verbrugge I, Martin BP, Salmon JM, Ghisi M, Baker A, et al. Differentiation therapy for the treatment of t (8 ; 21) acute myeloid leukemia using histone deacetylase inhibitors. Blood. 2014;123(9):1341–53.

217. Xu X, Xie C, Edwards H, Zhou H, Buck S a., Ge Y. Inhibition of histone deacetylases 1 and 6 enhances cytarabine-induced apoptosis in pediatric acute myeloid leukemia cells. PLoS One. 2011;6(2):1–11.

218. Gojo I, Tan M, Fang H Bin, Sadowska M, Lapidus R, Baer MR, et al. Translational phase I trial of vorinostat (suberoylanilide hydroxamic acid) combined with cytarabine and etoposide in patients with relapsed, refractory, high-risk acute myeloid leukemia. Clin Cancer Res. 2013;19(7):1838–51.

219. Kirschbaum M, Gojo I, Goldberg SL, Bredeson C, Kujawski LA, Yang A, et al. A phase 1 clinical trial of vorinostat in combination with decitabine in patients with acute myeloid leukaemia or myelodysplastic syndrome. Br J Haematol. 2014;167(2):185–93.

220. Garcia-manero G, Yang H, Bueso-ramos C, Ferrajoli A, Cortes J, Wierda WG, et al. Phase 1 study of the histone deacetylase inhibitor vorinostat (suberoylanilide hydroxamic acid [SAHA]) in patients with advanced leukemias and. Blood. 2009;111(3):1060–6.

221. Petruccelli L a, Pettersson F, Del Rincón S V, Guilbert C, Licht JD, Miller WH. Expression of leukemia-associated fusion proteins increases sensitivity to histone deacetylase inhibitor-induced DNA damage and apoptosis. Mol Cancer Ther. 2013;12(8):1591–604.

222. Saito A, Yamashita T, Mariko Y, Nosaka Y, Tsuchiya K, Ando T, et al. A synthetic inhibitor of histone deacetylase, MS-27-275, with marked in vivo antitumor activity against human tumors. Proc Natl Acad Sci U S A. 1999 Apr 13;96(8):4592–7.

223. Tatamiya T, Saito A, Sugawara T, Nakanishi O. Isozyme-selective activity of the HDAC inhibitor MS-275. In: Proc Amer Assoc Cancer Res. 2004.

224. Khan N, Jeffers M, Kumar S, Hackett C, Boldog F, Khramtsov N, et al. Determination of the class and isoform selectivity of small-molecule histone deacetylase inhibitors. Biochem J. 2008 Jan 15;409(2):581–9.

225. Bradner JE, West N, Grachan ML, Greenberg EF, Haggarty SJ, Warnow T, et al. Chemical phylogenetics of histone deacetylases. Nat Chem Biol. 2010;6(3):238–43.

226. Connolly RM, Rudek MA, Piekarz R. Entinostat : a promising treatment option for patients with advanced breast cancer. 2017;13:1137–48.

227. Subramanian S, Bates SE, Wright JJ, Espinoza-Delgado I, Piekarz RL. Clinical toxicities of histone deacetylase inhibitors. Pharmaceuticals. 2010;3(9):2751–67.

228. Yeruva SLH, Zhao F, Miller KD, Tevaarwerk AJ, Wagner LI, Gray RJ, et al. E2112: randomized phase iii trial of endocrine therapy plus entinostat/placebo in patients with hormone receptor-positive advanced breast cancer. npj Breast Cancer. 2018;4(1):1.

229. Rosato RR, Almenara JA, Grant S. The histone deacetylase inhibitor MS-275 promotes differentiation or apoptosis in human leukemia cells through a process regulated by generation of reactive oxygen species and induction of p21CIP1/WAF1 1. Cancer Res. 2003;63(13):3637–45.

230. Ramsey JM, Kettyle LMJ, Sharpe DJ, Mulgrew NM, Dickson GJ, Bijl JJ, et al. Entinostat prevents leukemia maintenance in a collaborating oncogene-dependent model of cytogenetically normal acute myeloid leukemia. Stem Cells. 2013;31(7):1434–45.

231. Duque-Afonso J, Yalcin A, Berg T, Abdelkarim M, Heidenreich O, Lübbert M. The

HDAC class I-specific inhibitor entinostat (MS-275) effectively relieves epigenetic silencing of the LAT2 gene mediated by AML1/ETO. Oncogene. 2011;30(27):3062–72.

232. Zhou L, Ruvolo VR, McQueen T, Chen W, Samudio IJ, Conneely O, et al. HDAC inhibition by SNDX-275 (Entinostat) restores expression of silenced leukemia-associated transcription factors Nur77 and Nor1 and of key pro-apoptotic proteins in AML. Leukemia. 2013;27(6):1358–68.

233. Gojo I, Jiemjit A, Trepel JB, Sparreboom A, Figg WD, Rollins S, et al. Phase 1 and pharmacological study of MS-275, a histone deacetylase inhibitor, in adults with refractory and relapsed acute leukemias. Blood. 2006;109(7):2781–91.

234. Prebet T, Sun Z, Figueroa ME, Ketterling R, Melnick A, Greenberg PL, et al. Prolonged administration of azacitidine with or without entinostat for myelodysplastic syndrome and acute myeloid leukemia with myelodysplasia-related changes: Results of the US Leukemia intergroup trial E1905. J Clin Oncol. 2014;32(12):1242–8.

235. Kuo Y-H, Landrette SF, Heilman S a, Perrat PN, Garrett L, Liu PP, et al. Cbf beta-SMMHC induces distinct abnormal myeloid progenitors able to develop acute myeloid leukemia. Cancer Cell. 2006;9(1):57–68.

236. Hyde RK, Liu PP. RUNX1 Repression Independent Mechanisms of Leukemogenesis by Fusion Genes CBFB-MYH11 and AML1-ETO (RUNX1-RUNX1T1). J Cell Biochem. 2010;110(5):1039–45.

237. Muzumdar MD, Tasic B, Miyamichi K, Li L, Luo L. A global double-fluorescent Cre reporter mouse. Genesis. 2007 Sep;45(9):593–605.

238. Cao W, Britos-Bray M, Claxton DF, Kelley C a, Speck N a, Liu PP, et al. CBF beta-SMMHC, expressed in M4Eo AML, reduced CBF DNA-binding and inhibited the G1 to S cell cycle transition at the restriction point in myeloid and lymphoid cells. Oncogene. 1997;15:1315–27.

239. Kuo Y-H, Zaidi SK, Gornostaeva S, Komori T, Stein GS, Castilla LH. Runx2 induces acute myeloid leukemia in cooperation with Cbfbeta-SMMHC in mice. Blood. 2009;113(14):3323–32.

240. Dull T, Zufferey R, Kelly M, Mandel RJ, Nguyen M, Trono D, et al. A third-generation lentivirus vector with a conditional packaging system. J Virol. 1998;72(11):8463–71.

241. Santoro F, Botrugno O a., Dal Zuffo R, Pallavicini I, Matthews GM, Cluse L, et al. A dual role for Hdac1: oncosuppressor in tumorigenesis, oncogene in tumor maintenance. Blood. 2013;121(17):3459–68.

242. Bahl K, Xie S, Spagnol G, Sorgen P, Naslavsky N, Caplan S. EHD3 protein is required for tubular recycling endosome stabilization, and an asparagine-glutamic acid residue pair within its Eps15 Homology (EH) domain dictates its selective binding to NPF peptides. J Biol Chem. 2016;291(26):13465–78.

243. Le Beau MM, Larson RA, Bitter MA, Vardiman JW, Golomb HM, Rowley JD. Association of an inversion of chromosome 16 with abnormal marrow eosinophils in acute myelomonocytic leukemia. A unique cytogenetic-clinicopathological association. N Engl J Med. 1983 Sep 15;309(11):630–6.

244. Arber DA, Orazi A, Hasserjian R, Borowitz MJ, Beau MM Le, Bloomfield CD, et al. The 2016 revision to the World Health Organization classification of myeloid neoplasms and acute leukemia. Blood. 2016;127(20):2391–406.

245. Castilla LH, Perrat P, Martinez NJ, Landrette SF, Keys R, Oikemus S, et al. Identification of genes that synergize with Cbfb-MYH11 in the pathogenesis of acute myeloid leukemia. Proc Natl Acad Sci U S A. 2004 Apr 6;101(14):4924–9.

246. Hart SM, Foroni L. Core binding factor genes and human leukemia. Haematologica. 2002 Dec;87(12):1307–23.

247. Speck N a, Gilliland DG. Core-binding factors in haematopoiesis and leukaemia. Nat Rev Cancer. 2002;2(7):502–13.

248. Speck N a. Core binding factor and its role in normal hematopoietic development. Curr Opin Hematol. 2001;8:192–6.

249. Warren a J, Bravo J, Williams RL, Rabbitts TH. Structural basis for the heterodimeric interaction between the acute leukaemia-associated transcription factors AML1 and CBFbeta. EMBO J. 2000 Jun 15;19(12):3004–15.

250. Gray SG, Ekström TJ. The human histone deacetylase family. Exp Cell Res. 2001;262(2):75–83.

251. Delcuve GP, Khan DH, Davie JR. Roles of histone deacetylases in epigenetic regulation: emerging paradigms from studies with inhibitors. Clin Epigenetics. 2012;4(1):5.

252. de Ruijter AJM, van Gennip AH, Caron HN, Kemp S, van Kuilenburg ABP. Histone deacetylases (HDACs): characterization of the classical HDAC family. Biochem J. 2003;370(Pt 3):737–49.

253. Nusinzon I, Horvath CM. Histone Deacetylases as Transcriptional Activators? Role Reversal in Inducible Gene Regulation. Sci Signal. 2005;2005(296):1–7.

254. Yanagisawa K, Horiuchi T, Fujita S. Establishment and characterization of a new

human leukemia cell line derived from M4E0. Blood. 1991;78(2):451–7.

255. Tang YY, Shi J, Zhang L, Davis A, Bravo J, Warren AJ, et al. Energetic and functional contribution of residues in the core binding factor β (CBFβ) subunit to heterodimerization with CBFα. J Biol Chem. 2000;275(50):39579–88.

256. Nagata T, Werner MH. Functional mutagenesis of AML1/RUNX1 and PEBP2 beta/CBF beta define distinct, non-overlapping sites for DNA recognition and heterodimerization by the Runt domain. J Mol Biol. 2001;308(2):191–203.

257. Giaimo BD, Ferrante F, Borggrefe T. Chromatin immunoprecipitation (ChIP) in mouse T-cell lines. J Vis Exp. 2017;2017(124).

258. Matthews GM, Mehdipour P, Cluse LA, Falkenberg KJ, Wang E, Roth M, et al. Functional-genetic dissection of HDAC dependencies in mouse lymphoid and myeloid malignancies. Blood. 2015;126(21):2392–404.

259. Friedman Ohana R, Kirkland TA, Woodroofe CC, Levin S, Uyeda HT, Otto P, et al. Deciphering the Cellular Targets of Bioactive Compounds Using a Chloroalkane Capture Tag. ACS Chem Biol. 2015;10(10):2316–24.

260. Gelmetti V, Zhang J, Fanelli M, Minucci S, Pelicci PG, Lazar MA. Aberrant Recruitment of the Nuclear Receptor Corepressor-Histone Deacetylase Complex by the Acute Myeloid Leukemia Fusion Partner ETO. Mol Cell Biol. 1998 Dec 1;18(12):7185–91.

261. He L-Z, Guidez F, Tribioli C, Peruzzi D, Ruthardt M, Zelent A, et al. Distinct interactions of PML-RARα and PLZF-RARα with co-repressors determine differential responses to RA in APL. Nat Genet. 1998;18(2):126–35.

262. Dovey OM, Foster CT, Conte N, Edwards SA, Edwards JM, Singh R, et al.

Histone deacetylase 1 and 2 are essential for normal T-cell development and genomic stability in mice. Blood. 2013;121(8):1335–44.

263. Streubel G, Fitzpatrick DJ, Oliviero G, Scelfo A, Moran B, Das S, et al. Fam60a defines a variant Sin3a-Hdac complex in embryonic stem cells required for self-renewal. EMBO J. 2017;36(15):2216–32.

264. Zapotocky M, Mejstrikova E, Smetana K, Stary J, Trka J, Starkova J. Valproic acid triggers differentiation and apoptosis in AML1/ETO-positive leukemic cells specifically. Cancer Lett. 2012 Jun 28;319(2):144–53.

265. Yazdanparast R, Mahdavi M, Moosavi MA. Induction of differentiation and apoptosis in three human leukemia cell lines by a new compound from Dendrostellera lessertii. Acta Biochim Biophys Sin (Shanghai). 2006;38(7):477–83.

266. Bruserud O. Induction of Differentiation and Apoptosis-- A Possible Strategy in the Treatment of Adult Acute Myelogenous Leukemia. Oncologist. 2000;5(6):454–62.

267. Mottamal M, Zheng S, Huang TL, Wang G. Histone Deacetylase Inhibitors in Clinical Studies as Templates for New Anticancer Agents. Molecules. 2015;20(3):3898–941.

268. Minucci, Nervi, Coco L, Pelicci. Histone deacetylases: a common molecular target for differentiation treatment of acute myeloid leukemias? Oncogene. 2001;20(24):3110–5.

269. Martens JHA, Stunnenberg HG. The molecular signature of oncofusion proteins in acute myeloid leukemia. FEBS Lett. 2010;584(12):2662–9.

270. Hiebert SW, Lutterbach B, Amann J. Role of co-repressors in transcriptional

repression mediated by the t(8;21), t(16;21), t(12;21), and inv(16) fusion proteins. Curr Opin Hematol. 2001;8(16):197–200.

271. Bai XT, Gu BW, Yin T, Niu C, Xi XD, Zhang J, et al. Trans-repressive effect of NUP98-PMX1 on PMX1-regulated c-FOS gene through recruitment of histone deacetylase 1 by FG repeats. Cancer Res. 2006;66(9):4584–90.

272. Hoogeveen AT, Rossetti S, Stoyanova V, Schonkeren J, Fenaroli A, Schiaffonati L, et al. The transcriptional corepressor MTG16a contains a novel nucleolar targeting sequence deranged in t (16; 21)-positive myeloid malignancies. Oncogene. 2002;21(43):6703–12.

273. Izutsu K, Kurokawa M, Imai Y, Ichikawa M, Asai T, Maki K, et al. The t(3;21) fusion product, AML1/Evi-1 blocks AML1-induced transactivation by recruiting CtBP. Oncogene. 2002;21(17):2695–703.

274. He LZ, Guidez F, Tribioli C, Peruzzi D, Ruthardt M, Zelent A, et al. Distinct interactions of PML-RARalpha and PLZF-RARalpha with co-repressors determine differential responses to RA in APL. Nat Genet. 1998;18(2):126–35.

275. Troke PJF, Kindle KB, Collins HM, Heery DM. MOZ fusion proteins in acute myeloid leukaemia. Biochem Soc Symp. 2006;73:23–39.

276. Lutterbach B, Westendorf JJ, Linggi B, Patten A, Moniwa M, Davie JR, et al. ETO, a Target of t(8;21) in Acute Leukemia, Interacts with the N-CoR and mSin3 Corepressors. Mol Cell Biol. 1998 Dec 1;18(12):7176–84.

277. Gelmetti V, Zhang J, Fanelli M, Minucci S, Pelicci PG, Lazar MA. Aberrant Recruitment of the Nuclear Receptor Corepressor-Histone Deacetylase Complex by the Acute Myeloid Leukemia Fusion Partner ETO. Mol Cell Biol.

1998;18(12):7185–91.

278. Zhang J, Kalkum M, Yamamura S, Chait BT, Roeder RG. E protein silencing by the leukemogenic AML1-ETO fusion protein. Science. 2004 Aug 27;305(5688):1286–9.

279. Wang J, Saunthararajah Y, Redner RL, Liu JM. Inhibitors of histone deacetylase relieve ETO-mediated repression and induce differentiation of AML1-ETO leukemia cells. Cancer Res. 1999;59(12):2766–9.

280. Racanicchi S, Maccherani C, Liberatore C, Billi M, Gelmetti V, Panigada M, et al. Targeting fusion protein/corepressor contact restores differentiation response in leukemia cells. EMBO J. 2005;24(6):1232–42.

281. Yang G, Thompson MA, Brandt SJ, Hiebert SW. Histone deacetylase inhibitors induce the degradation of the t(8;21) fusion oncoprotein. Oncogene. 2007;26(1):91–101.

282. Bots M, Verbrugge I, Martin BP, Salmon JM, Ghisi M, Baker A, et al. Differentiation therapy for the treatment of t(8;21) acute myeloid leukemia using histone deacetylase inhibitors. Blood. 2014 Feb 27;123(9):1341–52.

283. Odenike OM, Alkan S, Sher D, Godwin JE, Huo D, Brandt SJ, et al. Histone deacetylase inhibitor romidepsin has differential activity in core binding factor acute myeloid leukemia. Clin Cancer Res. 2008;14(21):7095–101.

284. Hong SH, David G, Wong CW, Dejean A, Privalsky ML. SMRT corepressor interacts with PLZF and with the PML-retinoic acid receptor alpha (RARalpha) and PLZF-RARalpha oncoproteins associated with acute promyelocytic leukemia. Proc Natl Acad Sci U S A. 1997;94(17):9028–33.

285. Di Croce L. Chromatin modifying activity of leukaemia associated fusion proteins. Hum Mol Genet. 2005;14(SPEC. ISS. 1):77–84.

286. Uribesalgo I, di Croce L. Dynamics of epigenetic modifications in leukemia. Brief Funct Genomics. 2011;10(1):18–29.

287. Ptasinska A, Assi SA, Mannari D, James SR, Williamson D, Dunne J, et al. Depletion of RUNX1/ETO in t(8;21) AML cells leads to genome-wide changes in chromatin structure and transcription factor binding. Leukemia. 2012;26(8):1829–41.

288. Martens JHA, Brinkman AB, Simmer F, Francoijs K-J, Nebbioso A, Ferrara F, et al. PML-RARα/RXR Alters the Epigenetic Landscape in Acute Promyelocytic Leukemia. Cancer Cell. 2010 Feb;17(2):173–85.

289. Singh AA, Mandoli A, Prange KHM, Laakso M, Martens JHA. AML associated oncofusion proteins PML-RARA, AML1-ETO and CBFB-MYH11 target RUNX/ETS-factor binding sites to modulate H3ac levels and drive leukemogenesis. Oncotarget. 2016;8(8):12855–65.

290. Wang L, Gural A, Sun X-J, Zhao X, Perna F, Huang G, et al. The leukemogenicity of AML1-ETO is dependent on site-specific lysine acetylation. Science. 2011 Aug 5;333(6043):765–9.

291. Reed-Inderbitzin E, Moreno-Miralles I, Vanden-Eynden S, Xie J, Lutterbach B, Durst-Goodwin K, et al. RUNX1 associates with histone deacetylases and SUV39H1 to repress transcription. Oncogene. 2006;25(April 2005):5777–86.

292. Zhang DE, Hetherington CJ, Chen HM, Tenen DG. The macrophage transcription factor PU.1 directs tissue-specific expression of the macrophage colony-

stimulating factor receptor. Mol Cell Biol. 1994;14(1):373–81.

293. Hubbert C, Guardiola A, Shao R, Kawaguchi Y, Ito A, Nixon A, et al. HDAC6 is a microtubule-associated deacetylase. Nature. 2002;417(6887):455–8.

294. Bacon T, Seiler C, Wolny M, Hughes R, Watson P, Schwabe J, et al. Histone deacetylase 3 indirectly modulates tubulin acetylation. Biochem J. 2015;472(3):367–77.

295. Pockwinse SM, Rajgopal A, Young DW, Mujeeb KA, Nickerson J, Javed A, et al. Microtubule-dependent nuclear-cytoplasmic shuttling of Runx2. J Cell Physiol. 2006;206(2):354–62.

296. Matsuyama A, Shimazu T, Sumida Y, Saito A, Yoshimatsu Y, Seigneurin-Berny D, et al. In vivo destabilization of dynamic microtubules by HDAC6-mediated deacetylation. EMBO J. 2002;21(24):6820–31.

297. Portran D, Schaedel L, Xu Z, Théry M, Nachury M V. Tubulin acetylation protects long-lived microtubules against mechanical ageing. Nat Cell Biol. 2017;19(4):391–8.

298. Morita K, Noura M, Tokushige C, Maeda S, Kiyose H, Kashiwazaki G, et al. Autonomous feedback loop of RUNX1-p53-CBFB in acute myeloid leukemia cells. Sci Rep. 2017;7(1):1–12.

Appendices

Appendix A: HDAC1 regulates RUNX1 acetylation which is critical for CBFβ-SMMHC-induced gene expression changes

A.1

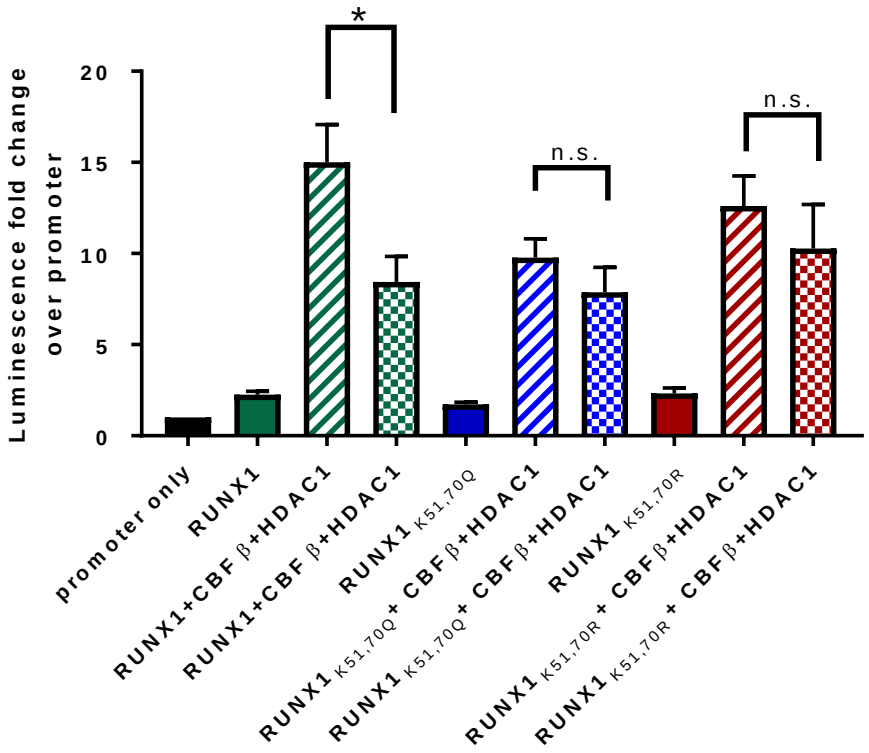

A.2

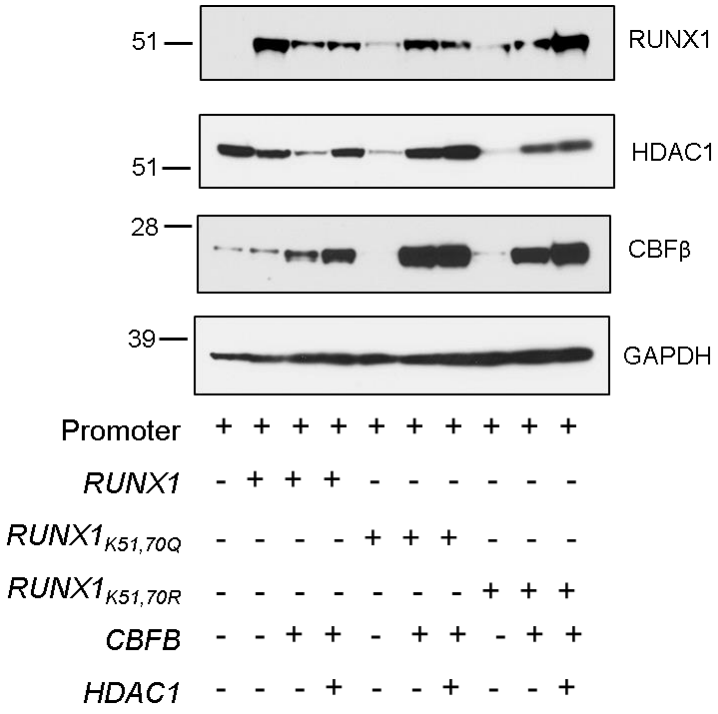

A.3

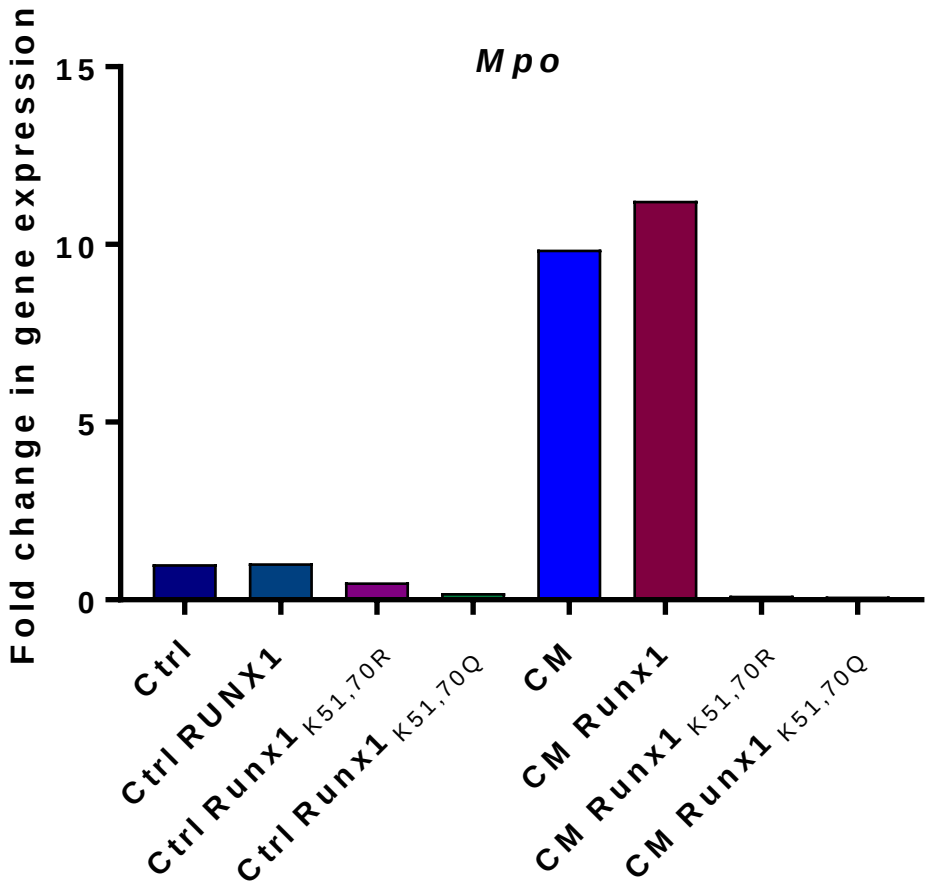

HDAC1 may mediate RUNX1 acetylation status which is critical for cooperation with CBFβ-SMMHC in gene expression. A.1) Luciferase assay was performed using the M-CSFR-Luc RUNX1 target promoter co-transfected with a constitutively expressed renilla luciferase containing plasmid to control for variations in transfection efficiency. The indicated plasmids were co-transfected along with the two luciferase plasmids into HEK293 cells for 48 hours, followed by lysis and luminescence analysis. Data is plotted as relative luminescence compared to promoter only. Significance was calculated using ANOVA. * = p≤0.05, ** = p≤0.01, n.s. = not significant. N ≥3. **(A.2)** A representative western blot confirming expression of transfected plasmids in HEK293 cells. **(A.3)** 32D cells with or without inducible CBFβ-SMMHC expression (CM or Ctrl) were transfected with RUNX1, $RUNX1_{K51,70R}$ or $RUNX1_{K51,70Q}$ expressing plamids. 24 hours after transfection, CM expression was induced. Cells were harvested 24 hours post induction of CM. RNA was extracted and used for qRT-PCR analysis of the indicated genes. RUNX1 and CM overexpression was confirmed. Data is normalized to beta actin and expressed as a fold change compared to the untransfected Ctrl cells. Data shown is from one representative experiment.

A.3

Appendix B: HDAC1 is required for localization of the CBFβ-SMMHC complex to gene promoters

B.1

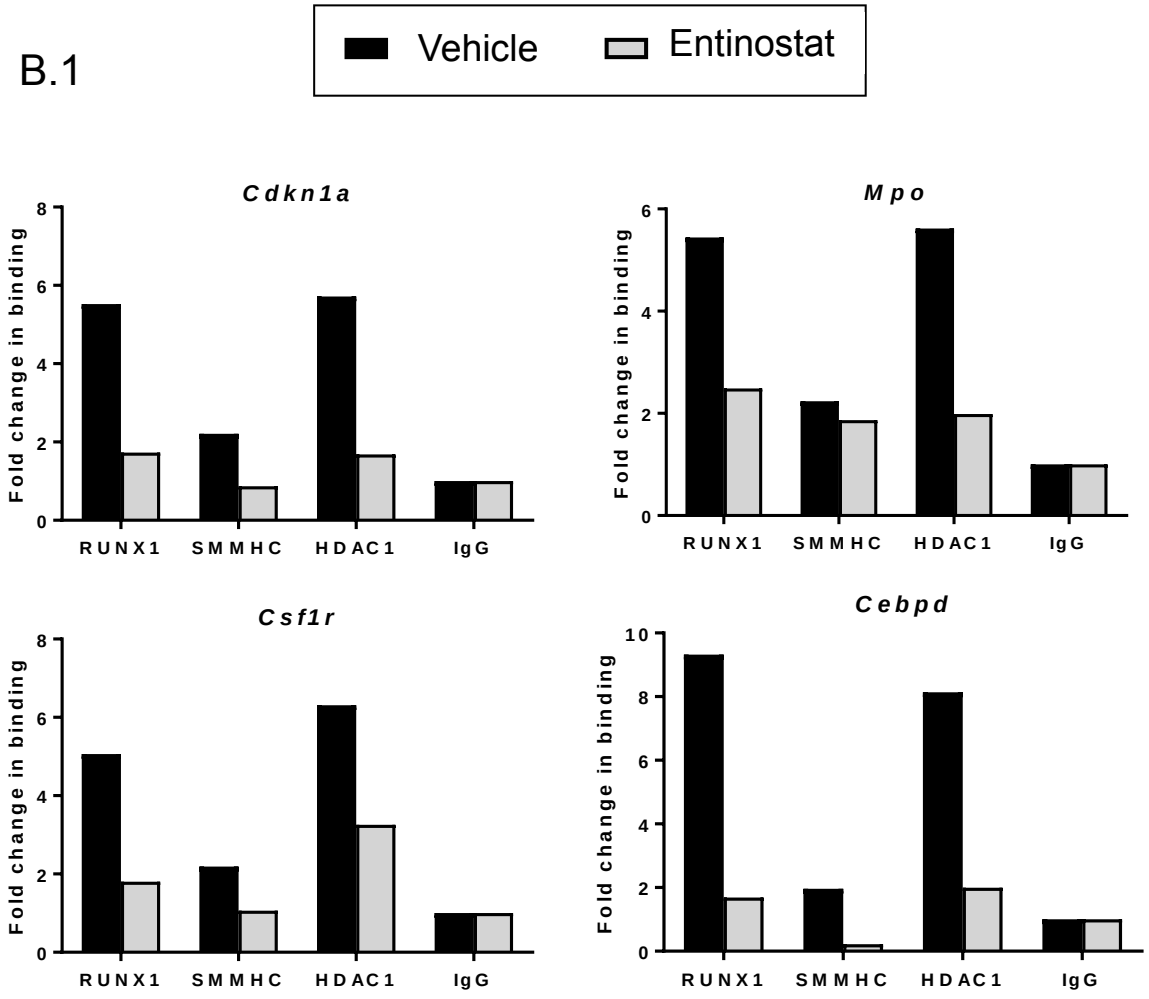

B.2

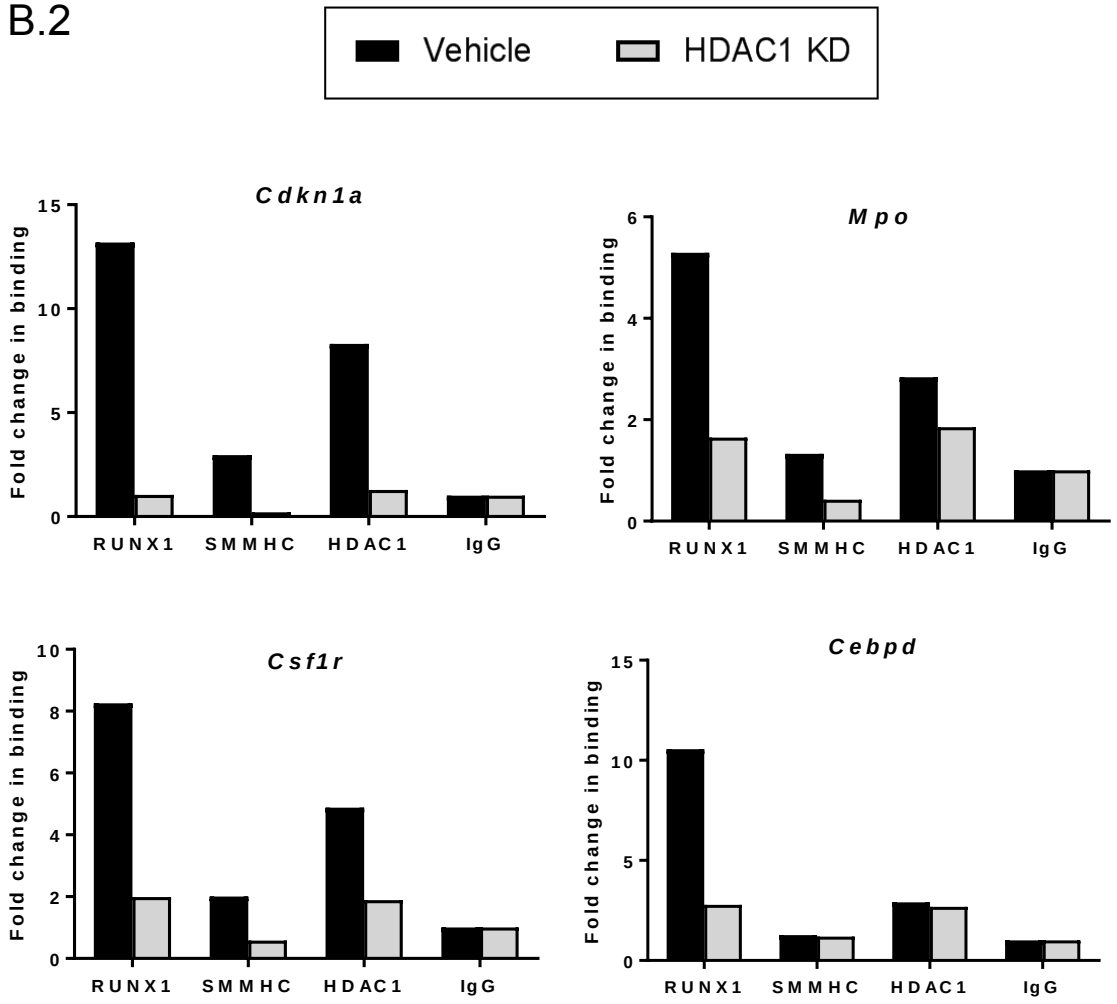

HDAC1 activity is required for the localization of CBFβ-SMMHC and RUNX1 to gene promoters. (B.1) Mouse *CM*$^{+}$ cells were treated with entinostat or DMSO for six hours in culture. ChIP was performed with the indicated antibodies followed by qRT-PCR for *Cdkn1a*, *Mpo*, *Cebpd*, or *Csf1r*. Data is from a single experiment. **(B.2)** Mice with *CM*$^{+}$ leukemia carrying stable incorporation of shRNA against HDAC1 were treated for seven days with 10 mM IPTG in the water bag to induce knockdown of HDAC1. Spleen cells from a mouse with confirmed HDAC1 KD and a control mouse were used for ChIP. ChIP was performed as in (B.1). Data is from a single experiment.

Appendix C: Tubulin may be deacetylated by HDAC1 and bound to RUNX1

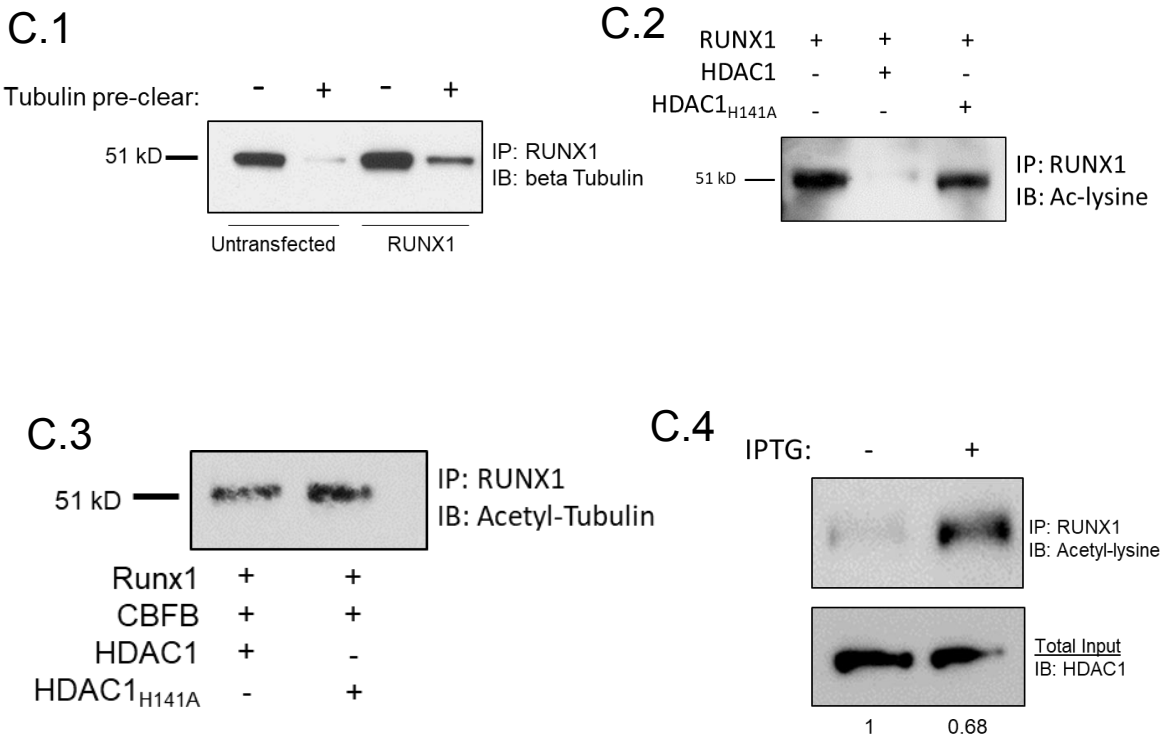

Tubulin is pulled down in IPs with RUNX1 and is a possible HDAC1 target. (C.1) COS-7 cell lysates, untransfected or transfected with a plasmid expressing RUNX1, were precleared with or without anti-beta tubulin antibody. Next, lysates were subjected to IP with anti-RUNX1 followed by western blot for beta tubulin. **(C.2)** COS-7 cells were transfected with plasmids expressing *RUNX1*, *HDAC1*, or $HDAC1_{H141A}$. Cell lysates were subjected to IP with RUNX1 and western blot with anti-acetyl-lysine. **(C.3)** COS-7 cells were transfected with plasmids expressing *RUNX1*, *CBFB*, *HDAC1*, or $HDAC1_{H141A}$ and lysates were subjected to IP with anti-RUNX1 antibody followed by western blot for acetyl-tubulin. **(C.4)** CM^{+} mouse cells containing IPTG-inducible shRNA against HDAC1 were treated with or without IPTG for 36 hours. Nuclear lysates were subjected to IP with anti-RUNX1 followed by western blot for acetyl-lysine. HDAC1 knockdown was confirmed in the inputs.

Appendix D: HDAC1 and CBFβ-SMMHC cooperate to downregulate CBFβ expression

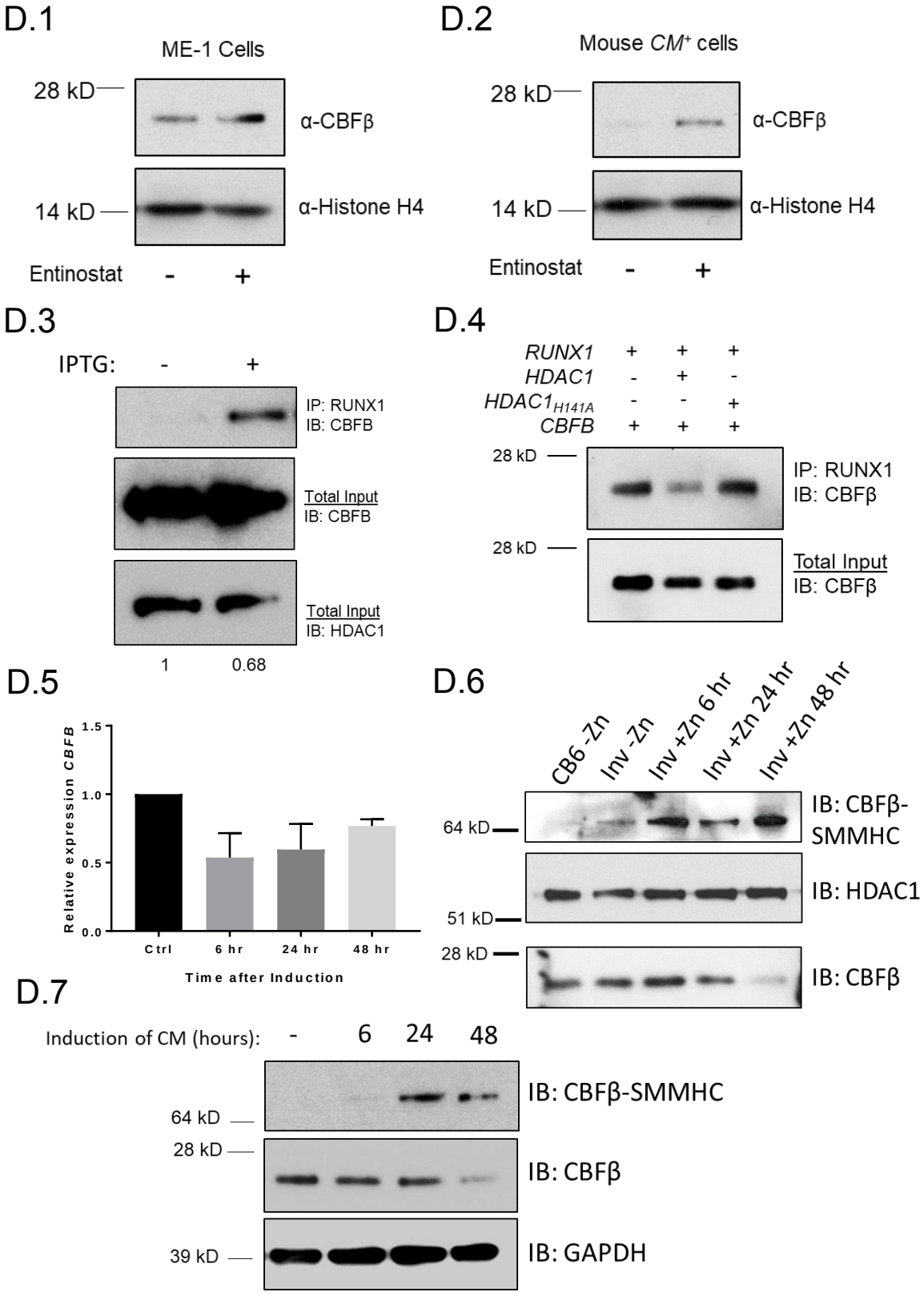

D.8

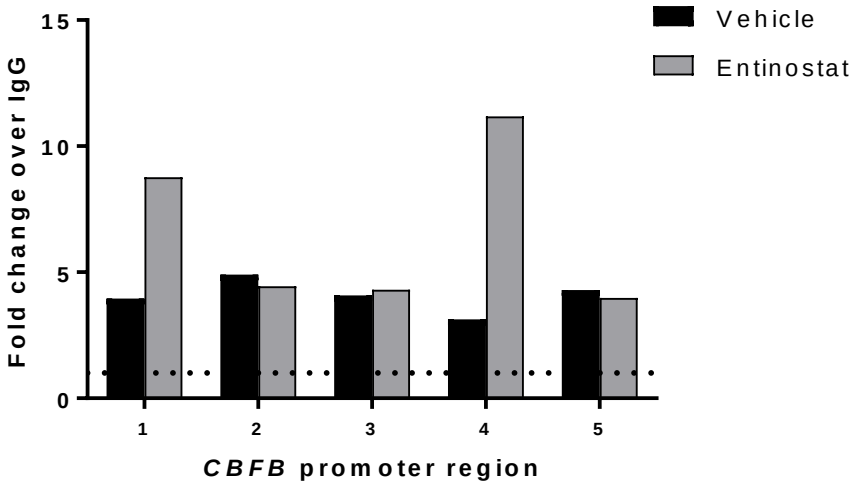

D.9

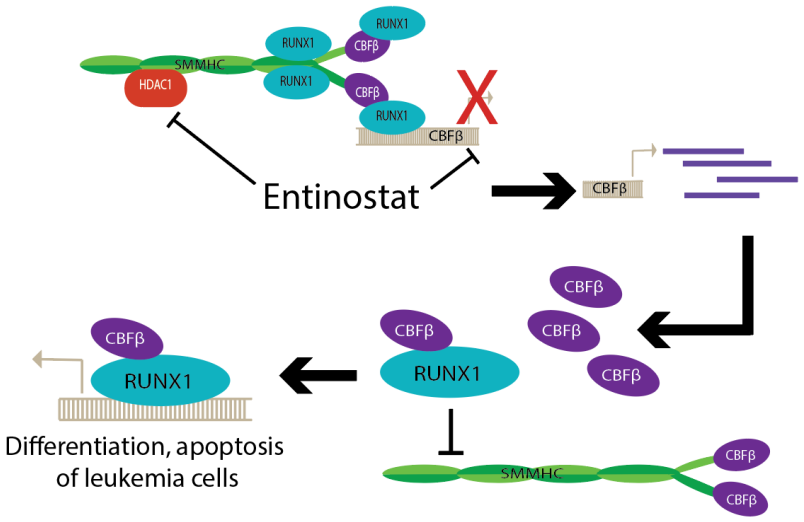

HDAC1 and CBFβ-SMMHC downregulate *CBFB* gene and protein expression. (D.1) ME-1 cells or **(D.2)** *CM*$^{+}$ mouse cells were treated with entinostat or vehicle control for 24 hours. Nuclear lysates were extracted and subjected to western blot with anti-CBFβ or histone H4 for loading control. **(D.3)** *CM*$^{+}$ mouse cells containing IPTG-inducible shRNA against HDAC1 were treated with or without IPTG for 36 hours. Nuclear lysates were extracted followed by immunoprecipitation with anti-RUNX1 and western blot for anti-CBFβ. Total inputs are shown below. **(D.4)** COS-7 cells were transfected with plasmids containing *RUNX1*, *CBFB*, *HDAC1*, or $HDAC1_{H141A}$ constructs. Nuclear lysates were subjected to IP with anti-RUNX1, followed by western blot with anti-CBFβ. Total input is shown below. **(D.5)** QRT-PCR was performed on cDNA from 32D INV cells at the indicated time points after induction of CBFβ-SMMHC, n = 3. **(D.6)** 32D CB6 or INV cells were induced with zinc and nuclear lysates were harvested at the indicated time points for western blot. anti-CBFβ was used to detect CBFβ-SMMHC (top panel) or wild-type CBFβ (bottom panel). **(D.7)** 32D INV cells were harvested at the indicated time points after induction of CBFβ-SMMHC. Total cell lysates were subjected to western blot as in D.6. **(D.8)** ChIP was performed on ME-1 cells with six hours of entinostat or vehicle treatment. Anti-SMMHC or total rabbit IgG was used for pulldown followed by qRT-PCR for five regions of the *CBFB* promoter. Data is plotted as SMMHC pulldown relative to IgG pulldown (represented by dotted line), n=1. **(D.9)** Model showing possible role of HDAC1, CBFβ-SMMHC, and entinostat in regulating CBFβ expression in inv(16) AML.